

1988

Spectrophotometric Determination of pH and Iron in Seawater: Equilibria and Kinetics

D. Whitney King
University of Rhode Island

Follow this and additional works at: https://digitalcommons.uri.edu/oa_diss

Terms of Use

All rights reserved under copyright.

Recommended Citation

King, D. Whitney, "Spectrophotometric Determination of pH and Iron in Seawater: Equilibria and Kinetics" (1988). *Open Access Dissertations*. Paper 1304.
https://digitalcommons.uri.edu/oa_diss/1304

This Dissertation is brought to you by the University of Rhode Island. It has been accepted for inclusion in Open Access Dissertations by an authorized administrator of DigitalCommons@URI. For more information, please contact digitalcommons-group@uri.edu. For permission to reuse copyrighted content, contact the author directly.

SPECTROPHOTOMETRIC DETERMINATION
OF pH AND IRON IN SEAWATER:
EQUILIBRIA AND KINETICS

BY

D. WHITNEY KING

A DISSERTATION SUBMITTED IN PARTIAL FULFILLMENT
OF THE REQUIREMENTS FOR THE DEGREE
OF DOCTOR OF PHILOSOPHY
IN
OCEANOGRAPHY

UNIVERSITY OF RHODE ISLAND

1988

Dissertation Abstract

The apparent dissociation constants, pK' , of five sulfonephthalein indicators (thymol blue, bromophenol blue, bromocresol green, bromocresol purple, and phenol red) were determined in 35 ‰ salinity seawater at 25 °C and over a pressure range from atmospheric to 1000 bars. The indicators were used to measure seawater pH over the above pressure ranges using the pK' and measured absorbance ratios of the acidic and basic components of a particular indicator. The pK' of the indicators were determined without the use of potentiometric pH measurements. The indicators provide a thermodynamically consistent free hydrogen ion pH scale independent of the problems of electrode drift and liquid junction error common to pH electrodes. The pH indicators can be readily adapted for in situ pH measurements.

The visible spectrum of each indicator was deconvoluted into four gaussian components using a nonlinear curve fitting approach. The spectrum of the basic form of the indicator was described by three components and the acid form by one peak. The gaussian components were defined in terms of their peak position, width, and height. Combining the gaussian parameters with the thermodynamic data for the indicators allowed quantitative modeling of an indicator's spectrum as a function of pH. A general equation was derived for the calculation of pH from two absorbance measurements of a solution which contains two or more indicators. The application of multiple indicators significantly expands the pH range over which pH measurements can be made with a single indicator. Using the modeled spectra for several indicators,

optimal indicator combinations for specific pH ranges were determined. The combination of phenol red and bromocresol green allowed determination of seawater pH over the range 8.2-3.0 which is suitable for oceanic pH and alkalinity determinations.

UV spectroscopy was used to determine the first hydrolysis constant of Fe(III), ${}^*_1\beta$, at 25 °C over a pressure range from atmospheric to 1000 bars. Based on these data the partial molal volume and compressibility change for the hydrolysis reaction were $-13.1 \text{ cm}^3\text{mol}^{-1}$ and $9.3 \times 10^{-4} \text{ cm}^3\text{mol}^{-1}\text{bar}^{-1}$ respectively. The ${}^*_1\beta$ values were determined independently of optical constants over the full pressure range. The results demonstrate that molal absorptivities of Fe^{3+} and FeOH^{2+} are not independent of pressure as assumed by previous investigators. An empirical equation provides values of ${}^*_1\beta$ as a function of temperature ($273 \leq T \leq 300$), ionic strength ($0.1 \leq I \leq 1.0$), and pressure ($0 \leq P \leq 1000$).

The pH indicators were used to study the effect of pressure on the second dissociation constant of bisulfate, K'_2 , and the rate of Fe (II) oxidation in seawater. The effect of pressure on bisulfate dissociation was determined over the pressure range atmospheric to 1000 bars from the compressional pH change of acidic seawater solutions. The partial molal volume and compressibility change for bisulfate dissociation was $-13.9 \text{ cm}^3\text{mol}^{-1}$ and $-6.54 \times 10^{-3} \text{ cm}^3\text{mol}^{-1}\text{bar}^{-1}$ respectively. An empirical equation provides values for K'_2 over the full range of oceanic temperatures, pressures, and salinities.

The rate of Fe(II) oxidation was established by monitoring the increase in the Fe(III) UV absorbance with time using a high pressure optical cell. Fe(II) concentrations were calculated from the iron

mass balance. The pseudo first order rate constant for Fe(II), k' , exhibited a second degree $[H^+]$ dependence over the pH range 7.0-8.2. At constant pH, k' increased by a factor of 6 with compression from atmospheric to 1000 bars. The change in k' was due to the increase in $[OH^-]$ with pressure. The pressure dependence was eliminated when the rate data were transformed to a constant pOH scale. The net effect is a small temperature dependent decrease in the predicted Fe(II) oxidation rates from surface to deep ocean environments.

The oxidation rate of Fe(II) in Narragansett Bay seawater was determined for both naturally occurring Fe(II) and for Fe(II) added at close to natural concentrations. The oxidation rate of added Fe(II) was in good agreement with the predicted rate based on rate constants for Fe(II) oxidation by O_2 and H_2O_2 . The concentration of Fe(II) in the surface waters of Narragansett Bay was between 6-11 $nmol\ kg^{-1}$. The oxidation rate of naturally occurring Fe(II) was slower than the predicted rate by an order of magnitude. Stabilization of Fe(II) by adsorption onto particles or by organic complexation could explain the reduced Fe(II) oxidation rate. The Fe(II) production rate required to maintain the observed quasi-steady state Fe(II) concentrations was $8 \pm 6\ nmol\ kg^{-1}\ hr^{-1}$. This production rate could be sustained by photochemical reduction of particulate Fe(III) to Fe(II).

ACKNOWLEDGMENTS

I would like to acknowledge my major professor, Dr. Dana Kester, who provided the guidance and facilities to make this work possible. His concern for his students and excellence as a teacher will always be remembered. I would also like to thank my lab-mates for making the laboratory a stimulating and enjoyable place to work. The assistance of Bill Miller and Jie Lin in the determination of H_2O_2 and Fe(II) is appreciated. Many thanks go to my parents who have always encouraged all of their children to make their own decisions and then backed our efforts with patience and understanding. Finally, my deepest thanks go to my wife, Jan, whose commitment, support, and love were invaluable during my graduate studies.

Preface

This thesis is written in manuscript format. It consists of seven manuscripts, seven appendices, and a thesis bibliography.

The manuscripts have been written in a format suitable for submission to marine and chemical journals. The first three manuscripts describe the development and application of sulfonephthalein colorimetric indicators for pH measurements in seawater at atmospheric and elevated pressures. The high pressure pH and optical measurement methods developed in these papers were used to determine the effect of pressure on bisulfate dissociation, Fe(III) hydrolysis, and Fe(II) oxidation as described in the fourth, fifth, and sixth manuscripts. The final manuscript examines the oxidation rate of Fe(II) at natural concentrations in Narragansett Bay.

The first manuscript "Determination of Seawater pH From 1.5 to 8.5 Using Colorimetric Indicators" describes the basic methodology for pH measurements using indicators. The paper presents experimentally determined values for the acid dissociation constants of the indicators in seawater media. Appendix I contains the derivation of the equations used to determine pH from the absorbance of seawater solutions containing a single indicator. Appendix II lists the absorbance and pH data used in the determination of the dissociation constants of the indicators.

The second manuscript "The Effect of Pressure on the Dissociation of Sulfonephthalein Indicators" extends the indicator pH measurement capability to high pressures. The relationship between indicator pK and ΔV is discussed in terms of electrostatic theory. Appendix III

lists the high pressure absorbance data used in the determination of buffer pH and indicator pK.

The third manuscript "Spectral Modeling of Sulfonephthalein Indicators: Application to pH Measurements Using Multiple Indicators" combines models for indicator absorbance spectra with indicator pK data to establish a general model for indicator absorbance as a function of indicator concentration, pH, and measurement wavelength. The methodology for pH measurement using multiple indicators is developed and optimization of multiple indicator pH measurements using indicator absorbance models is discussed. Appendix IV contains the derivation of the equations used to determine pH from absorbance of seawater solutions containing multiple indicators. Appendix V provides plots of observed and predicted absorbance spectra for the indicators which were not included in the manuscript.

The fourth manuscript "The Effect of Pressure on the Dissociation of Bisulfate in Seawater" describes the determination of the effect of pressure on bisulfate dissociation from compressional pH changes of acidic seawater solutions.

The fifth manuscript "The Effect of Pressure on the Hydrolysis of Fe(III)" presents the application of high pressure UV spectroscopy to the determination of the effect of pressure on the first hydrolysis constant of Fe(III). Appendix VI lists the pressure, pH, wavelength, and absorbance data used in the determination of ${}^*_1\beta$.

The sixth manuscript considers "The Effect of Pressure on the Oxidation Rate of Fe(II) in Seawater". Appendix VII describes a model for Fe(II) inorganic speciation which is used in the interpretation of

Fe(II) kinetic data.

The seventh and final manuscript "The Oxidation Rate of Fe(II) at Natural Concentrations in Narragansett Bay Seawater" presents rate constants for Fe(II) oxidation under natural conditions in Narragansett Bay seawater. The study used the new analytical method of King et al. (1988) to measure Fe(II) concentrations at natural levels.

Table of Contents

Thesis Abstract.....	ii
Acknowledgments.....	v
Preface.....	vi
List of Tables.....	xiii
List of Figures.....	xvi
Section I. Determination of Seawater pH From 1.5 to 8.5 Using Colorimetric Indicators.....	1
Abstract.....	2
Introduction.....	3
Theory.....	6
Experimental Methods.....	12
Results and Discussion.....	19
Conclusions.....	36
References.....	37
Section II. The Effect of Pressure on the Dissociation of Sulfonephthalein Indicators.....	40
Abstract.....	41
Introduction.....	42
Experimental	48
Results	53
Discussion.....	59
Summary.....	69
References.....	70

Section III.	Spectral Modeling of Sulfonephthalein Indicators: Application to pH Measurements Using Multiple Indicators.....	73
	Abstract.....	74
	Introduction.....	75
	Theory.....	76
	Experimental Section.....	84
	Results and Discussion.....	89
	References.....	105
Section IV.	The Effect of Pressure on the Dissociation of Bisulfate in Seawater.....	107
	Abstract.....	108
	Introduction.....	109
	Theory.....	111
	Methods.....	112
	Results and Discussion.....	114
	References.....	121
Section V.	The Effect of Pressure on the Hydrolysis of Fe(III).....	124
	Abstract.....	125
	Introduction.....	126
	Method.....	127
	Experimental.....	129
	Results.....	131
	Discussion.....	139
	References.....	141

Section VI.	The Effect of Pressure on the Oxidation Rate	
	of Fe(II) in Seawater.....	145
	Abstract.....	146
	Introduction.....	147
	Experimental.....	149
	Results and Discussion.....	160
	References.....	170
Section VII.	The Oxidation Rate of Fe(II) at Natural	
	Concentrations in Narragansett Bay Seawater.....	174
	Abstract.....	175
	Introduction.....	176
	Methods.....	177
	Results and Discussion.....	186
	Summary.....	193
	References.....	194
Appendices.....		197
	Appendix I: Derivation of equations used to calculate pH	
	from absorbances of single indicator solutions.....	197
	Appendix II: Indicator absorbance and pH data used for the	
	determination of indicator pK.....	200
	Appendix III: Indicator absorbance, pH and pK data used	
	in the determination of indicator pK as a	
	function of pressure.....	202
	Appendix IV: Derivation of equations used to calculate	
	pH from absorbances of multiple indicator	
	solutions.....	204

Appendix V: Plots of predicted and observed sulfonephthalein indicator spectra.....	210
Appendix VI: Fe(III) absorbance, pH, wavelength, and pressure data used in the determination of β as a function of pressure.....	221
Appendix VII: Fe(II) inorganic speciation model.....	223
Thesis Bibliography.....	231

List of Tables

Determination of Seawater pH From 1.5 to 8.5 Using Colorimetric Indicators

Table 1.	Values of λ_{iso} , λ_1 , E_1 , and E_2 for indicators in 35 ‰ seawater.....	20
Table 2.	Values for the pK_a of the indicators in 35 ‰ seawater.....	21

The Effect of Pressure on the Dissociation of Sulfonephthalein Indicators

Table 1.	Functional groups of the sulfonephthalein indicators.....	45
Table 2.	Values of λ_{iso} , λ_1 , E_{HA} , E_A , and C_A for indicators in 35 ‰ seawater at 25 °C and 0-1000 bars.....	54
Table 3.	ΔV values for the indicators and A and B constants from equation 8 for the buffers in 35 ‰ seawater at 25 °C.....	58
Table 4.	Values of σ for selected functional groups based on phenolic compounds.....	61

Spectral Modeling of Sulfonephthalein Indicators: Application to pH Measurements Using Multiple Indicators

Table 1.	Apparent dissociation constants of sulfonephthalein indicators in 35 ‰ salinity seawater at 25 °C.....	78
Table 2.	Isosbestic wavenumbers for the indicators in seawater, 0.68 M NaCl and Milli-Q media.....	90

Table 3.	Molar absorptivity of indicators at ν_{iso} in seawater, 0.68 m NaCl and Milli-Q media.....	91
Table 4.	Molar absorptivities of indicator gaussian components in seawater, 0.68 m NaCl and Milli-Q media.....	92
Table 5.	ν_{max} of indicator gaussian components in seawater, 0.68 m NaCl and Milli-Q media.....	93
Table 6.	ν_{half} of indicator gaussian components in seawater, 0.68 m NaCl and Milli-Q media.....	94
The Effect of Pressure on the Dissociation of Bisulfate in Seawater		
Table 1.	Literature values for K'_2 in seawater at 25 °C and 35 ‰ salinity.....	113
Table 2.	Solution pH and calculated bisulfate K'_2 and pK'_2 as a function of pressure ($t = 25$ °C, $S = 35$ ‰).....	115
Table 3.	Difference between pH_F and pH_T as a function of temperature and pressure.....	120
The Effect of Pressure on the Hydrolysis of Fe(III)		
Table 1.	Values for $-\log({}_1^*\beta)$ at 0, 355, 605, and 905 bars pressure and E_{Fe} , and E_{FeOH} at five wavelengths and 0, 355, 605, 905 bars pressure..	134
The Effect of Pressure on the Oxidation Rate of Fe(II) in Seawater		
Table 1.	Values of k' determined at 25°C in 35 ‰ salinity seawater using CFA and absorbance methods.....	161

The Oxidation Rate of Fe(II) at Natural Concentrations in
Narragansett Bay Seawater

Table 1. Oxidation rate of Fe(II) in Narragansett Bay
seawater..... 187

Appendices

Appendix II: Indicator absorbance and pH data used for the
determination of indicator pK

Table 1. Indicator absorbance and pH data used for the
determination of indicator apparent dissociation
constants..... 200

Appendix III: Indicator absorbance, pH and pK data used
in the determination of indicator pK as a
function of pressure

Table 1. Indicator absorbance and pH of buffer
solutions as a function of pressure at 25 °C in
35 ‰ salinity seawater..... 202

Table 2. Indicator absorbance and pK as a function of
pressure at 25 °C in 35 ‰ salinity seawater.. 203

Appendix VI: Fe(III) absorbance, pH, wavelength, and
pressure data used in the determination of β_1^*
as a function of pressure

Table 1. Absorbance of Fe(III) solutions as a function of
pH, wavelength, and pressure..... 221

Appendix VII: Fe(II) inorganic speciation model

Table I. Values of $\log K_1^0$, B, C, D, and ΔZ for
equation 2 and $\log K_1^*$ determined at 25 °C
in 35 ‰ salinity seawater..... 224

List of Figures

Determination of Seawater pH From 1.5 to 8.5 Using Colorimetric Indicators

Figure 1. Visible spectra of bromocresol green at six different pH..... 8

Figure 2. Diagram of the spectrophotometric system used to determine the isosbestic point wavelength of each indicator..... 16

Figure 3. Deviation of the pH_{ind} about the $pH_{ind}-pH_{EMF}$ regression line as a function of pH_{ind} 25

Figure 4. Deviation between pH_{ind} and pH_F as a function of pH_{ind} 27

Figure 5. Scaled acid and basic molar absorptivities of the indicators as a function of wavelength..... 30

Figure 6. Alkalinity titration of 35 ‰ seawater using both indicators and electrodes to monitor pH..... 35

The Effect of Pressure on the Dissociation of Sulfonephthalein Indicators

Figure 1. General structure of sulfonephthalein indicators..... 44

Figure 2. Diagram of the high pressure optical cell and internal cell..... 50

Figure 3. Change in the pK_a' of the indicators as a function of pressure.....	56
Figure 4. pK' as a function of $\Sigma\sigma$ for each indicator.	63
Figure 5. $\Delta V'$ for the indicators and ΔV for the substituted phenols as a function of the pK_a'	68
Spectral Modeling of Sulfonephthalein Indicators: Application to pH Measurements Using Multiple Indicators	
Figure 1. Visible spectra of phenol red in 0.68 M NaCl at six pH.....	83
Figure 2. Diagram of closed loop flow system used for isosbestic wavenumber determination and seawater alkalinity titrations.....	86
Figure 3. Observed and calculated spectra of bromocresol purple in seawater at pH 5.654.....	97
Figure 4. Predicted spectra of phenol red and bromocresol green in seawater as a function of pH and wavelength.....	100
Figure 5. Alkalinity titration of seawater solution.....	103
The Effect of Pressure on the Dissociation of Bisulfate in Seawater	
Figure 1. Calculated pK_2' for bisulfate as a function of pressure.....	117
The Effect of Pressure on the Hydrolysis of Fe(III)	
Figure 1. UV spectra of Fe(III) in 0.68 m NaClO ₄ at four pH.....	133

Figure 2. Values of $\log(\frac{*}{\beta})$ in 0.68 m NaClO ₄ at 25 °C as a function of pressure.....	137
The Effect of Pressure on the Oxidation Rate of Fe(II) in Seawater	
Figure 1. Diagram of the continuous flow analysis system used for Fe(II) determinations at atmospheric pressure.....	152
Figure 2. Fe(II) concentrations and Fe(III) absorbances as a function of time.....	154
Figure 3. Pseudo first order rate constant for Fe(II) as a function of pH.....	163
Figure 4. Pseudo first order rate constant for Fe(II) as a function of pOH.....	166
The Oxidation Rate of Fe(II) at Natural Concentrations in Narragansett Bay Seawater	
Figure 1. Flow system used to determine the oxidation rate of Fe(II) added to Narragansett Bay seawater.....	181
Figure 2. Flow system used to determine the oxidation rate of naturally occurring Fe(II).....	184
Figure 3. First order decay plots for Fe(II) oxidation.....	189
Appendices	
Appendix V: Plots of predicted and observed sulfonephthalein indicator spectra	
Figure 1. Observed and predicted spectra of thymol blue in seawater at pH 1.684.....	212
Figure 2. Observed and predicted spectra of bromophenol blue in seawater at pH 3.751.....	214

Figure 3. Observed and predicted spectra of bromocresol green in seawater at pH 4.625.....	216
Figure 4. Observed and predicted spectra of bromocresol purple in seawater at pH 5.654.....	218
Figure 5. Observed and predicted spectra of phenol red in seawater at pH 7.986.....	220
Appendix VII: Fe(II) inorganic speciation model	
Figure 1. Variation of Fe(II) species in 35 ‰ salinity seawater at 25 °C as a function of pH...	228
Figure 2. Variation of Fe(II) hydrolysis species in 35 ‰ salinity seawater at 25 °C as a function of pH.....	230

Determination of Seawater pH From 1.5 to 8.5
Using Colorimetric Indicators.

Abstract

The apparent dissociation constants of five sulfonephthalein indicators (thymol blue, bromophenol blue, bromocresol green, bromocresol purple, and phenol red) were determined in 35 ‰ seawater at 25 °C. Measurements of seawater pH were made using the ratio of the optical absorbance of the acid and basic component of a particular indicator and the apparent dissociation constant of the indicator. The suite of indicators allow quantitative determination of seawater pH over the pH range 1.5-8.5. For seven seawater samples ranging from pH 1.5-8.0 the average difference between pH measurements made with indicators and conventional electrodes was ± 0.005 . Measurement of seawater pH with indicators is not limited to single indicator additions. Simultaneous addition of phenol red and bromocresol green allow pH determination from 3.0-8.2 which is suitable for alkalinity titrations. The pK_a' of the indicators were determined without the use of potentiometric pH measurements. The pH indicators provide an absolute pH scale independent of the problems of electrode drift and liquid junction errors associated with potentiometric pH measurements.

INTRODUCTION

The pH of seawater is an important parameter in describing the chemistry of marine systems; it is necessary for defining acid-base equilibria, mineral solubility, and rates of kinetic processes. Most pH measurements in seawater have been made potentiometrically using a glass hydrogen ion electrode and a reference electrode with a liquid junction (Culberson, 1981). Currently, three different pH scales are used to calibrate pH electrodes in seawater: the National Bureau of Standards activity scale, pH_{NBS} (Bates, 1964), the total hydrogen ion scale, pH_{T} (Hansson, 1972), and the free hydrogen ion scale, pH_{F} (Bates, 1975). In the past ten years there has been debate over which pH scale is best suited for measurements in seawater (Culberson, 1981; Dickson, 1984; Perez and Fraga, 1987). The NBS scale has the advantage of being widely accepted outside the field of marine chemistry and buffer solutions are commercially available to calibrate the electrodes. However, non-thermodynamic assumptions used to establish the NBS scale and the inability to quantify reference electrode junction errors make the NBS scale subject to unknown systematic errors. When systematic errors are constant the reproducibility of pH_{NBS} is ± 0.003 pH units (Pytkowicz et al., 1966). Recently Whitfield et al. (1985) and Millero (1986) have demonstrated that the thermodynamically consistent total hydrogen ion scale and the free hydrogen ion scale are well suited for pH measurements in marine waters over a wide range of salinity. If appropriate buffer solutions are prepared, the accuracy of potentiometric pH_{T} or pH_{F} measurements in

seawater is better than ± 0.01 pH units.

Irrespective of which pH scale is chosen, potentiometric pH measurements have limitations. Electrode potentials, even under the best of conditions, take several minutes to stabilize when the electrode is transferred between two solutions of different composition. The time required for the stabilization of the electrodes sets a lower limit of 2-5 minutes per sample for measurements. Long term drift of pH electrodes can be as much as 0.6 mv/hour or approximately 0.01 pH/hour (Culberson, 1981). Long term electrode drift can make measurement of small pH changes over a period of time difficult to resolve. In addition to drift, the potential of the reference electrode can vary due to liquid junction irreproducibility. Liquid junction offsets occur when the liquid junction potential of the reference electrode in the buffer and the sample solutions are not equal. These offsets can be quite large when potentials are being compared between two solutions of different ionic composition such as NBS buffers and seawater (Whitfield et al., 1985). Even seawater measurements using the free hydrogen ion and total hydrogen ion scales can have significant junction offsets (0.5 mv) if the salinities of the buffers and sample are significantly different (Millero, 1986). Finally, because the measurements are only relative, pH electrodes must be referenced to buffer solutions of similar temperature, salinity, and pressure. In applications where pH electrodes can not be periodically recalibrated, such as in situ systems, changes in the response of the electrode due to changes in temperature, salinity or pressure can cause significant errors in calculated pH values.

Colorimetric indicators offer an alternative to potentiometric

methods for measuring pH. Indicators have the advantage of rapid equilibration time and eliminate the problem of electrode drift and liquid junction error. Most importantly, pH indicators can provide an absolute hydrogen ion concentration scale. In well defined media such as seawater, it is possible to establish the apparent equilibrium constants of indicators (K_a') over a practical range of salinities, temperatures and pressures. Once the apparent equilibrium constant of an indicator is known, measurement of pH using indicators can be made with an accuracy equal to or surpassing that of potentiometric pH measurements. While pH indicators have been used to measure pH for over 100 years (Kolthoff and Rosenblum, 1937), the use of pH indicators today has been mostly limited to qualitative pH estimates. Due to salt and medium effects on the dissociation constants of indicators, the apparent equilibrium constants in complex ionic media can not be predicted reliably (Bates, 1964). Accurate values for the K_a' of indicators are usually obtained by direct measurement in the medium of interest. Recently, Robert-Baldo et al. (1985) determined the pK_a' for phenol red in seawater as a function of temperature and salinity using potentiometric measurements as the pH standard for their experiments. Phenol red can be used to measure seawater pH over the range of 6.5-8.5.

Our work expands the application of pH indicators for seawater pH measurement. Five indicators, thymol blue, bromophenol blue, bromocresol green, bromocresol purple, and phenol red have been used to establish the working range of pH indicators from pH 1.5 to 8.5. The pK_a' of each indicator at 35 ‰ and 25 °C has been determined. The pK_a' of the indicators were determined independently of

potentiometric pH measurements.

THEORY

Acid-base indicators are weak acids which change color upon protonation or deprotonation of the indicator molecule. Figure 1 illustrates the color change of bromocresol green over a wide pH range. The pH of a solution can be determined by quantifying the absorbance of an indicator as a function of pH.

The acid-base equilibria for an indicator can be described by:

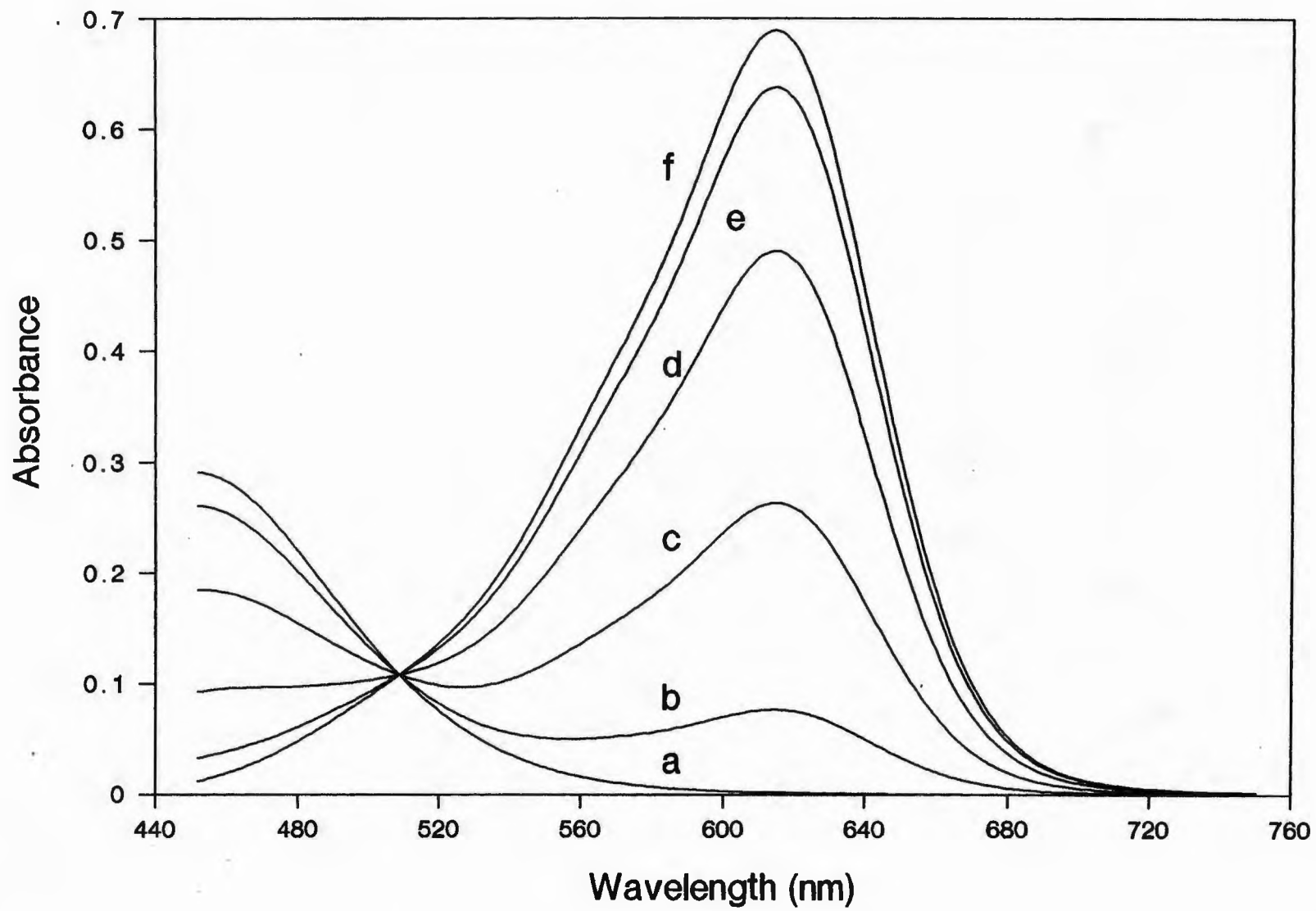


We define the K_a' for the indicator in terms of the free hydrogen ion concentration, $[\text{H}^+]$, and the total concentrations of the acid and basic forms of the indicator, (HA) and (A^-) respectively:

$$K_a' = \frac{[\text{H}^+](\text{A}^-)}{(\text{HA})} \quad (2)$$

The pH based on the indicator, pH_{ind} , is defined as the $-\log[\text{H}^+]$ which is the free hydrogen ion pH scale. The total concentration of A^- and HA are equal to the free concentration of the indicator species plus any indicator which has formed ion-pairs with the major components of seawater. The equilibrium constant for the indicator defined above is therefore an apparent equilibrium constant dependent

Figure 1. Visible spectra of bromocresol green at six different pH. Spectra a and f are the acid and basic components of the indicator respectively. Spectra b-e are composite absorbances of the acid and basic forms of the indicator at each pH. The pH_F of the solutions are: a=1.4, b=3.5, c=4.2, d=4.8, e=5.5, f=7.4.



on the ionic strength and the composition of the seawater solution in which it is defined.

The pH_{ind} of the solution can be determined from the pK_a' of the indicator and the concentration ratio of (A^-) to (HA) .

$$\text{pH}_{\text{ind}} = \text{pK}_a' + \log \frac{(\text{A}^-)}{(\text{HA})} \quad (3)$$

The ratio of (A^-) to (HA) can be determined colorimetrically by measuring the optical absorbance of an indicator at two wavelengths (see Appendix I):

$$\frac{(\text{A}^-)}{(\text{HA})} = \frac{(A_1/A_2 - E_{\text{HA}})}{(E_{\text{A}} - A_1/A_2)E_2} \quad (4)$$

A_1/A_2 is the ratio of the measured absorbances at wavelengths λ_1 and λ_2 . The constants E_{HA} , E_{A} , and E_2 are the ratios of the molar absorptivities, $\lambda \epsilon_i$, of (HA) and (A^-) at wavelengths λ_1 and λ_2 :

$$E_{\text{HA}} = \frac{\epsilon_{\text{HA}}(\lambda_1)}{\epsilon_{\text{HA}}(\lambda_2)} \quad (5)$$

$$E_{\text{A}} = \frac{\epsilon_{\text{A}^-}(\lambda_1)}{\epsilon_{\text{A}^-}(\lambda_2)} \quad (6)$$

$$E_2 = \frac{\epsilon_{\text{A}^-}(\lambda_2)}{\epsilon_{\text{HA}}(\lambda_2)} \quad (7)$$

The advantage of measuring absorbance ratios over single absorbance measurements is that equation 4 is independent of indicator concentration and pathlength. This is helpful since most indicators are poor primary standards. This approach is similar to the one presented by Robert-Baldo et al. (1985).

The constants E_{HA} and E_A are only a function of the molar absorptivities of HA and A^- respectively. At very acid or very basic pH_{ind} relative to the pK_a' of the indicator, the respective concentrations of HA and A^- can be assumed to be equal to the total concentration of the indicator, I_T . Therefore, values for E_{HA} and E_A can be measured directly in solutions according to equations 8 and 9.

For solutions with $pH_{ind} \ll pK_a'$, $(HA) = (I_T)$

$$E_{HA} = \frac{A_1}{A_2} = \frac{\epsilon_{HA}(HA)\ell}{\epsilon_{HA}(HA)\ell} \quad (8)$$

For solutions with $pH_{ind} \gg pK_a'$, $(A^-) = (I_T)$

$$E_A = \frac{A_1}{A_2} = \frac{\epsilon_{A^-}(A^-)\ell}{\epsilon_{A^-}(A^-)\ell} \quad (9)$$

where ℓ is the optical pathlength.

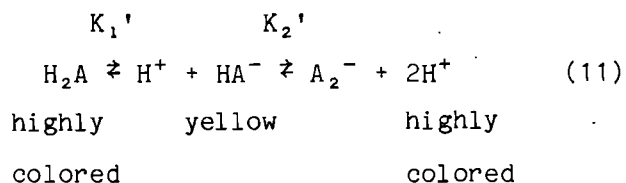
Combining equations 3 and 4, a final equation relating solution

pH_{ind} to A₁/A₂ of an indicator can be formulated.

$$\text{pH}_{\text{ind}} = \text{pK}'_a + \log \frac{(A_1/A_2 - E_{\text{HA}})}{(E_A - A_1/A_2)} - \log(E_2) \quad (10)$$

If λ_2 is chosen to be the wavelength of the isosbestic point of the indicator, E_2 has a value of unity and the $\log(E_2)$ term is eliminated in equation 10. The isosbestic point occurs at the wavelength where the molar absorptivities of A⁻ and HA are identical. The isosbestic point for bromocresol green is located at approximately 509 nm (Figure 1).

The sulfonephthalein indicators used in this work are not simple monoprotic acids as used in the derivation of equation 10. The general dissociation reaction for sulfonephthalein indicators consists of a two step dissociation of the diprotic acid as shown in equation 11:



However, since the first and second dissociation constants of the indicators are separated by more than a factor of 10⁶ ($\text{pK}'_2 - \text{pK}'_1 > 6$), the indicators can be treated as simple monoprotic acids within three pH units of pK'_1 or pK'_2 .

EXPERIMENTAL METHODS

Reagents

All solutions were prepared from reagent grade salts. Solutions were prepared using Milli-Q water and were stored in teflon bottles. Indicator stock solutions were prepared by adding the sodium salts of the indicators to artificial seawater solutions (ASW). The concentration of indicator stocks solutions was 1×10^{-3} m. Final indicator concentrations in measuring solutions were $1-2 \times 10^{-6}$ m. The concentrated indicator stock solutions were added directly to seawater samples to avoid diluting the sample. The change in the pH of the seawater samples due to the addition of the indicators was less than 0.001 pH units.

All experiments were performed using artificial seawater. Two types of artificial seawater were prepared according to a recipe of Kester et al. (1967) with the following exceptions; type one seawater, ASW(1), had all the weak acid salts including Na_2SO_4 , and NaF replaced with NaCl, and type two seawater, ASW(2), had NaHCO_3 , Na_2CO_3 , and NaB(OH)_4 replaced with NaCl. An ion-pairing model, based on NaCl as the reference medium, was used to calculate the effective ionic strength of 35 ‰ seawater (Kester, 1986). The effective ionic strength was 0.67 m at 25 °C. The effective ionic strengths of ASW(1) and ASW(2) were adjusted with NaCl until they matched that of 35 ‰ seawater. The total salt content of the ASW(1) and ASW(2) solutions was 33.3 and 35.5 g/kg respectively.

An HCl solution (1.656 molal) was standardized by titration of primary standard Na₂CO₃ solutions. The pH (pH range 1.0-2.5) of the ASW(1) solutions were established by gravimetric addition of the standard HCl stock solution. The NaCl concentration of the ASW(1) solutions was adjusted for HCl addition to maintain a constant effective ionic strength. Since the free hydrogen ion pH scale has been adopted in this work and ASW(1) contains no weak acids, the pH_{ind} of ASW(1) solutions was equal to the -log(HCl). Errors in the calculated pH due to impurities in the reagents were insignificant below pH 2.5. ASW(2) solutions of constant pH (pH range 2.6-8.5) were buffered by adding 0.01 m phthalate, phosphate, or Tris buffer to ASW(2) stock. The addition of the buffers to ASW(2) did not change the effective ionic strength of the solution by more than 1.5%. Since activity coefficients change slowly in the ionic strength range 0.5-0.8 (Kester, 1986), small changes in ionic strength will not influence the speciation of seawater to a significant extent.

Instrumentation

Spectra were obtained using a Shimadzu UV-260 spectrophotometer. Samples were contained in 10 cm thermostated quartz cells. The experiments were performed at 25.0 ± 0.1 °C. Spectral data were collected digitally over the wavelength range 750-400 nm and were transferred to a microcomputer for data analysis. The sampling resolution was 0.1 nm. The spectral data were smoothed using a seven point moving average. All spectra were baseline corrected using spectra of solutions of identical composition without added indicator.

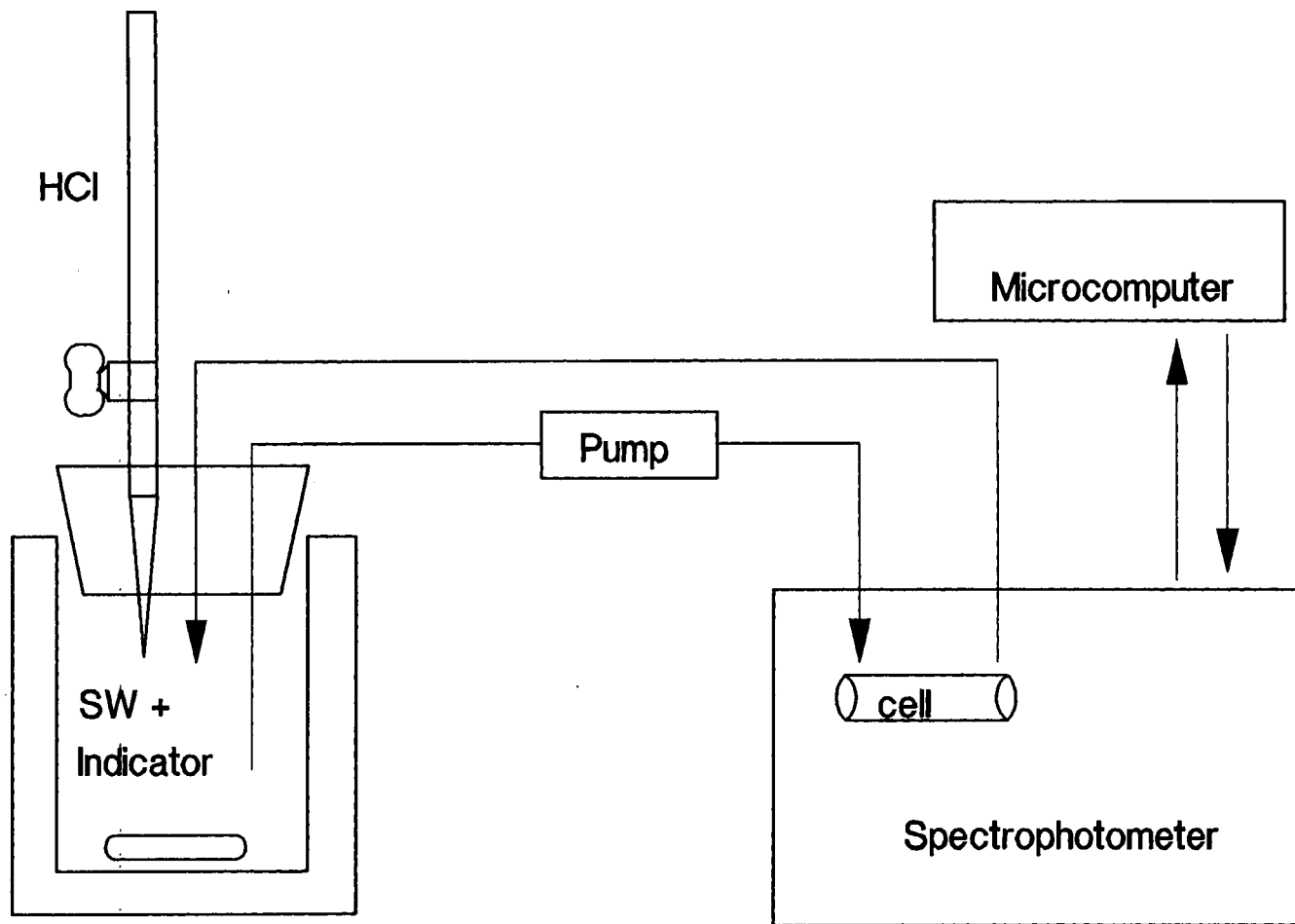
The background noise in the data was less than 0.0002 absorbance units. Background noise was calculated from the standard deviation of the absorbance measurements of the baseline solutions over a wavelength range 725-715 nm.

Potentiometric pH measurements were made with an Orion Ross 8102 combination pH electrode (4.0 m NaCl filling solution) and an Orion 701a pH meter. All pH measurements were made in a covered, thermostated, 50 ml polycarbonate beaker.

Determination of Isosbestic Point Wavelengths

The isosbestic point wavelength for each indicator was determined by measuring the wavelength of the intersection of three or more spectra of the same indicator. The spectra were obtained from indicator solutions with identical total indicator concentration but at different pH. Figure 2 is a diagram of the apparatus used to perform this experiment. A basic solution of ASW(2) with added indicator was contained in a 1000 ml covered, thermostated, pyrex vessel. The indicator solution was pumped in a closed loop from the pyrex vessel through a 10 cm cell in the spectrophotometer and back to the pyrex vessel. After the solution was well mixed, the pump was stopped and a spectrum was measured. Sequential spectra of the indicator at decreasing pH were obtained by titrating the indicator solution with small amounts of 3 m HCl. The exact wavelength of the isosbestic point was determined by the minimum in the plot of the standard deviation of the absorbance values for all of the spectra as a function of wavelength. The standard deviation of the three spectra at the

Figure 2. Diagram of the spectrophotometric system used to determine the isosbestic point wavelength of each indicator.



isosbestic point wavelength was less than 0.001 for all isosbestic determinations.

Determination of E_{HA} and E_A

As discussed in the theory section, E_{HA} and E_A values for an indicator were calculated from the ratio of A_1 to A_2 when the indicator is either all in the acid or basic form respectively. Estimates of the pK_a' of each indicator were used to determine the pH range for which equations 8 and 9 apply. It was assumed that the indicator was completely in the acidic or basic form when the pH of the indicator solution was more than ± 3 pH units from the pK_a' of the indicator. For the indicators bromophenol blue, bromocresol green, and bromocresol purple determination of E_{HA} and E_A was straightforward. Indicator solutions of the appropriate pH were prepared and the absorbance ratio A_1/A_2 measured. The E_A value for phenol red could not be determined in this manner due to brucite ($Mg(OH)_2$) precipitation from seawater solutions at $pH > 9.5$. Phenol red is not completely in the basic form until the $pH > 10.5$. Robert-Baldo et al. (1985) found that the maximum absorbance of phenol red exhibited very little medium dependence. We have found that the shape of the spectra of phenol red and the other four indicators are similar in NaCl and seawater (King and Kester, 1988). We therefore determined the value of E_A for phenol red in 0.67 NaCl at a pH of 10.5. The value for E_{HA} for thymol blue also could not be determined from absorbance ratios. The pH of thymol blue solutions would have to be less than $pH -2.4$ to obtain a direct determination of E_{HA} . The E_{HA} value for thymol blue was determined

by solving equation 10 in terms of E_{HA} and pK_a' as a function of pH and absorbance. The details of this calculation will be provided in the next section.

Determination of the pK_1' and E_{HA} of Thymol Blue

The absorbance ratio, A_1/A_2 , for thymol blue was measured in five ASW(1) solutions of gravimetrically known HCl molality at 25 °C. The values for E_{HA} and pK_1' (thymol blue) were calculated by solving equation 10 in terms of pK_1' and E_{HA} as a function of E_A and the five or more A_1/A_2 , pH_{ind} values from the ASW(1) solutions. The $\log(E_2)$ term in equation 10 is equal to zero since λ_2 was taken to be the isosbestic point. A nonlinear curve fitting program using the simplex algorithm (Caceci and Cacheris, 1984) was used to perform the calculations. The curve fitting program was written in Turbo Pascal and takes about one minute to converge on the solution using a microcomputer.

Determination of pK_2' for the Other Indicators

The known values for pK_1' , E_{HA} , and E_A for thymol blue were used to determine the pH_{ind} of three ASW(2) buffer solutions over the pH range 2.5-3.5. The indicator bromophenol blue was added to each of the three buffer solutions and the spectra were measured. The pK_2' of bromophenol blue was calculated by solving equation 10 for pK_2' in terms of the constants E_{HA} and E_A and the measured A_1/A_2 and pH_{ind} values for the three buffer solutions. Since the value of

E_{HA} and E_A were determined independently, the solution of equation 10 in terms of the pK_2' for bromophenol blue reduces to a simple linear problem.

The indicator bromophenol blue was used to determine the pH_{ind} of three more ASW(2) solutions over the pH range of 3.5-5.0. These three buffer solutions were used to determine the pK_2' of bromocresol green in a manner identical to the calculation of the pK_2' for bromophenol blue. This process was repeated two more times for bromocresol purple and phenol red.

RESULTS AND DISCUSSION

Optical Constants and pK' Values for the Indicators

Table 1 lists the isosbestic point wavelength ($\lambda_2 = \lambda_{iso}$), the wavelength of maximum absorbance (λ_1), and the values of E_{HA} and E_A for each indicator at 25 °C. Thymol blue is the only indicator for which the first dissociation constant was determined. Thymol blue is colored as an acid and is colorless (pale yellow) as a base, which is opposite to the characteristics of the other indicators.

Table 2 lists the calculated pK_a' and associated errors for each indicator in 35 ‰ seawater at 25 °C. The individual error reported for each indicator is the standard deviation of the curve fit used to calculate the pK_a' of each indicator. These values represent composite errors which include uncertainties in the pK_a' and the values of E_{HA} and E_A . The actual error in the pK_a' for each indicator is the individual error of the indicator plus the error in

Table 1. Values of λ_{iso} , λ_1 , E_{HA} , and E_A for indicators in 35 ‰ seawater at 25 °C.

Indicator	λ_{iso} (nm)	λ_1 (nm)	E_{HA}	E_A
Thymol Blue	487.9	540.0	4.643	0.173
Bromophenol Blue	495.7	590.0	0.015	8.846
Bromocresol Green	509.6	615.0	0.000	6.415
Bromocresol Purple	488.2	588.0	0.000	6.926
Phenol Red	479.7	558.0	0.010	5.773

Table 2. Values for the pK_a' of the indicators in 35 ‰ seawater at 25 °C.

Indicator	pK_a'	individual error ^a	cumulative error ^b
Thymol Blue ^c	1.439	0.006	0.006
Bromophenol Blue	3.695	0.003	0.007
Bromocresol Green	4.410	0.000	0.007
Bromocresol Purple	5.972	0.007	0.010
Phenol Red	7.492	0.004	0.010

a) individual errors due to curve fitting.

b) cumulative errors due to propagation of individual errors.

c) pK_1' was determined for thymol blue, pK_2' was determined for the other indicators.

the pK_a' of the other preceding indicators used in its determination. The actual or cumulative error is calculated from the propagation of individual errors.

It is difficult to compare thermodynamic values for thymol blue, bromophenol blue, bromocresol green, and bromocresol purple with values of other investigators. No previous measurements of the dissociation constants of these indicators have been made in seawater. Our value of 7.492 for the pK_a' of phenol red at 25 °C is the same as the pK_a' determined by Robert-Baldo et al. (1985). Robert-Baldo et al.'s value for the pK_a' of phenol red was determined using potentiometric pH measurements to establish the pH_{ind} of the phenol red test solutions. Their electrode was calibrated on the free hydrogen ion scale using Tris-seawater buffers (Rammett et al., 1977). We measured the pH_{ind} of a 0.023 m Tris-seawater buffer which was prepared 71% TrisHCl and 29% Tris. The difference between pH_{ind} and the pH of the buffer derived from the work of Rammett et al. was -0.006 ± 0.004 . The agreement is well within the combined uncertainties of the buffer pH and pH_{ind} .

Comparison Between Potentiometric and Colorimetric pH Measurements

Simultaneous measurements of solution pH using indicators, pH_{ind} , and EMF using electrodes were made on seven ASW(2) buffer solutions at 25 °C in order to evaluate the agreement between colorimetric and potentiometric methods of measuring pH over a large pH range. The linearity of the electrode response relative to the pH_{ind} was tested by regressing the EMF, E, of the test solutions against pH_{ind} . The

slope of the line was 59.07 ± 0.07 mv per decade which is within 0.1 % of the theoretical Nernst slope. Figure 3 is a plot of the deviation of the pH_{ind} about the regression line as a function of pH_{ind} . The average deviation of less than 0.004 pH units is quite good considering the deviation in pH due to uncertainties in EMF measurements alone is 0.002 pH units.

Four ASW(1) solutions of known pH were used to establish the E^* of the electrode on the free hydrogen ion scale. The pH_F of the test solutions were determined from EMF measurements according to equation 12:

$$pH_F = \frac{E - E^*}{k} \quad (12)$$

where k is the electrode slope. Figure 4 is a plot of the deviation between pH_{ind} and pH_F as a function of pH_{ind} . This type of comparison is very sensitive to the slope chosen to describe the electrode response. The hatched envelope surrounding the symbols represents the effect that a 0.5 % variation in the electrode slope has on the calculated deviation. Considering the uncertainties associated with the electrode slope and measurement errors, there does not appear to be a significant difference between pH_{ind} and pH_F .

Application of pH Indicators to Measurement in Seawater

Use of the indicators to measure the pH of seawater is a three step

Figure 3. Deviation of the pH_{ind} about the $\text{pH}_{\text{ind}}-\text{pH}_{\text{EMF}}$ regression line as a function of pH_{ind} . The labels indicate the indicator used to determine the pH_{ind} : T=thymol blue, B=bromophenol blue, G=bromocresol green, P=bromocresol purple, R=phenol red.

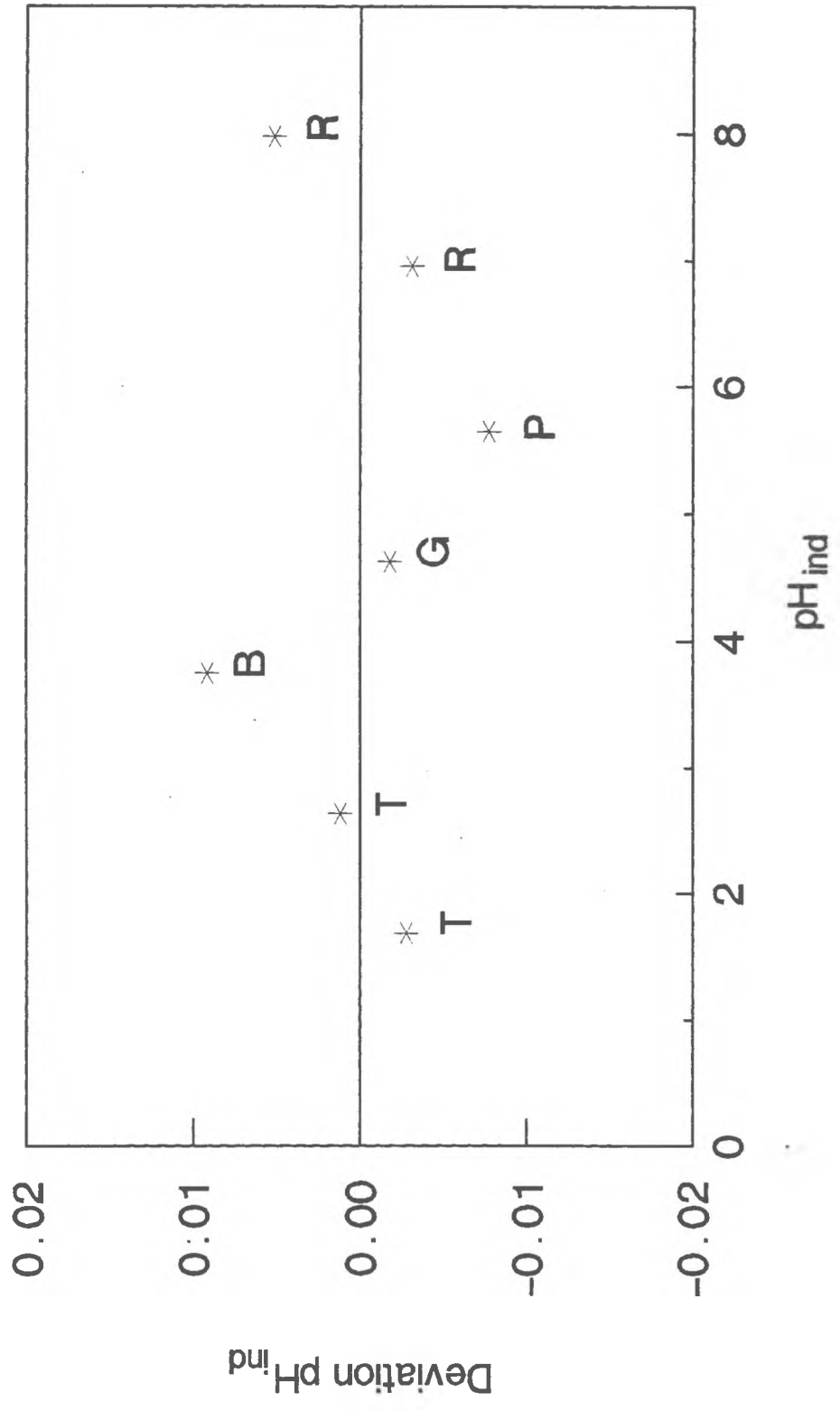
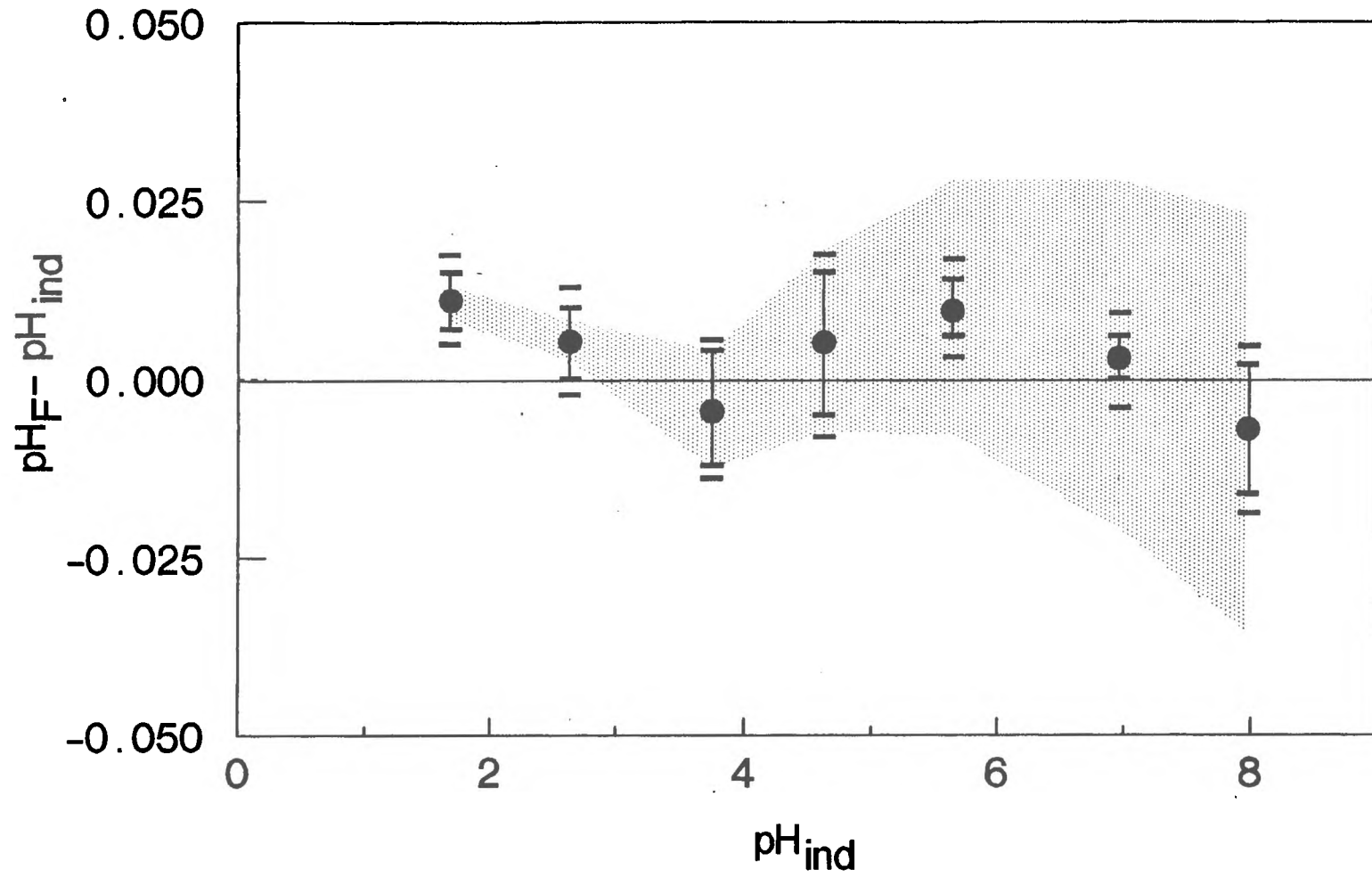


Figure 4. Deviation between pH_{ind} and pH_{F} as a function of pH_{ind} . The o symbol is the deviation assuming the electrode slope is Nernstian. Shaded area represents the range of the deviation if the electrode slope is non-Nernstian by $\pm 0.5\%$. Error bars are uncertainties due to measurement errors. Horizontal bars above the error bars represent the composite errors due to measurement errors and errors in pK_{a}' .

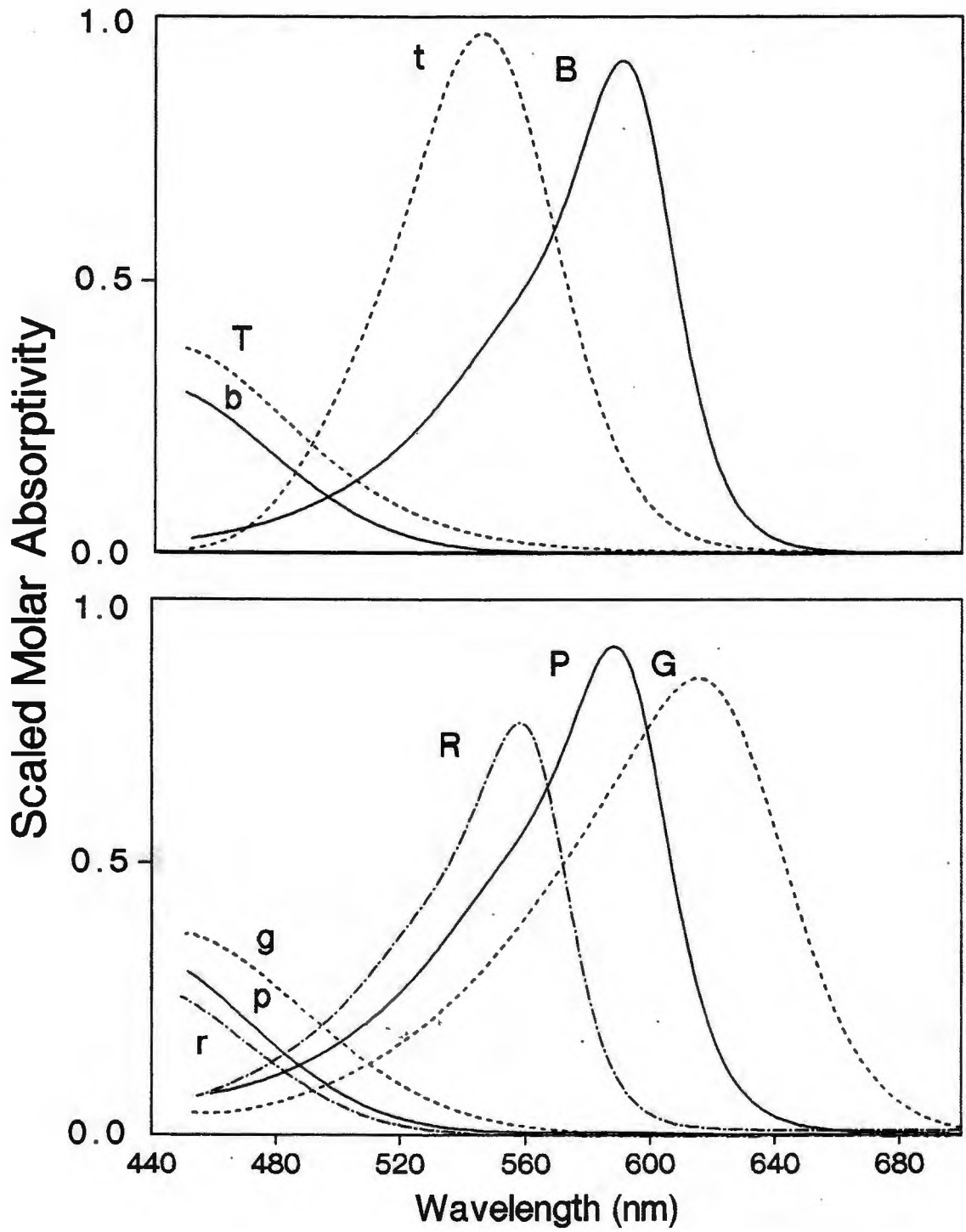


process. One, the wavelengths for A_1 and A_2 must be selected. Two, the constants E_{HA} , E_A , and E_2 must be determined for the wavelengths selected. Three, the measurement of A_1 and A_2 for each sample must be performed.

For the determination of the pK_a' of the indicators the wavelengths λ_1 and λ_2 were set at the wavelength of maximum indicator absorbance and the isosbestic point wavelength respectively. This choice maximizes the indicator signal and simplifies equation 10 by eliminating the $\log(E_2)$ term. These constraints are not necessary. The only criterion for the selection of λ_1 and λ_2 is that the resulting absorbance ratio A_1/A_2 change as a function of pH. The greater the change in A_1/A_2 with pH the greater the sensitivity of the pH determination. To maximize sensitivity, λ_1 should be near the indicators $\lambda_{\epsilon_{max}}$ and λ_2 should be at a wavelength where $\lambda_{\epsilon_{HA}}$ is greater than or equal to $\lambda_{\epsilon_{A^-}}$. Figure 5 is a plot of the scaled acid and basic molar absorptivities (λ_{ϵ_i}) of each indicator. These plots can be used as an aid for selection of λ_1 and λ_2 . The selection of λ_1 and λ_2 is not limited to individual wavelengths. A continuous wavelength range can be selected as long as the ratio of the integrated absorbances $A_1(int)$ and $A_2(int)$ continue to have a pH dependence. An example where a range of wavelengths might be used is an optical system which uses light emitting diodes (LED's) as the light source. Simple optical sensors of this type have been used by Johnson et al. (1986) and Betteridge et al. (1978) for nutrient and metal analysis. The wavelength range of the absorbance measurement could be the emission bandwidth of the LED.

Once λ_1 and λ_2 have been selected, the constants E_{HA} , E_A , and

Figure 5. Scaled acid and basic molar absorptivities of the indicators as a function of wavelength. The labels are defined in Figure 3. Lower and upper case labels indicate the acid and basic molar absorptivities respectively. The scaling factors for the indicators are: T=34200, B=79500, G=47500, P=58800, R=74700 ($\text{kg mol}^{-1} \text{cm}^{-1}$).



E_2 must be determined. Irrespective of whether λ_1 and λ_2 are individual wavelengths or integrated ranges, the constants E_{HA} and E_A are determined by taking the ratio of A_1 and A_2 in acid and basic seawater solutions respectively as described by equations 8 and 9. The constant E_2 is determined by measuring A_1/A_2 in a solution of known pH and solving equation 10 in terms of E_2 . The pH of a solution for E_2 determination can be measured by setting $\lambda_2 = \lambda_{iso}$ so that E_2 equals unity. Using this solution E_2 can be determined at any other λ_2 . Even in this situation the primary basis for the pH_{ind} scale is the gravimetrically determined HCl solutions used to establish pK_1' of thymol blue.

The pH determination of an unknown sample is then performed by measuring A_1/A_2 of the sample and calculating pH according to equation 10. The total indicator concentration does not need to be known but should be less than 5×10^{-5} in order to prevent changes in the sample pH due to added indicator. High indicator concentration should also be avoided to prevent dimerization of the indicator molecule (Kendrich and Gilkerson, 1987).

Application of Multiple pH Indicators.

A limitation of pH_{ind} is that a single indicator can only be used over a range within about ± 1.5 pH units of the pK_a' . The limited range of single indicator pH determinations can be significantly expanded if two or more indicators are added simultaneously to the sample. The addition of phenol red and bromocresol green to a seawater sample allows determination of pH_{ind} over the range 3.0-8.2.

Equation 13 can be used to calculate the pH_{ind} of a seawater solution with added phenol red and bromocresol green as a function of A_1/A_2 (Appendix IV).

$$\begin{aligned} & \alpha_G E_{2G} (A_1/A_2 - E_G) + \beta_G (A_1/A_2 - E_{HG}) \\ & = -\psi [\beta_R E_{2R} (A_1/A_2 - E_R) + \alpha_R (A_1/A_2 - E_{HR})] \quad (13) \end{aligned}$$

The same optical constants, E_A , E_{HA} , and E_2 , are used except the constants are labeled to be indicator specific: R for phenol red and G for bromocresol green. One additional constant, ψ , is the ratio of the absorbance of phenol red and bromocresol green at λ_2 when both indicators are completely in the acid form as described by equation 14.

$$\psi = A_2(\text{red})/A_2(\text{green}) = (TR)_2 \epsilon_{HR} / (TG)_2 \epsilon_{HG} \quad (14)$$

(TR) and (TG) are the total concentrations of phenol red and bromocresol green respectively. The pH dependence of equation 13 is incorporated in the β and α terms. The ratio of the base to total phenol red is β_R and the ratio of acid to the total phenol red is α_R . The same ratios are defined for bromocresol green, β_G and α_G . These ratios can be calculated for a general indicator according to equations 15 and 16.

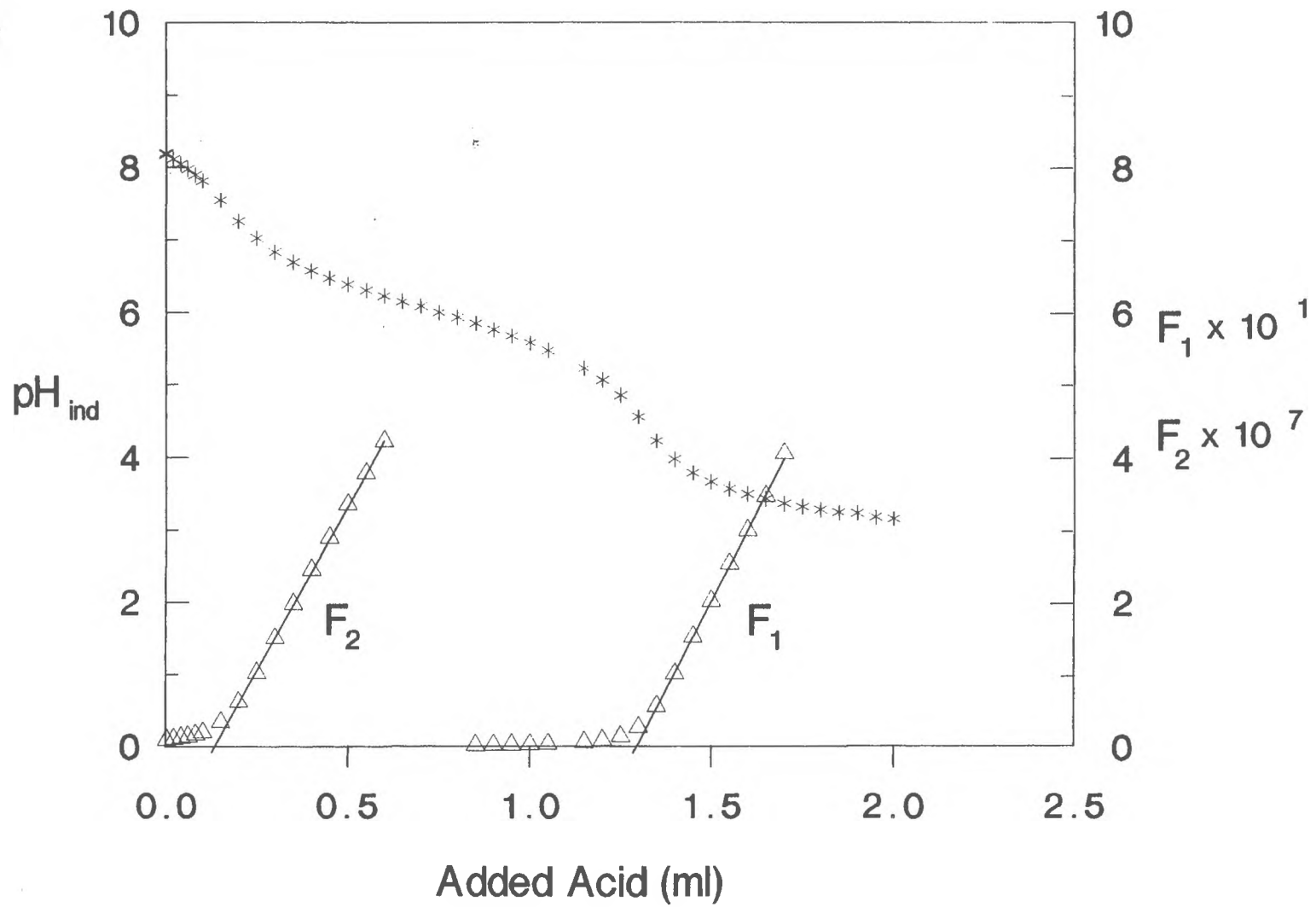
$$\beta_A = \frac{(A)}{(HA) + (A)} = \frac{K_A'}{K_A' + [H^+]} \quad (15)$$

$$\alpha_A = \frac{(HA)}{(HA) + (A)} = \frac{[H^+]}{K_A' + [H^+]} \quad (16)$$

If the optical constants are known and A_1/A_2 is measured the pH_{ind} can be determined by solving equation 13 for $[H^+]$. The optical constants E_{HR} , E_R , E_{2R} , E_{HG} , E_G , and E_{2G} are determined from single indicator additions as described in the previous section. The constant ψ is determined in a manner similar to the determination of E_2 in single indicator applications. Both indicators are added to a solution of known pH and equation 13 is solved for ψ . It is convenient to prepare a stock solution which contains both phenol red and bromocresol green because ψ need only be determined once for a given stock solution.

Measurements of pH using phenol red and bromocresol green were compared with measurements made with electrodes during an alkalinity titration of natural seawater. A sample of 35 ‰ Sargasso seawater was titrated in a closed system with HCl. Figure 6 is a plot of the titration curve. The agreement between indicator and electrode pH measurements was good with an average deviation of ± 0.018 over the pH range 3.0-8.2. The Gran functions F_1 and F_2 for the titration were calculated from the pH_{ind} measurements and the volume of added acid according to the method of Dyrssen and Sillen (1967). Ignoring the contributions of protolytic side reactions, the calculated total alkalinity and carbonate alkalinity were 2.31 and 2.07 mEq kg^{-1} respectively. These values are in good agreement with the total

Figure 6. Alkalinity titration of 35 ‰ seawater using both indicators and electrodes to monitor pH. The o symbol is the pH measured with an electrode. The solid line is the pH measured with the indicators phenol red and bromocresol green. Approximate indicator concentrations were 1.3×10^{-6} and 1.5×10^{-6} for phenol red and bromocresol green respectively.



alkalinity of 2.34 and carbonate alkalinity of 2.07 mEq kg⁻¹ for the same sample determined using pH measurements made with an electrode. The advantage of pH indicators over electrodes in this type of application is the speed at which the titration can be performed. The response time of the indicators is equal to the mixing time of the solution being titrated. A more detailed description of pH measurements using multiple indicators is presented by King and Kester (1988).

CONCLUSIONS

The apparent dissociation constants for five sulfonephthalein pH indicators have been determined in seawater at 25 °C. The pH indicators allow quantitative determination of seawater pH over the pH range of 1.5-8.5. The agreement between pH measured with indicators and potentiometric pH measurement is ± 0.005 which is within the combined uncertainties of the two methods. Multiple indicators can be combined to significantly expand the range over which pH measurements can be made. The combination of phenol red and bromocresol green can be used to monitor alkalinity titrations over the pH range 3.0-8.2. The pH indicators offer an alternative for measuring pH in seawater without the problems of electrode drift and liquid junction errors associated with potentiometric pH measurement. Most importantly, pH indicators offer an absolute pH scale on which to determine seawater pH.

References

- Bates, R. G. (1964) Determination of pH: Theory and Practice. Wiley and Sons, New York, 435 pp.
- Bates, R. G.; and Macaskill, J. B. (1975) Acid-base measurements in seawater. In: Analytical Methods in Seawater. Advances in Chemistry Series, No. 147. Gibbs Jr., R. P., editor, American Chemical Society, Washington, D.C., 110-123.
- Betteridge, D.; Dagless, E. L.; Fields, B.; and Graves, N. F. (1978) A highly sensitive flow-through phototransducer for unsegmented continuous-flow analysis demonstrating high-speed spectroscopy at parts per 10^9 level and a new method of refractometric determinations. *The Analyst*, 103(1230), 897-908.
- Caceci, M. S.; and Cacheris, W. P. (1984) Fitting curves to data. *Byte*, 9(5), 340-362.
- Culberson, C. H. (1981) Direct potentiometry, In: Marine Electrochemistry. Whitfield, M.; and Jagner, D., editors, Wiley and Son, New York, 188-261.
- Dickson, A. G. (1984) pH scales and proton-transfer reactions in saline media such as seawater. *Geochimica et Cosmochimica Acta*, 48, 2299-2308.

- Hansson, I. (1973) A new set of pH-scales and standard buffers for sea water. *Deep-Sea Research*, 20, 479-491.
- Johnson, K. S.; Beehler, C. L.; and Sakamoto-Arnold, C. M. (1986) A submersible flow analysis system. *Analytica Chimica Acta*, 179, 245-257.
- Kendrick, K. L.; and Gilkerson, W. R. (1987) The state of aggregation of methyl orange in water. *Journal of Solution Chemistry*, 16(4), 257-267.
- Kester, D. R. (1986) Equilibrium models in seawater: applications and limitations. In: *The Importance of Chemical Speciation in Environmental Processes*. Bernhard, M.; Brinckman, F. E.; and Sadler, P. J., editors, Dahlem Konferenzen 1986, Springer-Verlag Berlin, 337-363.
- Kester, D. R.; Duedall, I. W.; Connors, D. N.; and Pytkowicz, R. M. (1967) Preparation of artificial seawater. *Limnology and Oceanography*, 12(1), 176-179.
- King, D. W.; and Kester, D. R. (1988) Spectral modeling of sulfonephthalein indicators: Application to pH measurements using multiple pH indicators. In preparation.

- Kolthoff, I. M.; and Rosenblum, C. (1937) Acid-Base Indicators.
MacMillan Co., New York, 413 pp.
- Millero, F. J. (1986) The pH of estuarine waters. *Limnology and Oceanography*, 31(4), 839-837.
- Perez, F. F.; and Fraga, F. (1987) The pH measurements in seawater on the NBS scale. *Marine Chemistry*, 21, 315-327.
- Pytkowicz, R. M.; Kester, D. R.; and Burgener, B. C. (1966)
Reproducibility of pH measurements in seawater. *Limnology and Oceanography*, 11(3), 417-419.
- Ramette, R. W.; Culberson, C. H.; and Bates, R. G. (1977) Acid-base properties of tris(hydroxymethyl)aminomethane (Tris) buffers in seawater from 5 to 40 °C. *Analytical Chemistry*, 49(6), 867-870.
- Robert-Baldo, G. L.; Morris, M. J.; and Byrne, R. H. (1985)
Spectroscopic determination of seawater pH using phenol red. *Analytical Chemistry*, 57, 2564-67.
- Whitfield, M.; Butler, R. A.; and Covington, A. K. (1985) The determination of pH in estuarine waters. I. Definition of pH scales and the selection of buffers. *Oceanologica Acta*, 8(4), 423-432.

The Effect of Pressure on the Dissociation
of Sulfonephthalein Indicators.

Abstract

The apparent partial molal volume change, $\Delta V'$, for the dissociation of five sulfonephthalein indicators (thymol blue, bromophenol blue, bromocresol green, bromocresol purple, and phenol red) has been determined in 35 ‰ seawater at 25 °C. A correlation was observed between $\Delta V'$ and pK' indicating the importance of electrostatic interactions in the varying dissociation equilibria of this family of indicators. A similar correlation was observed between indicator structure and pK' . The pK' as a function of indicator structure was described using the Hammett equation.

1. Introduction

Sulfonephthalein indicators provide a rapid and highly accurate method for measuring pH in seawater at atmospheric pressure (Robert-Baldo et al., 1985; and Byrne, 1987; King and Kester, 1988a). The application of pH indicators for high pressure pH measurements requires accurate values for the dissociation constants of the indicators as a function of pressure. The effect of pressure on the pK' s of the indicators can be calculated from the change in partial molal volume, $\Delta V'$, of the proton dissociation. Unfortunately, values for $\Delta V'$ of sulfonephthalein indicators have not been determined in mixed electrolyte solutions such as seawater. In addition to providing the necessary data for high pressure pH measurements, $\Delta V'$ data can be used to examine the relationship between indicator structure and pK' on the effect of pressure on proton dissociation. Hamann and Linton (1974) have found that ΔV and pK values for substituted phenols can be correlated using a simple electrostatic model. Relationships of this type could be quite useful for predicting the $\Delta V'$ of indicators in the absence of experimental data. We have determined the effect of pressure on the pK' of five sulfonephthalein indicators in seawater media over the pressure range from atmospheric to 1000 bars. Correlations between indicator structure, pK' , and $\Delta V'$ were examined using Hammett type equations.

Figure 1 is a diagram of the general structure of the indicators (thymol blue, bromophenol blue, bromocresol green, bromocresol purple, and phenol red) used in this study. Table 1 lists the functional groups for each indicator. The sulfonephthalein indicators undergo a

Figure 1. General structure of sulfonephthalein indicators. The functional groups of specific indicators are listed in Table 1.

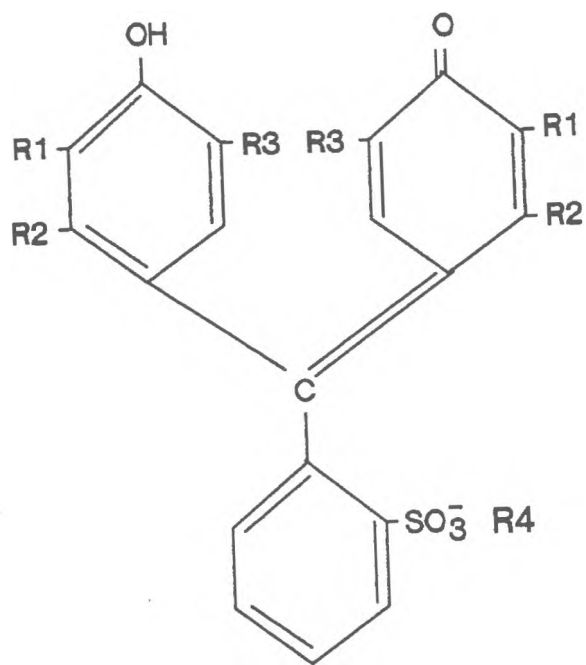


Table 1. Functional groups of the sulfonephthalein indicators; R1 to R4 are shown in Figure 1.

Indicator	Position			
	R1	R2	R3	R4
Thymol Blue	$(\text{CH}_3)_2\text{CH}$	H	H	H
Bromophenol Blue	Br	H	Br	-
Bromocresol Green	Br	CH_3	Br	-
Bromocresol Purple	Br	H	CH_3	-
Phenol Red	H	H	H	-

visible color change upon protonation or deprotonation of the indicator molecule. The pH of a solution with added indicator, pH_{ind} , can be determined if the ratio of the basic to acidic components of the indicator are measured optically and the apparent dissociation constant of the indicator, pK_a' , is known.

$$pH_{ind} = pK_a' + \log \frac{(A^-)}{(HA)} \quad (1)$$

In this work the pH is defined as the $-\log[H^+]$ where $[H^+]$ is hydrogen ion molality rather than using a hydrogen ion activity scale such as that of the National Bureau of Standards. The (A^-) and (HA) are the total concentrations of the basic and acidic forms of the indicator respectively. The K_a' is specific to a particular ionic medium (ionic strength and composition). Equation 2 defines pH_{ind} in terms of the optical absorbance of the indicator at two wavelengths as described by King and Kester (1988a).

$$pH_{ind} = pK_a' + \log \frac{(A_1/A_2 - E_{HA})}{(E_A - A_1/A_2)} - \log(E_2) \quad (2)$$

$$E_{HA} = \epsilon_1 \epsilon_{HA} / \epsilon_2 \epsilon_{HA} \quad (3)$$

$$E_A = \epsilon_1 \epsilon_A / \epsilon_2 \epsilon_A \quad (4)$$

$$E_2 = \epsilon_2 \epsilon_A / \epsilon_2 \epsilon_{HA} \quad (5)$$

A_1/A_2 is the ratio of the measured absorbances at wavelengths λ_1 and λ_2 . E_{HA} , E_A , and E_2 are optical constants which are a function of the molar absorptivities, $\lambda \epsilon_i$, of the acidic and basic components of the indicator at λ_1 and λ_2 . The wavelength of the isosbestic point of the indicator was chosen for λ_2 so that the constant E_2 equals unity. Under conditions of constant temperature and variable pressure the pH of a solution with added indicator can be determined if the pressure dependence of the optical constants and the pK_a' of the indicator are known. The pressure dependence on pK_a' is defined by equation 6 (Millero, 1983):

$$pK^P = pK^0 + \frac{\Delta V'}{2.303RT} P - \frac{0.5\Delta k'}{2.303RT} P^2 \quad (6)$$

where $\Delta V'$ and $\Delta k'$ are the apparent partial molal volume and compressibility change of the indicator respectively. P is the gauge pressure measured in bars. $\Delta V'$ and $\Delta k'$ are properties of the indicator that depend on the ionic strength and composition of the ionic medium in which they were defined. The pressure dependence on the optical constants is undetectable or small and can be described by the following linear equation:

$$E_i^P = E_i^0 + C_i P \quad (7)$$

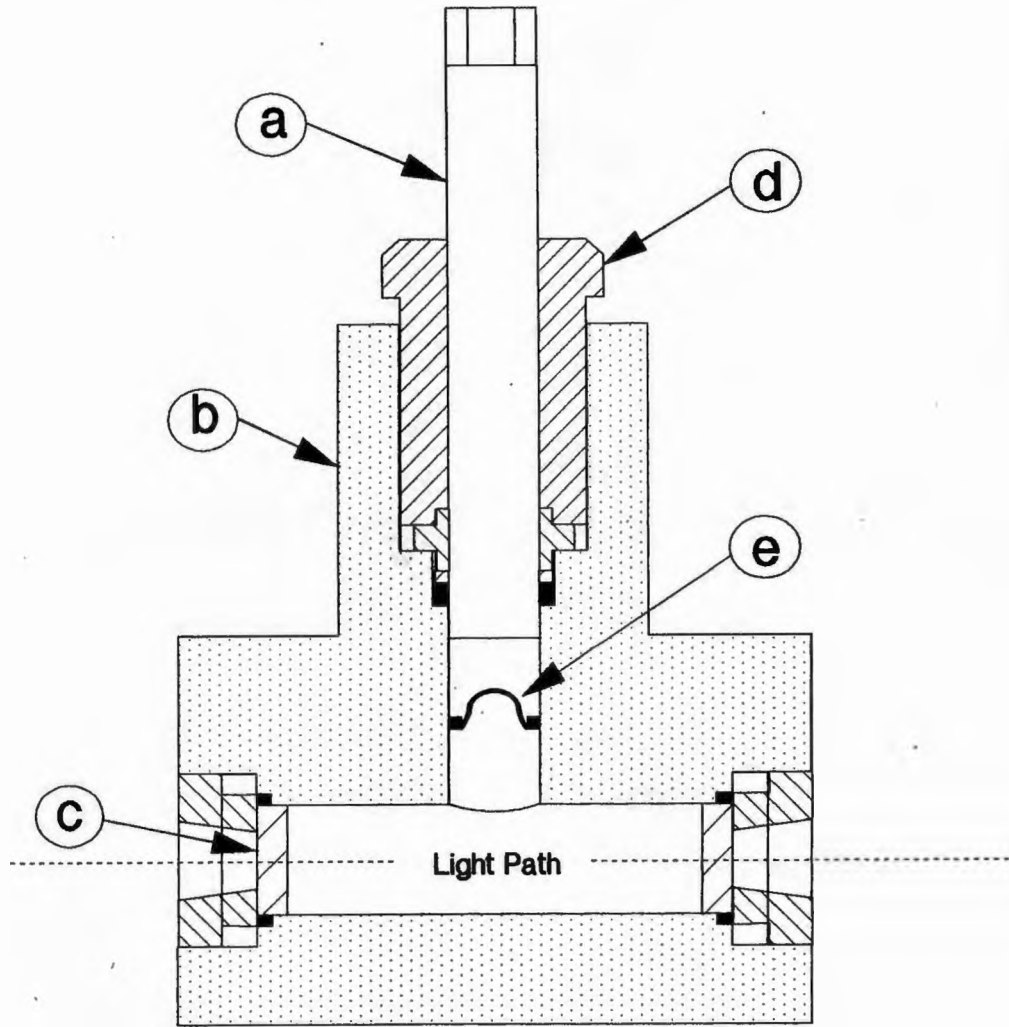
E_i^P is the optical constant at pressure P , E_i^0 is the optical constant at one atmosphere, and C_i is an empirical constant.

2. Experimental

All experiments were performed using artificial seawater solutions prepared from reagent grade salts and Milli-Q water as described by King and Kester (1988a). Concentrated indicator stock solutions (1×10^{-3} m) were prepared by adding sodium salts of the indicators to artificial seawater. Final indicator concentration was $1-2 \times 10^{-6}$ m. Two types of artificial seawater solutions were used; artificial seawater one, ASW(1), had all the weak acid salts including Na_2SO_4 , and NaF replaced with NaCl, and artificial seawater two, ASW(2), had all the carbonate and borate salts replaced with NaCl but sulfate and fluoride were present. ASW(1) solutions of known pH (pH range 1-3 on the free hydrogen ion concentration scale) were prepared by quantitative addition of HCl. Assuming HCl is completely dissociated in seawater solutions over the pressure range 0-1000 bars, the pH of the ASW(1) solutions on the free hydrogen ion scale will equal $-\log([\text{HCl}])$ and is independent of pressure. ASW(2) solutions of constant pH^0 were buffered using phthalate or maleate buffers.

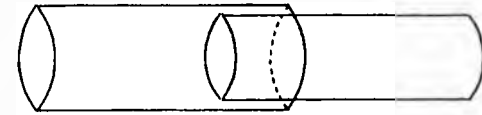
Spectra were measured using a Shimadzu UV-260 spectrophotometer. Spectral data were collected digitally over the wavelength range 750-450 nm and were transferred to a microcomputer for analysis. Spectra at high pressure were obtained using a custom designed high pressure optical cell manufactured by Harwood Engineering Co., Walpole, MA. Figure 2 is a sketch of the optical cell. Pressure was generated hydraulically inside the steel pressure chamber by compression of water using the piston. Removable high pressure optical windows are mounted

Figure 2. Diagram of the high pressure optical cell and internal cell.

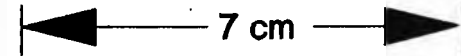


Labels

- a piston
- b cell body
- c high pressure windows
- d piston retaining screw
- e diaphragm



Internal Cell



at each end of the 7 cm sample chamber. The windows are constructed of single crystal sapphire and are transparent over a wavelength range of 900-220 nm (Epifinish Hemex windows, Crystal Systems Inc., Salem, MA). The sample was contained in an internal 1e Noble type telescoping quartz cell. The internal cell will expand and contract along its major axis to maintain hydrostatic equilibrium between the sample and the surrounding void fluid (1e Noble and Schlott, 1976). The decrease in pathlength of the internal cell compensates for 90 % of the increase in optical density of the sample with increasing pressure (Byrne, 1984). The void space surrounding the sample cell was filled with water. The entire inside surface of the high pressure cell was plated with nickel to reduce corrosion and contamination of the void fluid. A diaphragm in the neck of the cell prevents communication of the void fluid in the neck of the cell with the void fluid surrounding the sample cell. Changes in the optical absorbance of the cell due to void fluid contamination were not detectable over a time scale of 8 hours. The optical cell has a working pressure range of 0-1000 bars. Pressure was monitored to within 0.3% using an Entran Devices pressure transducer which was calibrated using a certified Heise bourdon tube gauge (Dresser Industries, Newtown, CT). The entire high pressure cell was thermostated to 25.0 ± 0.2 °C.

As described by King and Kester (1988a) E_{HA} and E_A at atmospheric pressure were determined from the absorbance ratio A_1/A_2 when the indicator is all in the acidic or basic form respectively. The effect of pressure on E_{HA} and E_A was determined by repeating the A_1/A_2 measurements as a function of pressure. The change in E_{HA} and E_H with pressure was fit to equation 7.

The indicator thymol blue was added to two different ASW(1) solutions and the absorbance ratio A_1/A_2 determined at five or more pressures over the range 0-1000 bars. The pH of the ASW(1) solutions are independent of pressure. The pK_1^P of thymol blue was determined by solving equation 2 in terms of pK_1^P as a function of the measured ratio A_1/A_2 at pressure P, the pH, and the constants E_A , E_{HA} . The values of pK_1^P as a function of pressure were fit to equation 6 to yield values of $\Delta V'$ and $\Delta k'$.

The indicator thymol blue was added to a buffered ASW(2) solution with an approximate pH^0 of 2.5 and the A_1/A_2 ratio was measured as a function of pressure. Using the pK^0 , $\Delta V'$, $\Delta k'$, E_A , and E_{HA} values for thymol blue, the pH^P of the solution was determined. The pH^P of the ASW(2) solution was fit to equation 8.

$$pH^P = pH^0 + \frac{A}{2.303RT}P - \frac{B}{2.303RT}P^2 \quad (8)$$

The constants A and B are empirical constants which are a function of the buffer, buffer concentration, and the pH^0 of the buffer solution. The indicator bromophenol blue was added to a separate aliquot of the same ASW(2) solution and the absorbance ratio A_1/A_2 for bromophenol blue measured as a function of pressure. The pH^P of the buffered ASW(2) solution was calculated using equation 8. The pK^P of bromophenol blue was determined by solving equation 2 for pK_2^P in terms of the measured A_1/A_2 ratio, pH^P , and the constants E_A and E_{HA} . As with thymol blue, the values of pK_2^P were fit to equation

6 to yield values of $\Delta V'$ and $\Delta k'$ for bromophenol blue.

Bromophenol Blue was used to determine the effect of pressure on the pH of a buffered ASW(2) solution with an initial $\text{pH}^0 = 3.7$. This solution was used to determine the effect of pressure on the pK_2 of bromocresol green. The above process was repeated two more times for bromocresol purple at $\text{pH}^0 = 5.4$ and phenol red at $\text{pH}^0 = 6.7$.

3. Results

Table 2 lists the isosbestic point wavelength ($\lambda_2 = \lambda_{\text{iso}}$), the wavelength of maximum absorbance (λ_1), and the values for E_A and E_{HA} at 25 °C and one atmosphere pressure for each indicator (King and Kester, 1988a). Over the pressure range 0-1000 bar the optical constants for thymol blue, bromophenol blue, bromocresol green, and bromocresol purple are independent of pressure. The constant E_A for phenol red decreases by 2.7 % from 0 to 1000 bars. The changes in E_{HA} and λ_{iso} for phenol red are not detectable. The value of E_A^{P} for phenol red can be calculated using equation 7 and the constants E_A^0 and C_i listed in Table 2.

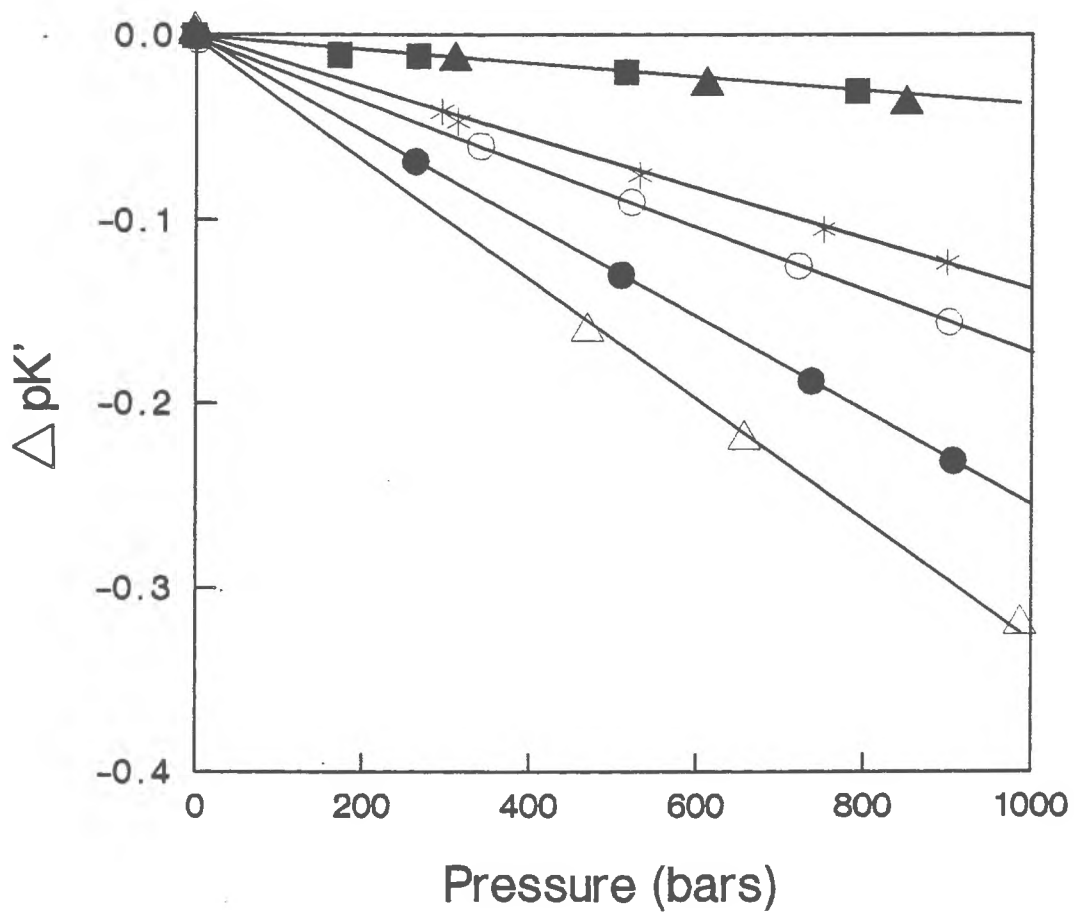
Figure 3 is the plot of the $\Delta \text{pK}'$ of the indicators as a function of pressure. The solid lines through the data are the fits to the data using equation 6. Table 3 gives the parameters A and B for the ASW buffers and $\Delta V'$ for the indicators. Replicate analyses were performed for the indicator thymol blue. The reported $\Delta V'$ value and associated error for thymol blue was calculated from the pooled data from both determinations. For all the indicators the $\Delta k'$ was insignificant.

The errors for $\Delta V'$ and A associated with fitting the observed data

Table 2. Values of λ_{iso} , λ_1 , E_{HA} , E_A , and C_A for indicators in 35 ‰ seawater at 25 °C and 0-1000 bars.

Indicator	λ_{iso}	λ_1	E_{HA}	E_A	$-C_A(10^4)$
Thymol Blue	487.9	540.0	4.643	0.173	0.0
Bromophenol Blue	495.7	590.0	0.015	8.846	0.0
Bromocresol Green	509.6	615.0	0.000	6.415	0.0
Bromocresol Purple	488.2	588.0	0.000	6.926	0.0
Phenol Red	479.7	558.0	0.010	5.773	2.729

Figure 3. Change in the pK_a' of the indicators as a function of pressure. The figure labels are: (■) and (▲) thymol blue, (*) bromophenol blue, (o) bromocresol green, (●) bromocresol purple, and (Δ) phenol red.



to equations 6 and 8 respectively are listed in Table 3 under individual error. The cumulative error is the individual error of an indicator or buffer plus the combined errors of the other indicators and buffers used in its determination. The cumulative error increases as more indicators and buffers are used to determine the effect of pressure on a particular solution. However, as can be seen in the last column of Table 3, the cumulative error for phenol red only results in an uncertainty of 0.010 in the calculated pH at 1000 bars pressure.

The indicators do not exhibit significant compressibility changes over the pressure range 0-1000 bars and therefore compressibility effects do not need to be considered for pH measurements in the oceanic pressure range. However, care should be taken in extrapolating our data to higher pressures. Compressibility effects may become significant at pressures greater than 1000 bars.

One previous measurement has been made on the effect of pressure on the dissociation of sulfonephthalein indicators. Grant (1973) determined the partial molal volume change for the dissociation of bromophenol blue ($-12.8 \text{ cm}^3\text{m}^{-1}$), bromocresol green ($-16.8 \text{ cm}^3\text{m}^{-1}$) and phenol red ($-11.6 \text{ cm}^3\text{m}^{-1}$) in 0.2 M NaNO_3 . The agreement between these values and our results is poor. A systematic difference between our apparent values ($\Delta V'$) determined in seawater and Grant's thermodynamic values (ΔV) determined in NaNO_3 is expected due to the change in the activity coefficients of the hydrogen ion and the indicator molecule with pressure. However, the differences in the two data sets do not reflect a systematic offset. Grant used a similar optical method to determine the ΔV of the indicators, but his absorbance measurements were made at only one wavelength in a fixed

Table 3. ΔV values for the indicators and A and B constants from equation 8 for the buffers in 35 ‰ seawater at 25 °C.

Solution (Indicator) ^{a,b}	pH ⁰ (pK ⁰)	-A ($-\Delta V'$)	$-10^3 B$ ($-10^3 \Delta k'$)	Individual error ^c	Cumulative error ^d	Error pH 1000 bars ^e
ASW(1):HCl	1.582					
ASW(1):HCl (thymol Blue) ^f	1.863 (1.439)	(2.26)		0.105	0.105	0.002
ASW(2):1 (bromophenol Blue)	2.470 (3.695)	6.70 (7.87)	2.00	0.005 0.122	0.105 0.161	0.002 0.003
ASW(2):2 (bromocresol green)	3.844 (4.410)	12.26 (9.73)		0.204 0.049	0.260 0.265	0.005 0.005
ASW(2):3 (bromocresol purple)	5.371 (5.972)	17.1 (14.49)		0.212 0.006	0.339 0.339	0.006 0.006
ASW(2):4 (phenol red)	6.696 (7.492)	27.38 (18.62)	2.56	0.002 0.453	0.339 0.590	0.006 0.010

- a) The ASW(1) or ASW(2) buffer solutions used in determining the pK_a' of the indicators are paired with their corresponding indicator.
- b) ASW(2):1 - ASW(2):3 are 0.01 m phthalate buffers. ASW(2):4 is a 0.01 maleate buffer.
- c) Individual error is the standard deviation of the regression line used to fit the data to equation 6 or 8.
- d) Cumulative error is the combined error calculated from the propagation of individual errors in $\Delta V'$ and A.
- e) Error in calculated pH^P at 1000 bars due to the cumulative errors in $\Delta V'$ and A.
- f) Equilibrium data for pK_1' for thymol blue, pK_2' for the other indicators.

pathlength cell. The poor agreement between the data sets is probably due to Grant's failure to correct for the change in optical density of the indicators with compression. In essence, Grant's ΔV values are apparent constants which are a function of the change in $\lambda\epsilon$ with pressure.

The effect of pressure on the second dissociation of maleate can be calculated from the change in the pH of the maleate buffer with pressure. The maleate buffer had a pH^0 of 6.7. At this pH the the first dissociation of maleic acid can be considered complete so that the change in pH of the buffer solution can be attributed solely to the effect of pressure on pK_2 . Under these conditions the calculated constants A and B for the buffer will equal the $\Delta V'$ and $\Delta k'$ of the buffer respectively. The calculated $\Delta V'$ value for maleate in seawater (-27.4 ± 0.3) is lower than the value of ΔV at infinite dilution (-24.4 ± 0.4) determined by Kitamura and Itoh (1987). Direct comparison of our values with the previous work at low ionic strength is difficult. The effect of pressure on the activity coefficients of maleate in seawater is a function of the change in the free activity coefficients and the ion-pairing of the buffer with pressure. Data are not available to make good estimates of the effect of pressure on the ion-pairing of maleate in seawater.

4. Discussion

As shown in Figure 1, the second dissociation of the indicators occurs at the phenolic acid group. The thymol blue indicator will not

be included in the following discussion since the first dissociation constant was determined for thymol blue.

For many organic weak acids, the change in the free energy of acid dissociation with the addition of functional groups is additive. This property has been described according to the Hammett equation (Perrin et al., 1981):

$$pK_S = pK_U - \rho(\Sigma\sigma) \quad (9)$$

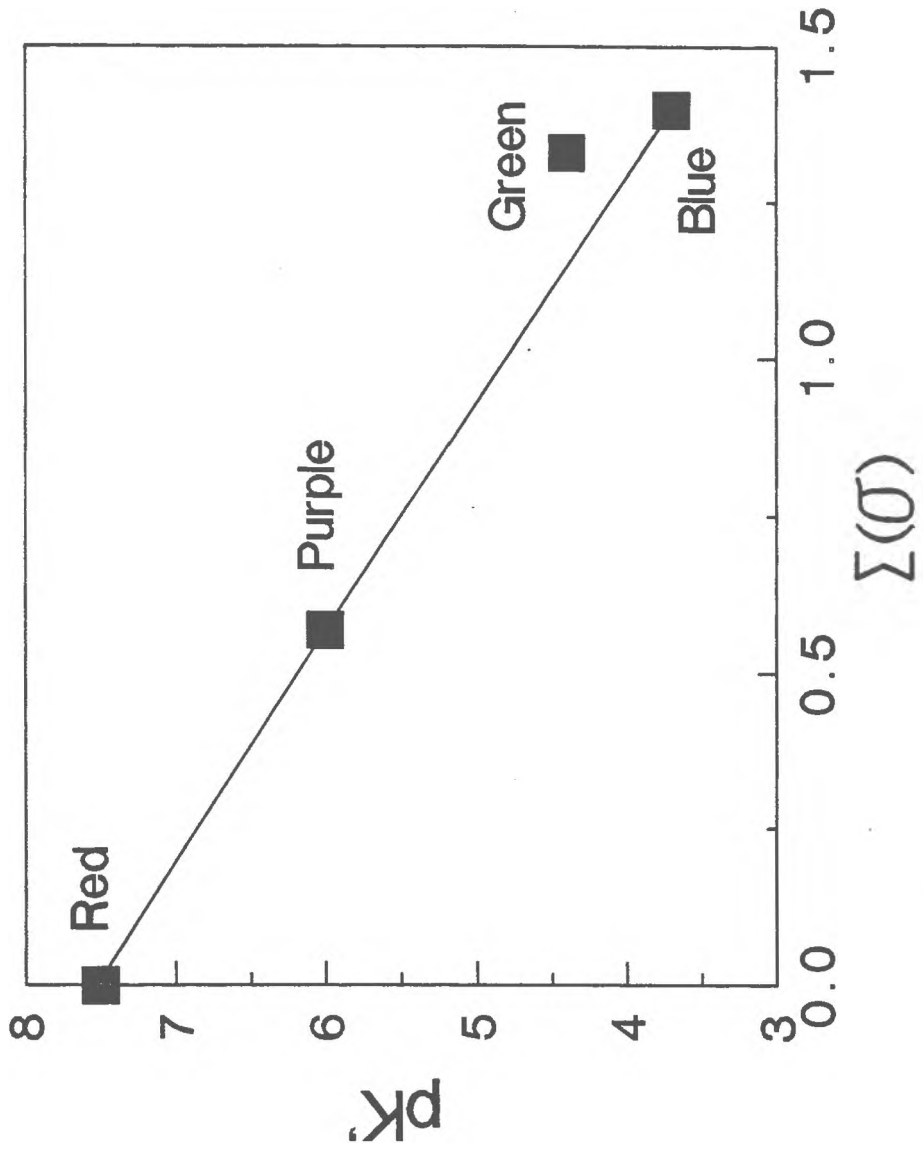
where pK_U and pK_S are the pK of the unsubstituted and substituted organic acids respectively, ρ is an empirical constant dependent only on the structure of the unsubstituted acid, and $\Sigma\sigma$ is the sum of the empirical functional group constants, σ . Values of σ for a large number of functional groups have been determined from the effect of functional group substitution on the pK of substituted phenols and other organic acids (Biggs and Robinson, 1961; Perrin et al., 1981). Within limits, the σ values determined using phenols could be applicable to other compounds with a similar phenolic structure such as the sulfonephthalein indicators. Table 4 lists the values of σ for Br and CH_3 , tabulated by Perrin et al. (1981). We used these values to calculate $\Sigma\sigma$ for the indicators. Figure 4 is a plot of the pK_2 of the indicators as a function of $\Sigma\sigma$. Phenol red was considered unsubstituted and therefore has a $\Sigma\sigma$ value of zero. The regression line in Figure 4 has a slope of 2.72 calculated using the data for phenol red, bromocresol purple, and bromophenol blue, thus providing the value of ρ for sulfonephthalein indicators. The pK'_a for bromocresol green is greater than expected for its $\Sigma\sigma$. This offset is

Table 4. Values of σ for selected functional groups based on phenolic compounds^a.

Functional Group	ortho	Position meta	para
CH ₃	-0.13	-0.07	-0.17
Br	0.70	0.39	0.27

a) from Perrin et al., 1981

Figure 4. pK' as a function of $\Sigma\sigma$ for each indicator.



consistent with steric hindrance of the Br by the CH₃ groups on bromocresol green. The Hammett equation will fail if steric hindrance of the functional groups occurs. Similar steric hindrance has been observed with 3,5-dimethyl-4-nitrophenol (Perrin et al., 1981).

The proximity of the functional groups to the acid center and the direction of the shift in the pK₂ of the indicators with substitution indicates that the interaction between the functional groups and the phenolic proton is electrostatic (Barlin and Perrin, 1972). Attempts to explain the linear free energy change of substituted organic acids from first principles have had variable success. The contributions of field and inductive effects on the overall polar effect are difficult to quantify (Barlin and Perrin, 1972). However, the theory by Kirkwood and Westheimer (1938) has been successful in describing the changes in pK of substituted carboxylic acids in terms of field effect models (Baker et al., 1967; Wilcox and Leung, 1968). According to the model, the change in the pK of an organic acid with substitution can be calculated using equation 10:

$$pK_S - pK_U = \frac{e}{2.3kT} \left[\left(\frac{\mu \cos \theta}{r^2 \epsilon} \right)_S - \left(\frac{\mu \cos \theta}{r^2 \epsilon} \right)_U \right] \quad (10)$$

where e is the electronic charge, k is the Boltzmann constant, T is the thermodynamic temperature, r is the distance between the midpoint of the dipole vector and the proton, μ is the dipole moment, θ is the angle between the dipole vector and the line joining the dipole moment and the reaction site, and ϵ is the effective dielectric constant. We

do not have sufficient data to apply this model to the indicator data, but the Kirkwood-Westheimer theory is useful to illustrate how ΔV and pK data of the indicators can be related in terms of electrostatic interactions.

Equation 11 is the general thermodynamic relationship relating the effect of pressure on the dissociation constant to the partial molal volume change of the acid dissociation.

$$\frac{\partial \log K}{\partial P} = \frac{-\Delta V}{2.303RT} \quad (11)$$

By differentiating equation 10 with respect to pressure and substituting for ΔV according to equation 11, equation 12 can be derived.

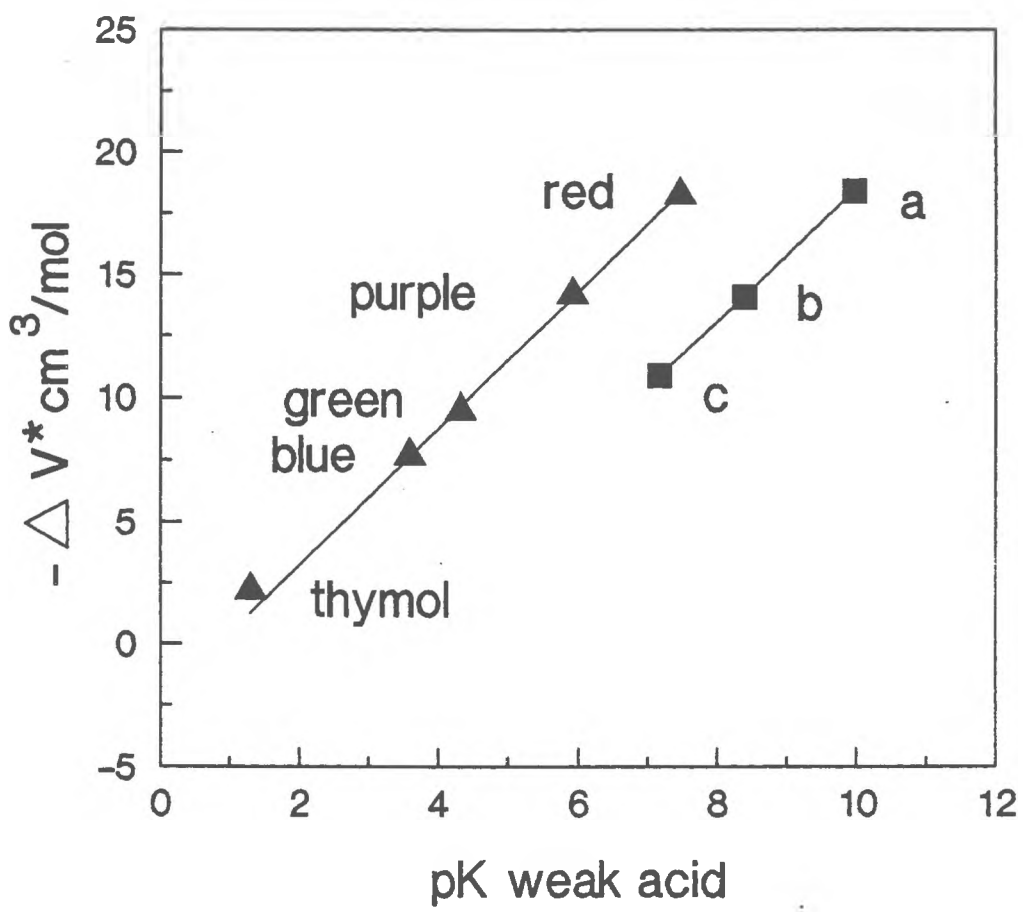
$$\Delta V_S - \Delta V_U = -RT(pK_S - pK_U) \left(\frac{\partial \ln \epsilon}{\partial P} \right) \quad (12)$$

As can be seen from equation 12, the expected change in ΔV for the indicators will be a function of the change in the pK of the indicators at one atmosphere pressure and the change in the $\ln \epsilon$ with pressure. Equation 12 is similar to the equation derived by Hamann and Linton (1974) for substituted phenols using a slightly different form of equation 10. In general, the form of equation 10 will not be important as long as the change in the pK of the organic acid with substitution

can be described in terms of electrostatics and the effective dielectric constant is the only pressure dependent term.

Figure 5 is a plot of $-\Delta V$ as a function of pK for the indicators. The data of Hamann and Linton (1974) for substituted phenols are included for comparison. As predicted from equation 12, a linear relationship is observed between the $\Delta V'$ and pK' of the indicators. The regression line through the indicator data has a slope of 2.87 which can be compared with a slope of 2.69 determined for the phenols. A theoretical slope in the range of the 2.69-2.64 can be calculated using values for $\partial \ln \epsilon / \partial P = 4.71-4.62 \times 10^{-5} \text{ bar}^{-1}$ measured by Owen et al. (1961) and Dunn and Stokes (1969) for pure water at 25 °C and one atmosphere pressure. The assumption is made that the change in the effective dielectric constant with pressure will equal that of pure water. The change in the dielectric constant of seawater with pressure has not been measured. However, it is expected that $\partial \ln \epsilon / \partial P$ for seawater will be slightly higher than for pure water if the number of water molecules in the outer ionic hydration spheres decrease with pressure.

Figure 5. $\Delta V'$ for the indicators and ΔV for the substituted phenols as a function of the pK_a' . The labels for the substituted phenols are:
a) phenol, b) 3-NO₂ phenol, c) 4-NO₂ phenol.



5. Summary.

The partial molal volumes of five sulfonephthalein indicators have been determined in 35 ‰ seawater at 25°C. These data can be used to measure the pH of seawater solutions over the entire oceanic pressure range. A good correlation between indicator structure and pK_2 exists for the indicators bromophenol blue, bromocresol purple, and phenol red. The change in the pK_2 with substitution for these indicators varies in accordance with the Hammett equation. The $\Delta V'$ for the indicators changes linearly with pK_2 which is consistent with electrostatic models for proton dissociation.

References

- Baker, F. W.; Parish, R. C.; and Stock, L. M. (1967) Dissociation constants of bicyclo[2.2.2]oct-2-ene-1-carboxylic acids, dibenzobicyclo[2.2.2]octa-2,5-diene-1-carboxylic acids, and cubanecarboxylic acids. *Journal of the American Chemical Society*, 89, 5677-5685.
- Barlin, G. B.; and Perrin, D. D. (1972) Dissociation constants in the elucidation of structure. In: *Elucidation of Organic Structures by Physical and Chemical Methods Part I, 2nd Edition.*, Bentley, K. W.; and Kirby, G. W., editors, Wiley-Interscience, New York, 611-676.
- Biggs, A. I.; and Robinson, R. A. (1961) The ionization constants of some substituted anilines and phenols: a test of the Hammett relation. *Journal of the Chemical Society*, 388-393.
- Byrne, R. H. (1984) Absorbance corrections in self-adjusting, variable path-length-diameter, high-pressure cells. *Review of Scientific Instruments*, 55(1), 131-132.
- Byrne, R. H. (1987) Standardization of standard buffers by visible spectrometry. *Analytical Chemistry*, 59(10), 1479-1481.

- Dunn, L. A.; and Stokes, R. H. (1969) Pressure and temperature dependence of the electrical permittivities of formamide and water. Transactions of the Faraday Society, 65, 2906-2912.
- Grant, M. W. (1973) Kinetics and thermodynamics of the formation of the monoglycinate complexes of cobalt(II), nickel(II), copper(II), and zinc(II) in water, at pressures from 1 bar to 3 kbar. Journal of the Chemical Society, Faraday Transactions 1., 69, 560-569.
- Hamann, S. D.; and Linton, M. (1974) Influence of pressure on the ionization of substituted phenols. Journal of the Chemical Society Faraday Transactions 1, 70, 2239-2249.
- King, D. W.; and Kester, D. R. (1988) Determination of seawater pH from 1.5 to 8.5 using colorimetric indicators. Marine Chemistry, accepted.
- Kirkwood, J. G.; and Westheimer, F. H. (1938) Electrostatic influence of substituents on the dissociation constants of organic acids. Journal of Chemical Physics, 6, 506.
- Kitamura, Y.; and Itoh, T. (1987) Reaction volume of protonic ionization for buffering agents. Prediction of pressure dependence of pH and pOH. Journal of Solution Chemistry, 16(9), 715-725.

- le Noble, W. J.; and Schlott, R. (1976) All quartz optical cell of constant diameter for use in high pressure studies. Review of Scientific Instruments, 47, 770.
- Millero, F. J. (1983) Influence of pressure on chemical processes in the sea. Chemical Oceanography. vol. 8., Riley, J. P.; and Chester, R. editors, Academic Press, London, 2-88.
- Owen, B. B.; Miller, R. C.; Milner, C. E.; and Cogan, H. L. (1961) Dielectric constant of water as a function of temperature and pressure. Journal of Physical Chemistry, 65, 2065.
- Perrin, D. D.; Dempsey, B.; and Serjeant, E. P. (1981) pKa Prediction for Organic Acids and Bases, Chaptman and Hall, London, 146 pp.
- Robert-Baldo, G. L.; Morris, M. J.; and Byrne, R. H. (1985) Spectroscopic determination of seawater pH using phenol red. Analytical Chemistry, 57, 2564-2567.
- Wilcox, C. F.; and Leung, C. (1968) Transmission of substituent effects. Dominance of field effects. Journal of the American Chemical Society, 90, 336-341.

Spectral Modeling of Sulfonephthalein Indicators:
Application to pH Measurements Using Multiple Indicators.

Abstract

The visible spectra of five sulfonephthalein indicators (thymol blue, bromophenol blue, bromocresol green, bromocresol purple, and phenol red) were deconvoluted into four Gaussian components. The spectra of the basic form of indicator was described by three components and the acidic form by one peak. The combination of the spectral model, pH and pK data allowed quantitative prediction of indicator spectra as a function of pH. A general equation was derived for the calculation of pH from two absorbance measurements of a solution which contains one or more indicators. The application of multiple indicators significantly expands the pH range over which pH measurements can be made. Using the modeled spectra for several indicators, optimal indicator combinations and measurement wavelengths for specific pH ranges were determined. The combination of phenol red and bromocresol green allowed determination of seawater pH over the range 3.0-8.2 which is suitable for oceanic pH and alkalinity determinations.

Introduction:

In recent years there has been increasing application of colorimetric indicators for pH determination in well defined media such as seawater (Robert-Baldo et al., 1985; Byrne, 1987; King and Kester, 1988a; King and Kester, 1988b). Indicators offer several advantages over potentiometric methods of pH measurement. Indicators have a rapid response time to pH changes, are immune to problems of electrode drift and liquid junction errors, and can be readily adapted for pH measurements at high pressure (King and Kester, 1988b). In seawater media, the accuracy of indicator pH measurements is equal to or greater than pH measurements made with electrodes (King and Kester, 1988a). Finally, the rapidly developing field of fiber optics is providing a wide variety of optical systems which can be employed to make optical pH measurements.

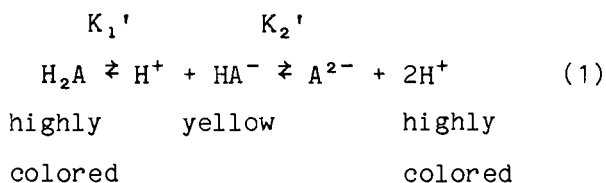
The pH measurements using a single indicator are restricted to a range within ± 1.5 pH units of the pK_a . If multiple indicators are used, this pH range can be significantly expanded. The development of multiple indicator systems for pH measurement, while conceptually straightforward, can be quite tedious experimentally. Many different combinations of indicator concentrations and measurement wavelengths must be explored to maximize the sensitivity of the pH measurement. Optimization becomes more complex for optical systems which do not use monochromatic light, such as systems using light emitting diodes as a light source. We developed a numerical model to describe the spectra of one or more indicators as a function of pH. The model can be used

to predict optimal indicator concentrations and measurement wavelengths for a particular pH range.

In this paper we present a general equation which can be used to calculate pH from absorbance measurements of a solution containing one or more indicators. A model has been developed which can describe the visible spectra of five sulfonephthalein indicators (thymol blue, bromophenol blue, bromocresol green, bromocresol purple, and phenol red) as a function of pH. The model has been used to select optimal measurement wavelengths and concentrations for a multiple indicator system containing phenol red and bromocresol green. These indicators were used to measure seawater pH over the range 3.0-8.2 during alkalinity titrations.

Theory

Sulfonephthalein indicators are diprotic acids whose dissociation is described by the equation 1.



For this class of indicators the first and second dissociation constants are separated by a factor of more than 10^6 . Therefore, over limited pH ranges the indicators can be treated as simple monoprotic acids. The first dissociation of thymol blue was used in this study.

The second dissociation was used for the other indicators.

The pH of a solution with a single added indicator can be determined using the equation (King and Kester, 1988a)

$$\text{pH} = \text{pK}_a' + \log \frac{(A_1/A_2 - E_{\text{HA}})}{(E_A - A_1/A_2)} - \log(E_2) \quad (2)$$

where pK_a' is the negative log of the apparent dissociation constant of the indicator in the solution being measured. Values for the pK'_a of the indicators in seawater are listed in Table I. This work is based on the free hydrogen ion pH scale: $\text{pH} = -\log[\text{H}^+]$, with brackets denoting hydrogen ion molality (Ramette et al., 1977 and Dickson, 1984). A_1 and A_2 are the absorbances of the indicator at wavelengths λ_1 and λ_2 respectively, and E_{HA} , E_A , and E_2 are optical constants. The optical constants are defined

$$E_{\text{HA}} = {}_1\varepsilon_{\text{HA}}/{}_2\varepsilon_{\text{HA}} \quad (3)$$

$$E_A = {}_1\varepsilon_A/{}_2\varepsilon_{\text{HA}} \quad (4)$$

$$E_2 = {}_2\varepsilon_A/{}_2\varepsilon_{\text{HA}} \quad (5)$$

where $\lambda\varepsilon_i$ is the molal absorptivity of i at wavelength λ . HA and A are the acidic and basic forms of the indicator respectively. E_{HA} and E_A can be determined from the absorbance ratio, A_1/A_2 , of the solution with added indicator when the indicator is either all in the acidic or basic form. E_2 can be determined by measuring A_1/A_2 in a solution of known pH and solving for E_2 (King and Kester, 1988a). The

Table I. Apparent dissociation constants of sulfonephthalein indicators in 35 ‰ salinity seawater at 25 °C.^a

Indicator	pK' _a
Thymol Blue	1.439
Bromophenol Blue	3.695
Bromocresol Green	4.410
Bromocresol Purple	5.972
Phenol Red	7.492

a) From King and Kester, 1988a.

advantage of the absorbance ratio technique is that pH determination is independent of indicator concentration.

The single indicator equations can be expanded to allow pH determination with two or more indicators. Using bromocresol green and phenol red as an example of a two indicator system; the pH can be determined by solving equation 6 for $[H^+]$ as a function of A_1 and A_2 (Appendix IV).

$$\begin{aligned} & \beta_G(E_{2G} A_1/A_2 - E_G E_{2G}) + \alpha_G(A_1/A_2 - E_{1G}) \\ & = -\psi[\beta_R(E_{2R} A_1/A_2 - E_R E_{2R}) + \alpha_R(A_1/A_2 - E_{1R})] \quad (6) \end{aligned}$$

The pH dependence is included in the β and α terms for each indicator which are defined

$$\beta_A = \frac{K_A'}{K_A' + [H^+]} \quad (7)$$

$$\alpha_A = \frac{[H^+]}{K_A' + [H^+]} \quad (8)$$

where K_A' is the apparent equilibrium constant (Pytkowicz, 1969 and Dickson, 1984). The terms E_{HG} , E_G , E_{2G} , and E_{HR} , E_R , E_{2R} are the indicator-specific optical constants for bromocresol green and phenol red respectively. ψ is the ratio of the absorbance of phenol red to bromocresol green at λ_2 when both indicators are completely in

the acid form as described by equation 9.

$$\psi = A_2(\text{red})/A_2(\text{green}) = (\text{TR})_2 \epsilon_{\text{HR}} / (\text{TG})_2 \epsilon_{\text{HG}} \quad (9)$$

TR and TG are the total concentrations of phenol red and bromocresol green respectively. Indicator stock solutions of known concentration are difficult to prepare. Therefore, ψ is most conveniently determined by solving equation 6 for ψ using a solution of known pH in a manner similar to the determination of E_2 for individual indicators. For two indicators the solution of equation 6 for $[\text{H}^+]$ reduces to a simple quadratic.

Equation 6 can be expanded to include more than two indicators. The general form of equation 6 is defined by equation 10. The first indicator is labeled as M and is defined as the master indicator. The second through n indicators will be labeled A, B, C,n etc.

$$\begin{aligned} & \beta_M(E_{2M}A_1/A_2 - E_M E_{2M}) + \alpha_M(A_1/A_2 - E_{HM}) \\ = & -\psi_A [\beta_A(E_{2A}A_1/A_2 - E_A E_{2A}) + \alpha_A(A_1/A_2 - E_{HA})] \\ & -\psi_B [\beta_B(E_{2B}A_1/A_2 - E_B E_{2B}) + \alpha_B(A_1/A_2 - E_{HB})] \\ & \dots -\psi_n [\beta_n(E_{2n}A_1/A_2 - E_n E_{2n}) + \alpha_n(A_1/A_2 - E_{Hn})] \quad (10) \end{aligned}$$

For each indicator the optical constants E_n , E_{Hn} , E_{2n} , and ψ_n must be determined. The constant ψ_n is the ratio of the absorbance (T_n) to (T_M) at λ_2 when both indicators are in the acid form. ψ_n is analogous to ψ defined in equation 9 if bromocresol green and phenol red were considered the master and n indicators respectively. For three or more indicators equation 10 is solved for $[\text{H}^+]$ using

numerical iteration.

Irrespective of the number of indicators employed, two basic rules should be followed to obtain the maximum precision in pH measurements. One, the absorbance values should fall in the absorbance range of the maximum photometric accuracy of the measuring system (usually 0.05-1.0 absorbance units). Two, the absorbance ratio, A_1/A_2 , must be changing as a function of pH over the pH range of interest. The greater $d(A_1/A_2)/dpH$ the more sensitive the pH measurement.

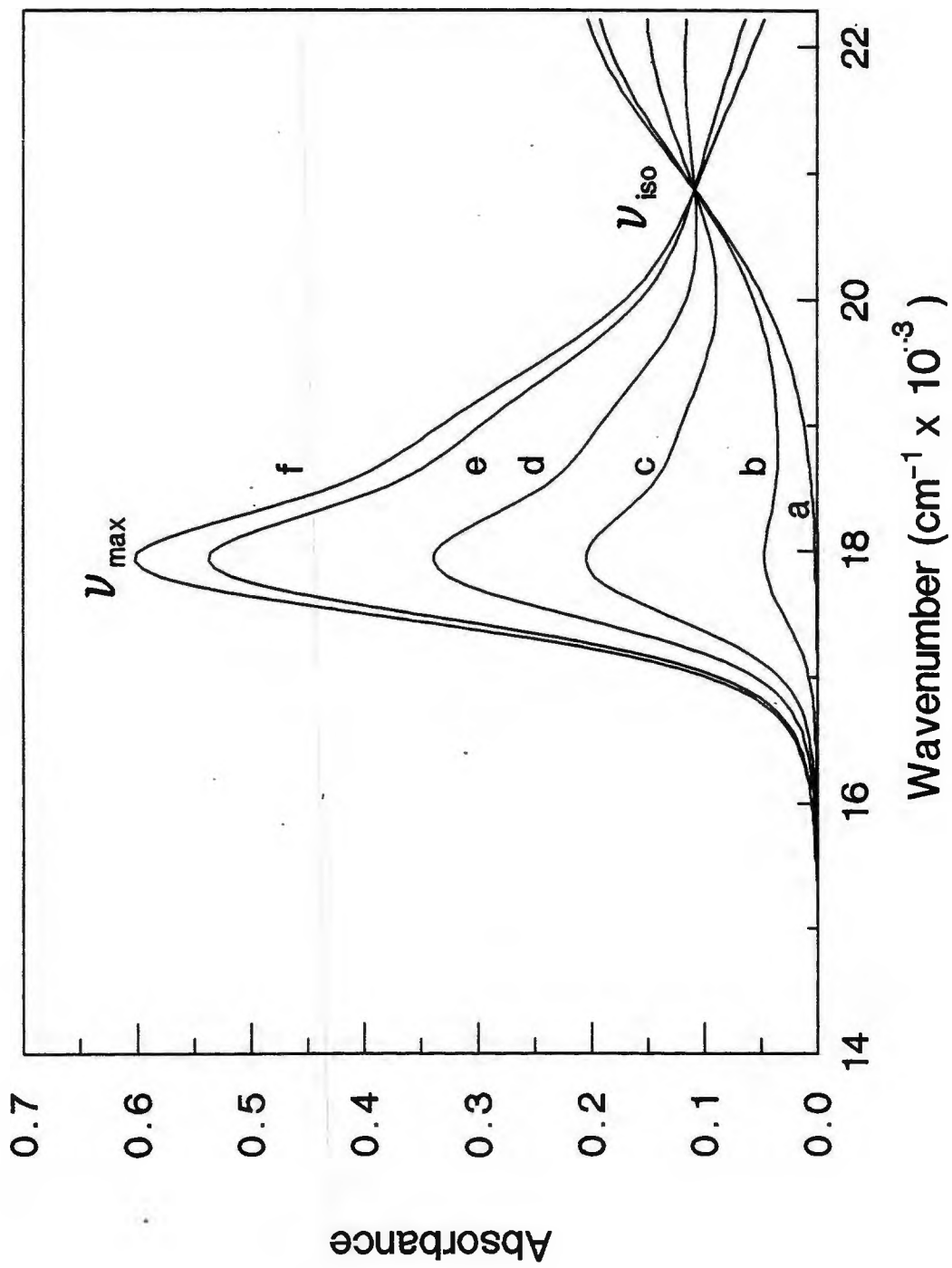
By judicious selection of indicators, indicator concentration, and measurement wavelength the above criteria can be met. To aid in the indicator and wavelength selection process we have developed a model to predict the absorbance spectra of solutions containing one or more sulfonephthalein indicators.

Figure 1 is a plot of absorbance as a function of wavenumber, ν , for the indicator phenol red at six different pH. The spectra are plotted as a function of wavenumber to be linear with energy which facilitates curve fitting. Wavenumber is equal to $(1 \times 10^7 \text{ nm cm}^{-1})/\lambda$. The absorbance of the indicator as a function of pH and wavenumber can be calculated according to equation 11

$$A_\nu = [TA]l\{\alpha(\nu\epsilon_{HA}) + \beta(\nu\epsilon_A)\} \quad (11)$$

where $[TA]$ is the total indicator concentration, l is the pathlength, and $\nu\epsilon_{HA}$ and $\nu\epsilon_A$ are the molal absorptivities at wavenumber ν of the acidic and basic forms of the indicator respectively. If $\nu\epsilon_{HA}$ and $\nu\epsilon_A$ are expressed as a function of ν using a simple model, then the spectrum of the solution can be predicted from pH,

Figure 1. Visible spectra of phenol red in 0.68 m NaCl at six pH. Spectra a and f are the acidic and basic chromophores of the indicator respectively. Spectra b-e are composite absorbances of the acidic and basic forms of the indicator in solutions at different pH. The pH of the solutions are: a=4.4; b=6.4; c=7.2; d=7.6; e=8.4; f=10.4.



pK_a' , [TA] and ν data.

The $\nu\epsilon$ of the acidic and basic chromophores of each indicator were fit using one or more Gaussian peaks. The Gaussian peak is defined by three parameters: the peak position, ν_{max} , the peak width at half height, $\Delta\nu_{1/2}$, and the maximum molar absorptivity, ϵ_{max} .

The Gaussian function for $\nu\epsilon$ is

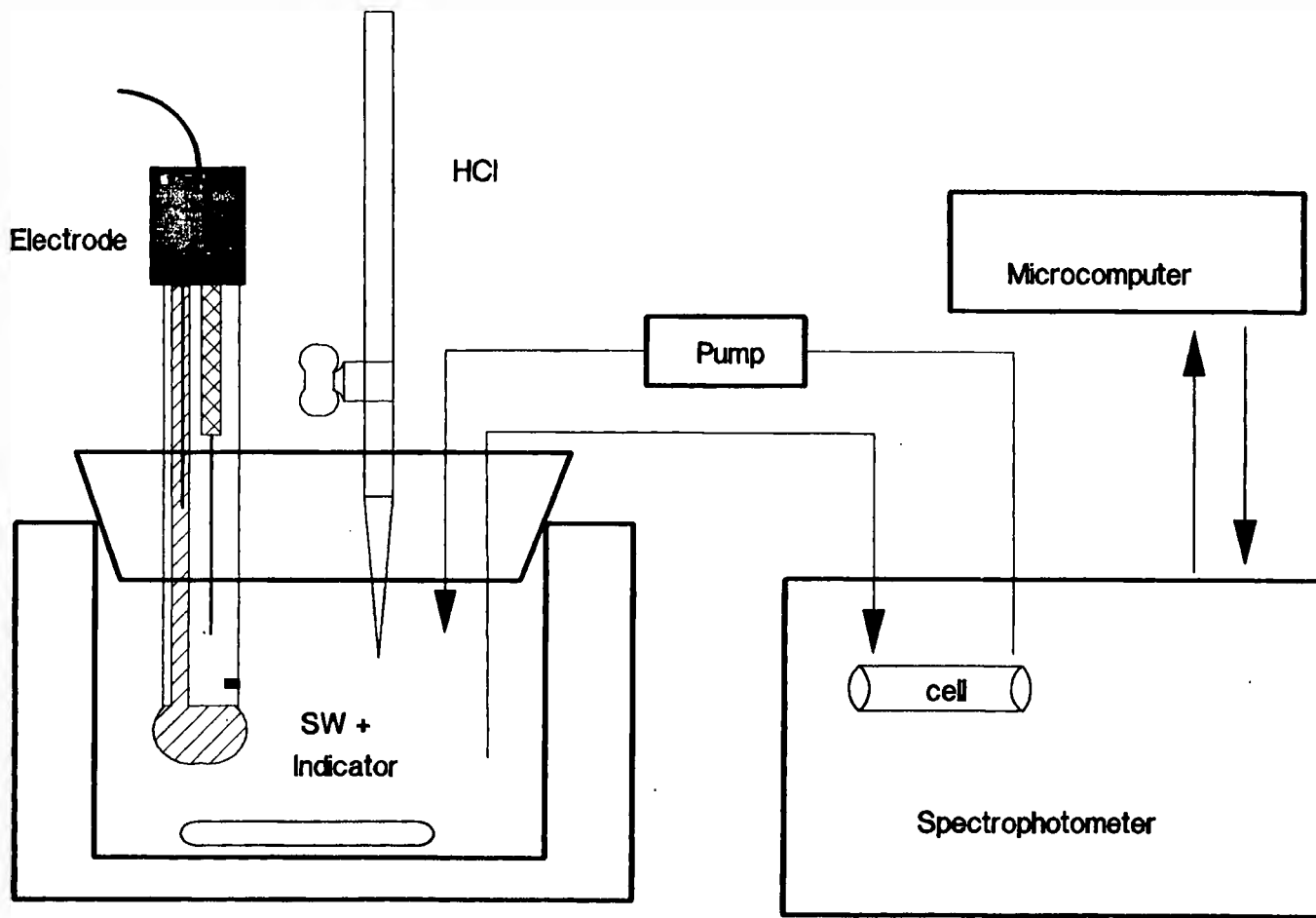
$$\nu\epsilon = \epsilon_{max} 2 \{ [2(\nu - \nu_{max}) / \Delta\nu_{1/2}]^2 \} \quad (12)$$

Gaussian components within a spectrum are additive (Brown and Kester, 1980). Therefore, the predicted $\nu\epsilon$ resulting from multiple Gaussian peaks will be the sum of $\nu\epsilon$ of each component peak. Except for thymol blue, the basic spectra of each indicator was fit with three Gaussian components and the acidic spectra with one peak. Thymol blue is an exception since the first acid dissociation was used. As a result, thymol blue is colored as an acid (red) and colorless (pale yellow) as a base. One Gaussian peak was used to fit the basic spectra of thymol blue and two components were used to fit the acidic spectra.

EXPERIMENTAL SECTION

Instrumentation: A Shimadzu UV recording spectrophotometer was used for all absorbance measurements. The Shimadzu was interfaced to a microcomputer for data acquisition and processing. Figure 2 is a diagram of the closed loop flow system used throughout the experiments. The flow system was convenient for making sequential

Figure 2. Diagram of closed loop flow system used for isosbestic wavenumber determination and seawater alkalinity titrations.



spectra of solutions containing the same concentration of indicator at different pH. An Orion Ross 8102 combination pH electrode was used in the flow system for comparison between potentiometric and indicator pH measurements.

Reagents: All solutions were stored in teflon bottles and prepared with purified distilled Milli-Q water and reagent grade salts. Stock solutions, 1×10^{-3} molal, of thymol blue, bromophenol blue, bromocresol green, bromocresol purple, and phenol red were prepared in artificial seawater from the sodium salts of the indicators (Kodak). Final indicator concentrations were $1-2 \times 10^{-6}$ molal. Seawater, 0.68 m NaCl, and Milli-Q solutions of constant pH (pH range 1.0-9.5) were buffered by adding 0.01 m phthalate, phosphate, or Tris buffer to the solutions. The pH of the buffered solutions were adjusted with additions of HCl and NaOH.

Determination of Isosbestic Wavenumbers and Molal Absorptivities:

Isosbestic wavenumbers of the indicators were determined by measuring the wavenumber of intersection of three or more spectra in solutions of different pH (King and Kester, 1988a). Isosbestic wavenumbers were determined for each indicator in seawater, 0.68 m NaCl, and Milli-Q media. Molal absorptivities for each indicator were determined from absorbance measurements of gravimetrically prepared indicator solutions at the isosbestic wavenumber of each indicator.

Measurement of Acidic and Basic Indicator Spectra: Spectra of the acidic and basic forms of each indicator for curve fitting were

obtained using solutions with pH more than ± 3 pH units from the pK_a' of each indicator. The spectra of basic phenol red in seawater could not be determined due to brucite ($Mg(OH)_2$) precipitation from seawater at $pH > 9.5$. Phenol red is not completely in the basic form until the $pH > 10.5$. We used the curve fitting results for basic phenol red in 0.68 m NaCl as an estimate for phenol red in seawater. As will be shown later, the small medium dependence on the curve fitting parameters makes this a good approximation. Due to the low pK_a' of thymol blue, 1.44, direct determination of the acid spectra of thymol blue was not possible. Curve fits of the acidic spectra of thymol blue were obtained by fitting both the acidic and basic spectra of thymol blue in solutions with known concentrations of the acidic and basic forms thymol blue. In seawater, the acidic and basic thymol blue concentrations were determined from pH and pK_a' data. In NaCl and Milli-Q media, pK_a' data is not available. The concentration of basic thymol blue in these solutions was established from the absorbance of the basic peak divided by ϵ_{max} determined independently in basic media. The acidic thymol blue concentration was calculated by difference.

Gaussian Curve Fits of Indicator Spectra: A nonlinear curve fitting program based on the simplex algorithm (Caceci and Cacheria, 1984) was used to fit one or more Gaussian components to the indicator spectra. Each spectrum was composed of approximately 250 (ν, A_ν) data pairs over the wavenumber range 14,000 - 22,000 cm^{-1} . The concentration of the indicator was determined from the absorbance of the indicator at ν_{iso} . The indicator concentrations were used to convert the

(ν, A_ν) data pairs into $(\nu, \nu\epsilon)$ data pairs for curve fitting. The curve fitting program was written in Turbo Pascal and takes about one hour to converge using a 5 MHz microcomputer with math coprocessor.

Results and Discussion

Isosbestic Wavenumbers and Molal Absorptivity of the Indicators: Table II lists the isosbestic wavenumber for each indicator in seawater, 0.68 m NaCl, and Milli-Q. For all the indicators there is not a significant difference in the isosbestic wavenumber among media. The standard deviation of 7 cm^{-1} for bromocresol green and bromocresol purple is small and within the experimental uncertainties of our isosbestic wavenumber determinations. Due to the lack of media dependence, the mean isosbestic wavenumber was used for all determinations. Table III lists the molal absorptivity of each indicator at ν_{ISO} in the three different media. While there is some scatter in the values of ϵ_{ISO} for each indicator in the different media, there is not a consistent media dependent trend. The indicator salts are not good gravimetric standards. They were not dried before preparation of the indicator solutions to avoid possible thermal alteration. For pH measurements this is not a concern since wavelength ratios are always used and concentration terms cancel. However, hydration and weighing precision of the indicator salts will contribute a 2% uncertainty to ϵ_{ISO} values. A 2% uncertainty is consistent with the standard deviation in ϵ_{ISO} between media.

Curve Fitting Parameters: Tables IV, V, and VI present values for

Table II. Isosbestic Wavenumbers for the Indicators in Seawater, 0.68 m NaCl and Milli-Q Media.

Indicator	ν_1^a	ν_{iso}			
		Seawater	NaCl	Milli-Q	Mean
Thymol Blue	18519	20492	20500	20496	20496 \pm 3 ^b
Bromophenol Blue	16949	20178	20173	20173	20175 \pm 2
Bromocresol Green	16260	19631	19627	19616	19625 \pm 7
Bromocresol Purple	17007	20492	20475	20488	20485 \pm 7
Phenol Red	17921	20851	20851	20838	20846 \pm 6

a) ν_1 are the approximate values of ν at maximum absorbance (± 40 cm^{-1}) provided for general comparison between indicators.

b) Uncertainties reported as standard deviation about the mean for each media.

Table III. Molar Absorptivity of Indicators at ν_{iso} in Seawater, 0.68 m NaCl and Milli-Q Media^a

Indicator	Media			Mean
	Seawater	Milli-Q	NaCl	
Thymol Blue	6830	7167	6863	6953 \pm 152 ^b
Bromophenol Blue	7950	7635	7831	7805 \pm 130
Bromocresol Green	6170	5930	6033	6033 \pm 124
Bromocresol Purple	7640	7151	7261	7351 \pm 209
Phenol Red	10460	10875	10277	10537 \pm 250

a) Molar absorptivities determined at mean isosbestic wavelengths.

b) Uncertainties reported as standard deviation about the mean for each media.

Table IV. Molar Absorptivities of Indicator Gaussian Components in Seawater, 0.68 m NaCl and Milli-Q Media

Indicator	Peak	Seawater	NaCl	Milli-Q	Mean
Thymol Blue	acid 1	24637	38703	42785	35374 ± 7774 ^a
	acid 2	19445	17224	21344	19445 ± 1654
	base 1	12420	12563	12612	12532 ± 81
Bromophenol Blue	acid 1	22201	22526	22389	22372 ± 133
	base 1	48923	50434	49173	49510 ± 661
	base 2	26797	27011	28931	27580 ± 960
	base 3	13017	12160	12370	12516 ± 365
Bromocresol Green	acid 1	16394	16100	16120	16204 ± 134
	base 1	23935	24149	26628	24904 ± 1222
	base 2	17501	19090	17650	18080 ± 716
	base 3	7711	6348	5826	6628 ± 795
Bromocresol Purple	acid 1	18457	18324	15522	17434 ± 1354
	base 1	33539	28143	29810	30497 ± 2256
	base 2	22395	23385	23539	23106 ± 507
	base 3	9954	9901	9025	9627 ± 426
Phenol Red	acid 1	21064	20404	20639	20702 ± 273
	base 1	35996	35996	42924	39460 ± 3464
	base 2	29212	29212	31103	30158 ± 946
	base 3	11557	11557	10368	10963 ± 595 ^b

a) Uncertainties reported as standard deviation about the mean for each media.

b) Mean for basic peaks of phenol red are based only on NaCl and Milli-Q data.

Table V. ν_{\max} of Indicator Gaussian Components in Seawater, 0.68 m NaCl and Milli-Q Media

Indicator	Peak	Media			Mean
		Seawater	NaCl	Milli-Q	
Thymol Blue	acid 1	18168	18160	18189	18172 ± 12 ^a
	acid 2	18989	19152	19324	19155 ± 137
	base 1	22491	22834	22617	22647 ± 142
Bromophenol Blue	acid 1	22455	22466	22405	22442 ± 27
	base 1	16857	16862	16868	16862 ± 4
	base 2	17670	17643	17701	17671 ± 24
	base 3	18775	18836	18854	18822 ± 34
Bromocresol Green	acid 1	22170	22165	22127	22154 ± 19
	base 1	16066	16088	16082	16079 ± 9
	base 2	16988	17145	17002	17045 ± 71
	base 3	18401	18998	18706	18702 ± 244
Bromocresol Purple	acid 1	22718	22087	22675	22493 ± 288
	base 1	16919	16917	16906	16914 ± 6
	base 2	17748	17685	17627	17687 ± 49
	base 3	19264	19593	19372	19410 ± 137
Phenol Red	acid 1	22575	22672	22521	22589 ± 62
	base 1	17833	17833	17855	17844 ± 10
	base 2	18524	18524	18759	18642 ± 127
	base 3	20192	20192	20517	20355 ± 162 ^b

a) Uncertainties reported as standard deviation about the mean for each media.

b) Mean for basic peaks of phenol red is based only on NaCl and Milli-Q data.

Table VI. v_{half} of Indicator Gaussian Components in Seawater, 0.68 m NaCl and Milli-Q Media

Indicator	Peak	Media			Mean
		Seawater	NaCl	Milli-Q	
Thymol Blue	acid1	1528	1657	1562	1582 ± 55 ^a
	acid2	2489	2173	2081	2248 ± 175
	base1	4355	4456	5068	4626 ± 315
Bromophenol Blue	acid1	3683	3631	3694	3669 ± 27
	base1	934	956	937	942 ± 10
	base2	1680	1731	1788	1733 ± 44
	base3	3520	3476	3500	3499 ± 18
Bromocresol Green	acid1	4205	4141	4267	4204 ± 51
	base1	1350	1376	1432	1386 ± 34
	base2	2161	2340	2269	2257 ± 74
	base3	3950	4028	4011	3996 ± 33
Bromocresol Purple	acid1	3855	3826	3105	3595 ± 347
	base1	978	917	961	952 ± 26
	base2	1941	2012	2088	2014 ± 60
	base3	3940	4040	3937	3972 ± 48
Phenol Red	acid1	3505	3417	3653	3525 ± 97
	base1	907	907	981	944 ± 37 ^b
	base2	1923	1923	1935	1929 ± 6
	base3	3580	3580	2771	3254 ± 404

a) Uncertainties reported as standard deviation about the mean for each media.

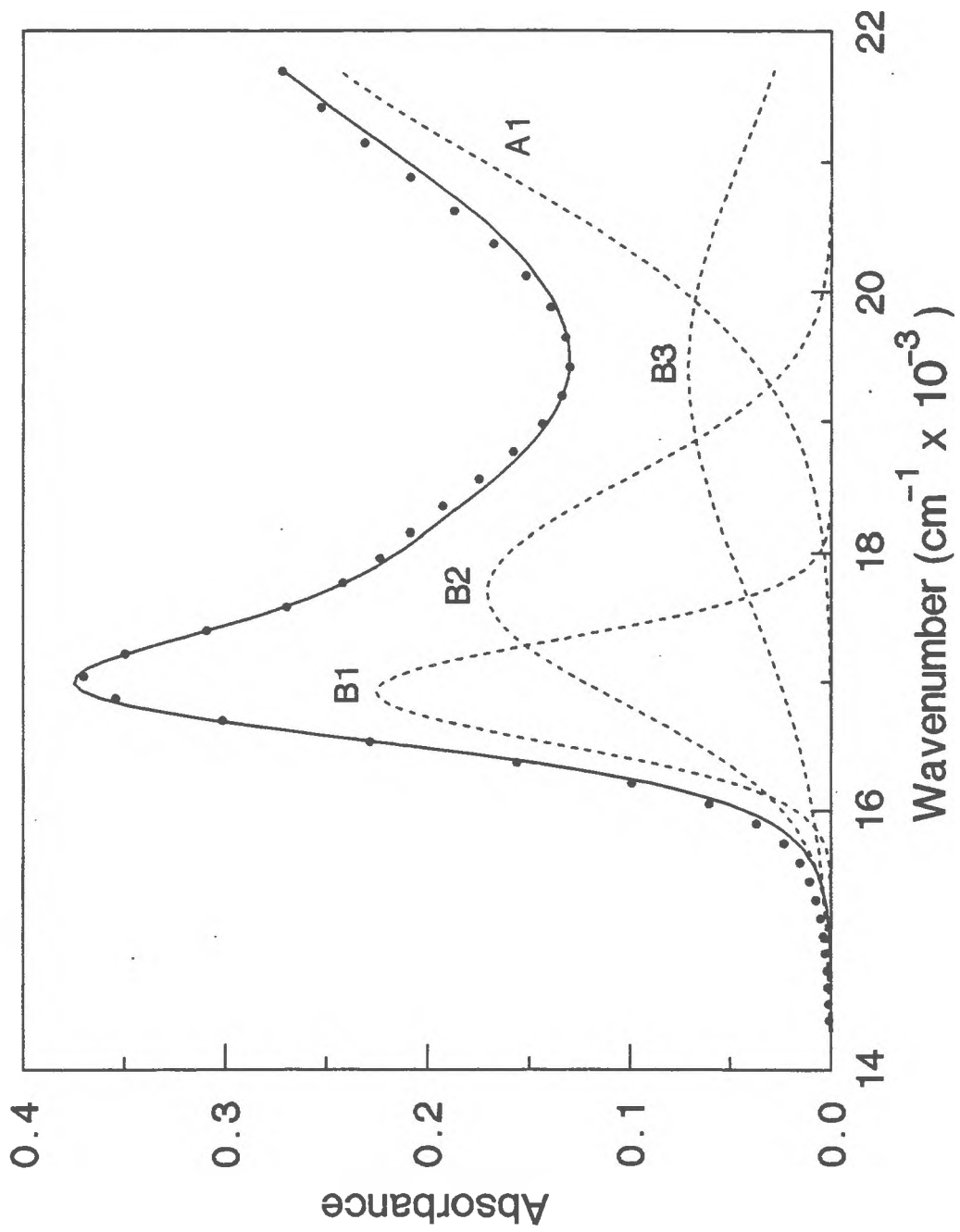
b) Mean for basic peaks of phenol red is based only on NaCl and Milli-Q data.

ϵ_{\max} , ν_{\max} , and $\Delta\nu_{1/2}$ for each indicator in seawater, 0.68 m NaCl, and Milli-Q media. The agreement between observed and modeled $\nu\epsilon$ for each indicator was very good. In most cases the average deviation between modeled and observed $\nu\epsilon$ was less than 2%. The Gaussian peak parameters did not have a significant trend among media. Except for the first acid peak for thymol blue, the values for ϵ_{\max} among media agree within 10%. Values for ν_{\max} are in excellent agreement with the relative standard deviation less than 2%. $\Delta\nu_{1/2}$ values in different media agree within 5% for most components with slightly higher deviations for the acid peak of bromocresol purple and the third basic component of phenol red. Due to the lack of medium dependence on the Gaussian peak parameters, estimates of indicator spectral shape in simple salt solutions can use the mean values for ϵ_{\max} , ν_{\max} , and $\Delta\nu_{1/2}$ presented here. It should be noted that pK'_a values for the indicators will exhibit a medium dependence and will be affected by medium composition and ionic strength.

Figure 3 illustrates the observed and calculated spectra for bromocresol purple. The calculated spectrum was based on values of $\nu\epsilon_{\text{HA}}$ and $\nu\epsilon_{\text{A}}$, pH, pK'_a , and the concentration of bromocresol purple. The agreement between the observed and calculated spectra demonstrates that models for the acidic and basic chromophore spectral shape, determined in acidic and basic media, can be combined with thermodynamic data to provide an accurate representation of an indicator's spectrum at intermediate pH.

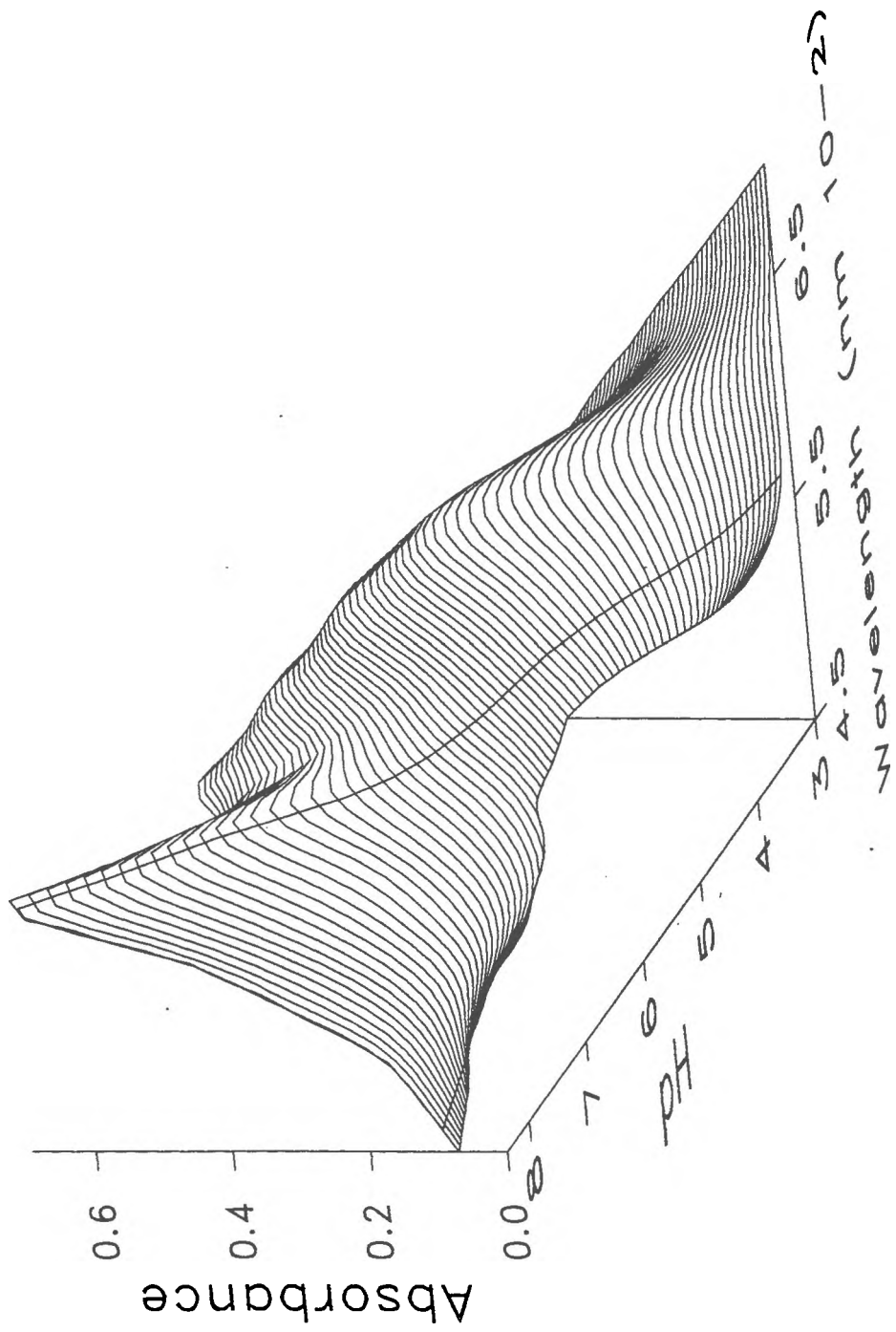
Prediction of Multiple Indicator Spectra: The predicted spectra of

Figure 3. Observed and calculated spectra of bromocresol purple in seawater at pH 5.654. The solid line is the observed spectrum. The dashed lines labeled A1, B1, B2, and B3 denote the acidic and first, second, and third basic Gaussian components. The ● symbol is the calculated spectrum based on the sum of the Gaussian components.



solutions containing multiple indicators can be obtained from linear addition of individual spectra of two or more indicators. A practical application in which multiple indicators are required is the determination of seawater alkalinity by acid titration. Continuous seawater alkalinity titrations require pH measurements over the range 3.0-8.3. A combination of phenol red and bromocresol green indicators is well-suited for pH measurements over this pH range. In order to optimize the wavelengths of measurement and indicator concentrations, spectra of a seawater solution containing both indicators were calculated as a function of pH. Figure 4 is a plot of the predicted spectra. The spectra are plotted as a function of wavelength to simplify discussion, but the model and computations are based on wavenumbers. At pH 8.3 the absorbance maximum at 560 nm is due to the basic form of phenol red. The shoulder at 615 nm is due to the basic form of bromocresol green. The acidic forms of both indicators have moderate absorbances below 470 nm which accounts for the gradual increase in absorbance at shorter wavelengths with decreasing pH. Based on calculated $d(A_1/A_2)/dpH$ values and the range in absorbance for several wavelengths, 560 and 460 nm were selected for wavelengths 1 and 2 respectively. The absorbance at 560 nm decreases steadily from pH 8.3-6, flattens from 6-5, and then decreases again from pH 5-3. The absorbance at 460 nm increases slowly over the full pH range 8.3-3. The optimal molal concentration ratio of bromocresol green to phenol red was 1.2 to 1. Slightly higher bromocresol green concentrations increase the absorbance of bromocresol green at 560 nm at low pH. The selected wavelengths provide maximum pH measurement sensitivity over the pH range 8.3-6 and 5-3. This is well suited for our application

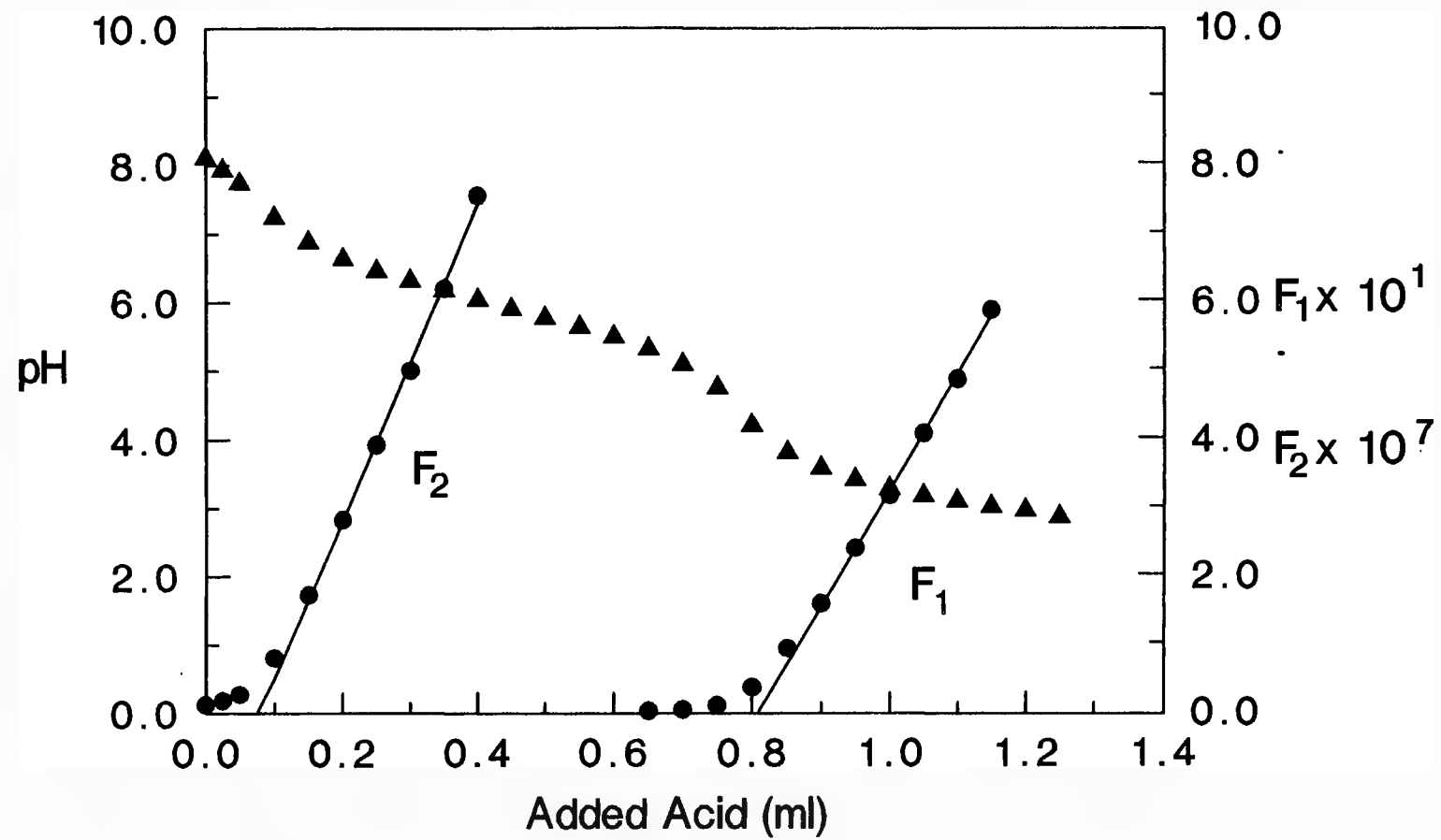
Figure 4. Predicted spectra of phenol red and bromocresol green in seawater as a function of pH and wavelength. The solid lines perpendicular to the surface contours are located at 560 and 460 nm.



since titration end points are at pH 7.7 and 4.2. While we have not pursued this possibility, increased precision in pH measurements should be possible if $\lambda_1 = 560$ nm above pH 5.5 and $\lambda_1 = 615$ nm below pH 5.5. A wavelength shift during the titration involves greater experimental complexity when using a spectrophotometer. For applications warranting a dedicated instrument using LED light sources and computer controlled data acquisition, a multiple wavelength system may be useful.

Alkalinity Titrations: The indicator combination of bromocresol green and phenol red was used to measure pH of a seawater solution during alkalinity titrations. The titration was performed in the flow system shown in figure 2. Absorbance was measured at the optimal wavelengths of 560 and 460 nm. The optical constants E_A , E_{HA} , and E_{2A} for phenol red and bromocresol green were determined directly in seawater media. A stock solution containing both phenol red and bromocresol green was prepared and ψ for this solution determined by solving equation 6 for ψ using several solutions of known pH. The pH of the calibration solutions was determined with an electrode but can also be readily determined with a single indicator. Since ψ is a function of the indicator ratio and not the total concentration, ψ can be determined once for a given stock solution. The stock solutions should be prepared weekly. Figure 5 shows the results of an alkalinity titration using indicators for pH measurements. The agreement between indicator and electrode pH measurements was ± 0.016 over the full range of the titration. Ignoring protolytic side reactions the total alkalinity and carbonate alkalinity can be determined using Gran plots as described by Dyrssen and Sillen (1967). The total alkalinity and

Figure 5. Alkalinity titration of seawater solution. The ▲ symbols denote the pH measured with the indicator combination phenol red and bromocresol green. The first and second Gran functions are labeled F1 and F2 respectively.



carbonate alkalinity were 2.21 ± 0.01 and 2.01 ± 0.01 mequiv kg^{-1} respectively for 2 replicate determinations. Total alkalinity and carbonate alkalinity determined using pH measurements made with an electrode agreed within 2 %.

Measurement of pH with indicators has several advantages over electrode pH measurement in well defined media such as seawater. The rapid response times of indicators can significantly decrease measurement times from minutes to seconds. Increased measurement rates are particularly advantageous during titrations where many pH measurements must be made. Indicators can be used for pH measurement at high pressures which will make in situ measurement of pH and alkalinity possible in the deep ocean. Finally, indicators do not require periodic calibration once the optical constants have been determined in the media of interest.

References

- Brown, M. F.; and Kester, D. R. (1980) Ultraviolet spectroscopic studies related to iron complexes in marine systems. *Thalassia Jugoslavica*, 16(2-4), 191-201.
- Byrne, R. H. (1987) Standardization of standard buffers by visible spectrometry. *Analytical Chemistry*, 59(10), 1479-1481.
- Caceci, M. S.; and Cacheris, W. P. (1984) Fitting curves to data *Byte*, 9(5), 340-362.
- Dickson, A. G. (1984) pH scales and proton-transfer reactions in saline media such as seawater. *Geochimica Cosmochimica Acta*, 48, 2299-2308.
- Dyrssen, D.; and Sillen, L. G. (1967) Alkalinity and total carbonate in sea water. A plea for p-T-independent data. *Tellus*, 19b, 113-121.
- King, D. W.; and Kester, D. R. (1988a) Determination of seawater pH from 1.5 to 8.5 using colorimetric indicators. *Marine Chemistry*, accepted.
- King, D. W.; and Kester, D. R. (1988b) The effect of pressure on the dissociation of sulfonephthalein indicators. *Journal of Solution Chemistry*, submitted.

Pytkowicz, R. M. (1969) Use of apparent equilibrium constants in chemical oceanography, geochemistry, and biochemistry. *Geochemical Journal*, 3, 181-184.

Ramette, R. W., C. H. Culberson, and R. G. Bates (1977) Acid-base properties of tris(hydroxymethyl)aminomethane (Tris) buffers in seawater from 5 to 40 °C. *Analytical Chemistry*, 49(6), 867-670.

Robert-Baldo, G. L.; Morris, M. J.; and Byrne, R. H. (1985) Spectroscopic determination of seawater pH using phenol red. *Analytical Chemistry*, 57, 2564-2567.

The Effect of Pressure on the Dissociation of Bisulfate
in Seawater.

Abstract

The effect of pressure on the dissociation of bisulfate was determined in 35 ‰ salinity seawater at 25 °C. The dissociation constant, K_2' , was determined over the pressure range from atmospheric to 1000 bars from the compressional pH change of acidic seawater solutions. The partial molal volume and compressibility change for bisulfate dissociation was $-13.9 \text{ cm}^3\text{mol}^{-1}$ and $-6.54 \times 10^{-3} \text{ cm}^3\text{mol}^{-1}\text{bar}^{-1}$ respectively. The high pressure K_2' data were combined with K_2' values at atmospheric pressure to provide an empirical equation for K_2' which can be used to relate free hydrogen ion and total hydrogen ion pH scales over the full range of oceanic temperatures, pressures, and salinities.

Introduction

There are currently three different pH scales used to calibrate pH electrodes in marine waters; the NBS activity scale, the total hydrogen ion scale, and the free hydrogen ion scale (Dickson, 1984). While the NBS scale is still in widespread use, the thermodynamically more rigorous total hydrogen ion and free hydrogen ion scales are gaining increasing acceptance (Whitfield et al., 1985; Millero, 1986). The total hydrogen ion and free hydrogen ion pH scales are defined by equations 1 and 2 respectively:

$$\text{pH}_T = -\log(\text{H}^+) \quad (1)$$

$$\text{pH}_F = -\log[\text{H}^+] \quad (2)$$

where parenthesis and brackets denote the respective free and total concentrations. The total hydrogen ion concentration is operationally defined as the free hydrogen ion concentration plus the bisulfate concentration.

$$(\text{H}^+) = [\text{H}^+] + (\text{HSO}_4^-) \quad (3)$$

The (HSO_4^-) can be calculated from the apparent acid dissociation constant, K'_2 , for HSO_4^- , $[\text{H}^+]$, and total sulfate concentration, T_{SO_4} .

$$K_2 = \frac{[H^+](SO_4^{2-})}{(HSO_4^-)} \quad (4)$$

$$(HSO_4^-) = T_{SO_4} \left(\frac{[H^+]}{[H^+] + K_2} \right) \quad (5)$$

Combining equations 2, 3 and 5 the two pH scales can be related:

$$pH_T = pH_F - \log \left\{ 1 + \left(\frac{T_{SO_4}}{[H^+] + K_2} \right) \right\} \quad (6)$$

T_{SO_4} can be calculated from seawater salinity. At the pH of natural seawater, the $[H^+]$ term in the right side of equation 6 is negligible. Values for K_2 as a function of temperature and salinity have been determined by several investigators (Khoo et al., 1977; Bates and Calais 1981; and Millero, 1986). Unfortunately, a systematic study of the effect of pressure on K_2 has not been made. During a series of experiments designed to determine the effect of pressure on the dissociation of sulfonephthalein indicators (King and Kester, 1988), we measured the pH change due to compression of artificial seawater solutions containing sulfate. These data were used to determine the effect of pressure on K_2 at 25 °C in 35‰ salinity seawater.

Theory

All the experiments were performed using artificial seawater prepared to have a major ion composition identical to natural seawater except all the carbonate and borate was replaced with chloride. Over the pH range 1.5 to 2.0, HSO_4^- will be the only significant protolytic species in the ASW(2) solutions. The buffering capacity of HF, the only other weak acid in solution, is less than 0.5% of the buffering capacity of HSO_4^- due to its low concentration and pK' of 2.65. Under these conditions, the change in the free hydrogen ion concentration with compression can be attributed to proton dissociation from HSO_4^- .

$$[\text{H}^+]_p = [\text{H}^+]_o + (\text{HSO}_4^-)_o - (\text{HSO}_4^-)_p \quad (7)$$

K'_{2p} as a function of pressure can be determined from a similar mass balance:

$$K'_{2p} = \frac{\{[\text{H}^+]_o + \chi\} \{(\text{SO}_4^{2-})_o + \chi\}}{\{(\text{HSO}_4^-)_o - \chi\}} \quad (8)$$

where the subscripts o and p denote values at atmospheric and pressure P respectively, and χ is the change in $[\text{H}^+]$ with compression. Values for $(\text{HSO}_4^-)_o$ and $(\text{SO}_4^{2-})_o$ were determined from pH and K'_{2p} data at atmospheric pressure using equations 5 and 9 respectively.

$$(\text{SO}_4^{2-}) = T_{\text{SO}_4} \left(\frac{K_2'}{[\text{H}^+] + K_2'} \right) \quad (9)$$

The change in K_2' with pressure can be fit to equation 10 to yield values for the partial molal volume change, $\Delta V'$, and partial molal compressibility change, $\Delta k'$, for bisulfate dissociation.

$$\text{p}K_p = \text{p}K_0 + \frac{\Delta V'}{2.303RT} P - \frac{0.5\Delta k'}{2.303RT} P^2 \quad (10)$$

Methods

All reagents were prepared from reagent grade salts dissolved in distilled deionized Milli-Q water. The composition of the seawater and indicator solutions are described in detail elsewhere (King and Kester, 1988b). All pH measurements were made on the free hydrogen ion pH scale using sulfonephthalein pH indicators. A high pressure optical system was used for all high pressure pH measurements (King and Kester, 1988). Pressure is reported in gauge pressure from one atmosphere. Literature values for K_2' at atmospheric pressure are listed in Table I; we selected the intermediate value of 0.0826 determined by Culberson et al. (1970) for our calculations.

Table I. Literature values for K_2' in seawater at 25 °C and 35 ‰ salinity.

K_2'	Reference
0.0781	Millero (1986)
0.0800	Bates and Calais (1981)
0.0840	Khoo et al. (1977)
0.0826	Culberson et al. (1970)
0.0885	Dyrssen and Hansson (1973)
0.0962	Harvie et al. (1984)
0.1010	Millero (1983)

Results and Discussion

Table II lists the observed pH change for two ASW(2) solutions as a function of pressure. The calculated K'_2 and pK'_2 at each pressure are also included. Figure 1 is a plot of the calculated pK'_2 as a function of pressure. There was not a significant difference between the pK'_2 values determined using different solutions. Equation 8 is overconstrained if several solutions with different pH_0 are used to determine pK'_2 . We didn't solve equation 8 in this manner because our pH measurements were not made at common pressures. However, the agreement between the two determinations provides evidence of the validity of our approach.

A nonlinear fit of equation 10 to the combined data yielded $\Delta V'$ and $\Delta k'$ values of $-13.9 \text{ cm}^3\text{mol}^{-1}$ and $-6.54 \times 10^{-3} \text{ cm}^3\text{mol}^{-1}\text{bar}^{-1}$. Our values can be compared to previously estimated values for $\Delta V'$ and $\Delta k'$ of -16.67 and -2.28×10^{-3} . The agreement is good considering the previously estimated values were obtained from ΔV and Δk data at infinite dilution and a medium correction using HCO_3^- as a model (Millero, 1983). Culberson (1981) has pointed out that the high pressure potentiometric data of Disteche and Disteche (1967) can be used to provide an estimate of the pressure effects on K'_2 in seawater. Disteche and Disteche measured the potential change as a function of pressure of the following cell:

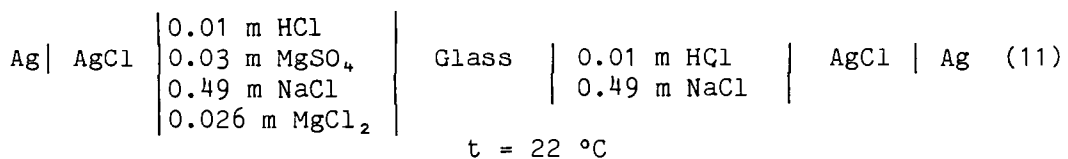
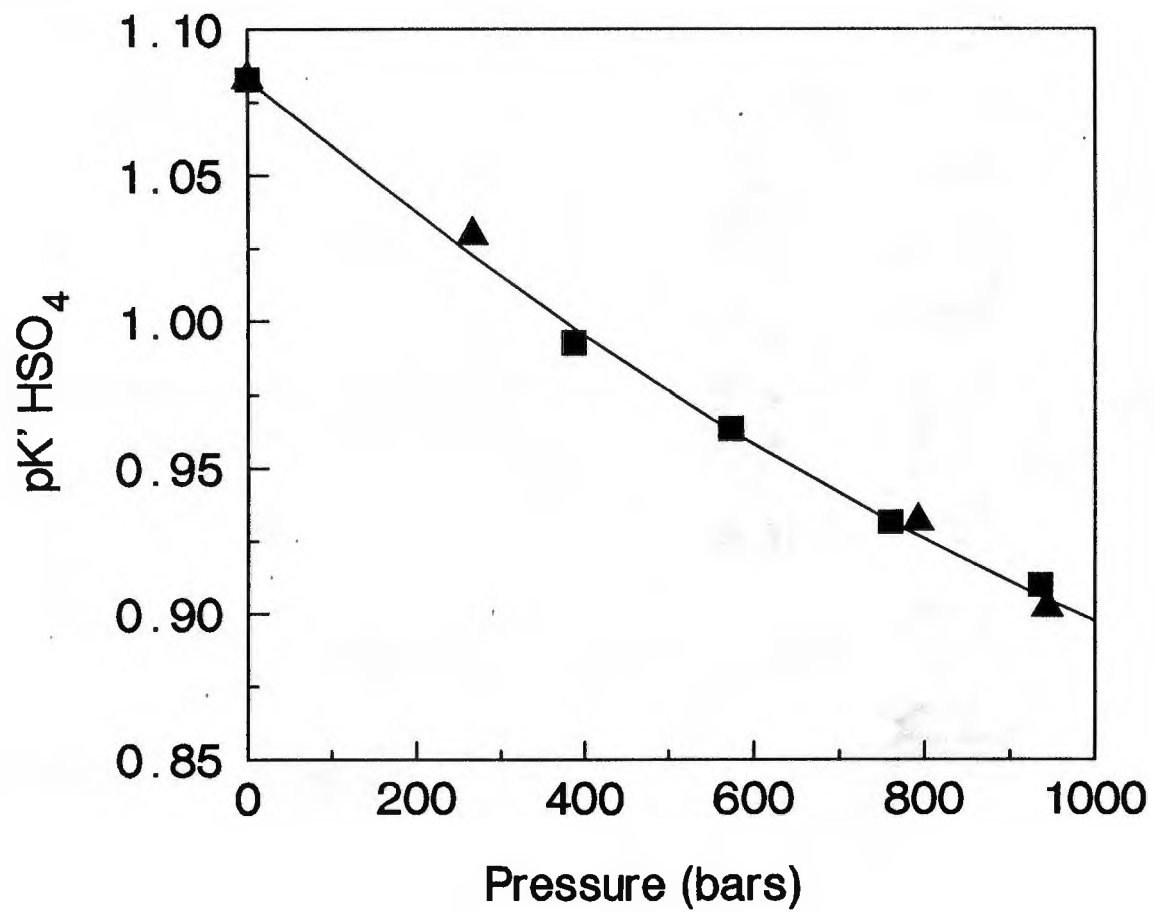


Table II. Solution pH and calculated bisulfate K_2' and pK_2' as a function of pressure ($t = 25\text{ }^\circ\text{C}$, $S = 35\text{ }^\circ/\text{oo}$).

Pressure (bars)	pH	$\Delta[\text{H}^+]$ (χ)	K_2' (molal)	pK_2'
Solution 1, $\text{pH}_0 = 1.899$				
0	1.899	--	0.083	1.083
266	1.888	3.191E-04	0.093	1.029
793	1.871	8.564E-04	0.117	0.932
944	1.866	1.008E-03	0.125	0.902
Solution 2, $\text{pH}_0 = 2.070$				
0	2.070	--	0.083	1.083
387	2.051	3.803E-04	0.102	0.993
573	2.045	4.953E-04	0.109	0.963
760	2.039	6.173E-04	0.117	0.931
936	2.036	6.964E-04	0.123	0.910

Figure 1. Calculated pK_2^* for bisulfate as a function of pressure.

Data labels: ▲, $pH_0 = 1.899$; ■, $pH_0 = 2.070$.



The change in the cell potential was linear with pressure. At 1000 bars, ΔE was 3.5 ± 0.3 mv which is equal to a ΔpH of 0.06. Accepting the assumption of Culberson (1981) that the change in the cell potential with pressure is due to dissociation of HSO_4^- , $K_2^!_p$ can be calculated using equation 8. We estimate the $[H^+]_0$ for the left hand side of the cell to be 0.0076 m based on the $HSO_4^- - SO_4^{2-}$ equilibria. The calculated change in $pK_2^!$ with compression to 1000 bars was -0.34 ± 0.3 which is equivalent to a $\Delta V'$ -19.4 ± 1.6 cm^3 mol^{-1} . Comparison of this result with our $\Delta V'$ value requires several considerations. First, the media used by Distech and Distech did not contain Ca^{2+} which could have an effect on SO_4^{2+} speciation. Second, due to the significant buffering capacity of the free proton below pH 3, calculation of the effect of pressure on $K_2^!$ is dependent on accurate values for pH_0 . Because pH_0 was not measured directly, we were forced to estimate pH_0 from the medium composition. Finally, as can be seen from Figure 1 and the estimates of Millero (1983), the effect of pressure on $pK_2^!$ is not linear. Our $\Delta V'$ value would increase by approximately 10% if compressibility changes were not considered.

Our $\Delta V'$ and $\Delta k'$ values determined at 25 °C and 35 ‰ salinity seawater can be extrapolated to other temperatures using HCO_3^- as a model (Millero, 1983). The equations are:

$$\Delta V' = -15.26 + 0.0466t + 0.316 \times 10^{-3}t^2 \quad (12)$$

$$10^3 \Delta k' = -8.79 + 0.0900t \quad (13)$$

Over the salinity range of the deep sea, variation in $\Delta V'$ and $\Delta k'$ due

to salinity variations will be minor. The high pressure K_2' data can be combined with operational values for K_2' at atmospheric pressure (Millero, 1986) to yield a general equation for K_2' as a function of temperature, pressure, and salinity:

$$pK_2' = A/T + B + \Delta V'P/2.303RT - 0.5 \Delta k'P^2/2.303RT \quad (14)$$

$$A = -1,226.966 + 65.6\sqrt{S} \quad (15)$$

$$B = 6.09405 - 0.4502\sqrt{S} + 1.3525 \times 10^{-2}S \quad (16)$$

where S is the salinity and $T = t + 273.15$. Equations 14 and 6 allow interconversion of pH_T and pH_F over the full range of oceanic temperatures, pressures, and salinities. The calculated difference between the two pH scales over a range of temperatures and pressures is listed in Table III.

Table III. Difference between pH_F and pH_T as a function of temperature and pressure. ΔpH calculated using equations 14 and 16 for 35 ‰ salinity seawater.

Pressure (bars)	Temperature (°C)				
	5	10	15	20	25
0	0.089	0.099	0.110	0.122	0.134
200	0.079	0.089	0.099	0.110	0.122
400	0.072	0.081	0.091	0.101	0.112
600	0.066	0.074	0.084	0.093	0.104
800	0.061	0.069	0.078	0.087	0.097
1000	0.058	0.065	0.073	0.082	0.092

References

- Bates, R. G.; and Calais, J. G. (1981) Thermodynamics of the dissociation of BisH^+ in seawater from 5 to 40 °C. *Journal of Solution Chemistry*, 10, 269-279.
- Culberson, C. H. (1981) Direct potentiometry In: *Marine Electrochemistry.*, Whitfield, M.; and Jagner, D., editors, Wiley and Son, New York, 188-261.
- Culberson, C. H.; Pytkowicz, R. M.; and Hawley, J. E. (1970) Seawater alkalinity determination by the pH method. *Journal of Marine Research*, 28, 15-21.
- Dickson, A. G. (1984) pH scales and proton-transfer reactions in saline media such as seawater. *Geochimica et Cosmochimica Acta*, 48, 2299-2308.
- Disteche, A. and S. Disteche (1967) The effect of pressure on the dissociation of carbonic acid from measurements with buffered glass electrode cells. *Journal Electrochemical Society*, 114(4), 330-340.
- Dyrssen, D.; and Hansson, I. (1973) Ionic medium effects in seawater - a comparison of acidity constants of carbonic acid and boric acid in sodium chloride and synthetic seawater. *Marine Chemistry*, 1, 137-149.

Harvie, C. E.; Moller, N.; and Weare, J. H. (1984) The prediction of mineral solubilities in natural waters: The Na-K-Mg-Ca-H-Cl-SO₄-OH-HCO₃-CO₃-CO₂-H₂O system to high ionic strengths at 25 °C. *Geochimica et Cosmochimica Acta*, 48, 723-751.

Khoo, K. H.; Ramette, R. N.; Culberson, C. H.; and Bates, R. G. (1977) Determination of hydrogen ion concentration in seawater from 5 to 40 °C: Standard potentials at salinities from 20 to 45 ‰. *Analytical Chemistry*, 49, 29-34.

King, D. W.; and Kester, D. R. (1988a) The effect of pressure on the dissociation of sulfonephthalein indicators. *Journal of Solution Chemistry*, submitted.

King, D. W.; and Kester, D. R. (1988b) Determination of seawater pH from 1.5 to 8.5 using colorimetric indicators. *Marine Chemistry*, accepted.

Millero, F. J. (1983) The estimation of the pK_{HA}^* of acids in seawater using the Pitzer equation. *Geochimica et Cosmochimica Acta*, 47(12), 2121-2129.

Millero, F. J. (1983) Influence of pressure on chemical processes in the sea. *Chemical Oceanography* vol. 8., Riley, J. P.; and Chester, R. editors Academic Press, London, 2-88.

Millero, F. J. (1986) The pH of estuarine waters. *Limnology and Oceanography*, 31(4), 839-837.

Whitfield, M.; Butler, R. A.; and Covington, A. K. (1985) The determination of pH in estuarine waters. I. Definition of pH scales and the selection of buffers. *Oceanologica Acta*, 8(4), 423-432.

The Effect of Pressure on the Hydrolysis of Fe(III).

Abstract

UV spectroscopy was used to determine the first hydrolysis constant of Fe (III), ${}^*_1\beta$, at 25 °C over a pressure range from atmospheric to 1000 bars. Based on these data the partial molal volume and compressibility change for the hydrolysis reaction were $-13.1 \text{ cm}^3\text{mol}^{-1}$ and $9.3 \times 10^{-4} \text{ cm}^3\text{mol}^{-1}\text{bar}^{-1}$ respectively. The ${}^*_1\beta$ values were determined independently of optical constants over the full pressure range. The results demonstrate that molal absorptivities of Fe^{3+} and FeOH^{2+} are not independent of pressure as assumed by previous investigators. An empirical equation provides values of ${}^*_1\beta$ as a function of temperature ($273 \leq T \leq 300$), ionic strength ($0.1 \leq I \leq 1.0$), and pressure ($0 \leq P \leq 1000$).

Introduction

The speciation of Fe(III) in seawater is important in controlling the solubility (Byrne and Kester; 1976a), redox potential (Kester et al., 1975), and availability of Fe(III) to marine organisms (Anderson and Morel, 1982). Over the past ten years the solubility and speciation of Fe(III) at atmospheric pressure has been well established (Kester et al., 1975; Byrne and Kester, 1976a; 1976b; 1978; 1981; Elrod and Kester, 1980; and Brown and Kester, 1980). However, the effect of pressure on the speciation of Fe(III) is not well defined. Several investigators have determined the effect of pressure on the first hydrolysis constant of Fe(III) in a range of media (Jost, 1976; Hasinoff, 1979; Swaddle and Merback, 1981; and Martinez et al., 1985). Unfortunately, all the determinations were made using UV spectroscopy without correction for the effect of pressure on the molar absorptivities of the Fe(III) species. In this work the effect of pressure on the first hydrolysis constant of Fe (III), ${}^*_1\beta$, was determined in 0.68 molal NaClO₄ media. A modification of the UV spectroscopic method used by Byrne and Kester (1978) was employed to determine ${}^*_1\beta$ over the pressure range 0 - 1000 bars. The method provides values for ${}^*_1\beta$ which are independent of the optical system used to make the high pressure absorbance measurements.

Method

The first hydrolysis of Fe(III) is defined:



where brackets denote free molal concentrations and ${}_1^*\beta$ is a stoichiometric constant dependent on the temperature, pressure, and ionic strength (Kester, 1986). The $[\text{FeOH}^{2+}]$ and total Fe(III) concentration, TFe, can be related to $[\text{Fe}^{3+}]$ and $[\text{H}^+]$ according to equations 2 and 3 respectively.

$$[\text{FeOH}^{2+}] = \frac{{}_1^*\beta[\text{Fe}^{3+}]}{[\text{H}^+]} \quad (2)$$

$$\text{TFe} = [\text{Fe}^{3+}]\{1 + {}_1^*\beta/[\text{H}^+]\} \quad (3)$$

Based on a value of 2.5×10^{-9} for the second hydrolysis constant of Fe(III) (Byrne and Kester, 1978), $\text{Fe}(\text{OH})_2^+$ contributed less than 0.1% of the total Fe(III) concentration and can be ignored for $\text{pH} < 3$. Similarly, the formation of the $\text{Fe}_2(\text{OH})_2^{4+}$ dimer was not significant in this study due to the low Fe(III) concentrations and relatively low pH (Byrne and Kester, 1978). We have adopted NaClO_4 as the background electrolyte and assumed that Fe(III) - ClO_4^- interactions were

negligible (Byrne and Kester, 1978).

Defining the molal absorptivities of Fe^{3+} and FeOH^{2+} at wavelength λ as $\lambda\epsilon_1$ and $\lambda\epsilon_2$, respectively, the absorbance of an Fe(III) solution as a function of hydrogen ion concentration is described:

$$\lambda A = [\text{Fe}^{3+}]l\{\lambda\epsilon_1 + \lambda\epsilon_2 \frac{*}{i}\beta/[\text{H}^+]\} \quad (4)$$

where l is the pathlength of the optical cell. The UV spectra of Fe (III) exhibits an isosbestic point at 272 nm where the molal absorptivities of Fe^{3+} and FeOH^{2+} are equal. At the isosbestic wavelength, equation 4 can be simplified as follows:

$$iA = [\text{Fe}^{3+}]l_i\epsilon\{1 + \frac{*}{i}\beta/[\text{H}^+]\} \quad (5)$$

where iA and $i\epsilon$ are the absorbance and molal absorptivity at the isosbestic wavelength. By taking the ratio of equations 4 and 5 the concentration and pathlength terms cancel.

$$\frac{\lambda A}{iA} = \frac{\{\lambda\epsilon_1 + \lambda\epsilon_2 \frac{*}{i}\beta/[\text{H}^+]\}}{\{1 + \frac{*}{i}\beta/[\text{H}^+]\}} \quad (6)$$

The constants $\lambda\epsilon_1$ and $\lambda\epsilon_2$ are ratios of the molal absorptivities of Fe^{3+} and FeOH^{2+} as defined by equations 7 and 8.

$$\lambda E_1 = \lambda \epsilon_1 / i \epsilon \quad (7)$$

$$\lambda E_2 = \lambda \epsilon_2 / i \epsilon \quad (8)$$

Equation 6 was used to establish ${}^*_1\beta$ from absorbance ratios and $[H^+]$ data using a nonlinear least squares method. At constant pressure, the three constants ${}^*_1\beta$, E_1 and E_2 were determined by solving equation 6 in terms of three ($[H^+]$, $\lambda A/iA$) coordinate pairs. Byrne and Kester (1978) have shown that determination of ${}^*_1\beta$ using a similar least squares approach was independent of wavelength. We pooled ($[H^+]$, $\lambda A/iA$) measurements made at five wavelengths for each of three Fe(III) solutions. Each solution had a different pH. The use of multiple wavelength data improved the determination of ${}^*_1\beta$ by overconstraining the solution to equation 6. The two optical constants, E_1 and E_2 , were determined for each wavelength. Therefore, solution of equation 6 using pooled data from five wavelengths required determination of 11 constants from 15 equations.

A nonlinear least squares program using the simplex algorithm (Caceci and Cacheris, 1984) was used for all nonlinear solutions. The algorithm was written in Turbo Pascal and runs on a microcomputer. The program took about 2 minutes to converge to a solution.

Experimental

All solutions were prepared using Milli-Q water and were stored in teflon bottles. A background electrolyte of 0.68 m NaClO₄ was used for all experiments. The NaClO₄ (Fisher Scientific) was filtered through a 0.4 μ m filter prior to use. The Fe(III) solutions were prepared in

the NaClO_4 electrolyte solution from $\text{Fe}(\text{ClO}_4)_3$ salts (G.Fredereck Smith) with a final concentration 6×10^{-6} m. The $\text{Fe}(\text{III})$ solutions were stored in black teflon bottles to avoid photoreduction of $\text{Fe}(\text{III})$. The pH of the $\text{Fe}(\text{III})$ solutions was adjusted with HClO_4 .

The pH of the $\text{Fe}(\text{III})$ solutions were determined using an Orion Ross 8102 combination pH electrode with a 4.0 m NaCl filling solution. The electrode was calibrated on the free hydrogen ion concentration scale (Dickson, 1984) using three 0.68 m NaClO_4 solutions of known free hydrogen ion concentration. The electrode calibration solutions were prepared by gravimetric addition of HClO_4 to the NaClO_4 background electrolyte. The HClO_4 was standardized relative to a primary standard Na_2CO_3 solution. The response of the electrode was within 0.02% of the theoretical Nernst slope. The pH of the $\text{Fe}(\text{III})$ solutions ranged from 1.6 to 3.1. The HClO_4 used to establish pH will be completely dissociated in the NaClO_4 media. Since no weak acids were added to the system which could change the proton balance, $[\text{H}^+]$ will be independent of pressure. Changes in the pH with pressure due to protolytic impurities or $\text{Fe}(\text{III})$ hydrolysis will be insignificant due to the buffering capacity of the free proton at pH 3.1 and below.

Absorbance measurements were made with a Shimadzu UV-260 recording spectrophotometer. Spectral data were acquired digitally over the wavelength range 400-190 nm and were transferred to a microcomputer for data analysis. Spectra of $\text{Fe}(\text{III})$ solutions at different pH were measured over the pressure range from atmospheric to 1000 bars using a high pressure optical cell. The cell consists of a steel pressure chamber and a 1e Noble type quartz internal cell (1e Noble and Schlott, 1976) with a 7 cm pathlength. Details of the high pressure cell are

presented elsewhere (King and Kester, 1988). Pressure is reported as gauge pressure above one atmosphere. All spectra were referenced to Milli-Q water at 1 bar in the reference light path. The Fe(III) spectra were corrected by subtracting a baseline spectrum of the NaClO₄ background electrolyte. The NaClO₄ spectrum did not change with pressure.

Results

Spectra of Fe(III) solutions at several pH and atmospheric pressure are shown in Figure 1. Similar spectra were obtained at 355, 605, and 905 bars. The isosbestic point wavelength was determined at each pressure from the intersection of spectra of three Fe (III) solutions. The mean isosbestic point wavelength for all pressures was 272 ± 1 nm. There was no pressure dependent trend in isosbestic point wavelength. The mean isosbestic point wavelength was based on all determinations. The isosbestic point wavelength found in this study agrees with the isosbestic point wavelength of 272 nm determined by other investigators (Sidall and Vosburgh, 1951; Byrne and Kester, 1978).

Absorbance ratios, $\lambda A / i A$, were measured at five wavelengths: 290, 295, 300, 310, and 330 nm on three solutions at pH 1.613, 2.284, and 3.048. The measurements were repeated at 0, 355, 605 and 905 bars pressure. The fifteen coordinate pairs, ($[H^+]$, $\lambda A / i A$), determined at each pressure were fit to equation 6 to yield values for the optical constants and $\epsilon^*_{i\beta}$. The calculated value for $\epsilon^*_{i\beta}$ and the optical constants are listed in Table 1. The results show an

Figure 1. UV spectra of Fe (III) in 0.68 m NaClO₄ at four pH.

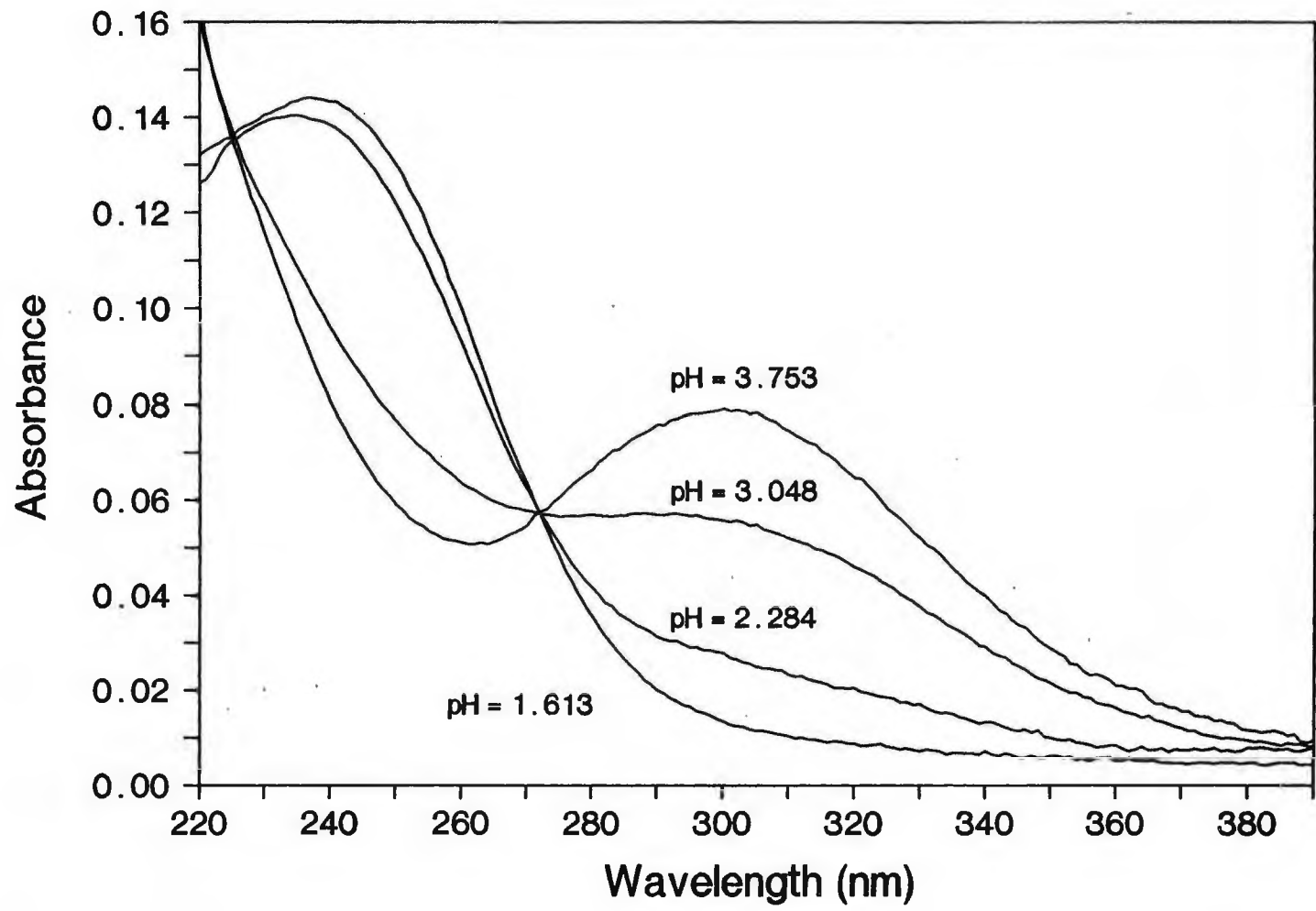


Table 1. Values for $-\log({}_1\beta^*)$ at 0, 355, 605, and 905 bars pressure and E_{Fe} , and E_{FeOH} at five wavelengths and 0, 355, 605, 905 bars pressure.

$-\log({}_1\beta^*)$	λ	E_1	E_2
	Pressure = 0 bars		
2.73	290	0.268	1.348
	295	0.203	1.375
	300	0.154	1.378
	310	0.094	1.303
	330	0.064	0.946
	Pressure = 355 bars		
2.65	290	0.285	1.196
	295	0.214	1.207
	300	0.160	1.205
	310	0.098	1.149
	330	0.064	0.833
	Pressure = 605 bars		
2.59	290	0.297	1.118
	295	0.223	1.104
	300	0.168	1.083
	310	0.105	0.996
	330	0.061	0.715
	Pressure = 905 bars		
2.52	290	0.305	1.060
	295	0.226	1.031
	295	0.169	1.002
	310	0.104	0.916
	330	0.068	0.645

increase in ${}^*_1\beta$ with increasing pressure. The optical constants also change with pressure. The value of E_1 increases with increasing pressure while E_2 decreases. Absorbance ratios were used for all the determinations so that changes in E_1 and E_2 are not due to variations in the pathlength or optical density of the solution with pressure. These results demonstrate that molal absorptivities or ratios of molal absorptivities measured at atmospheric pressure should not be assumed to be independent of pressure.

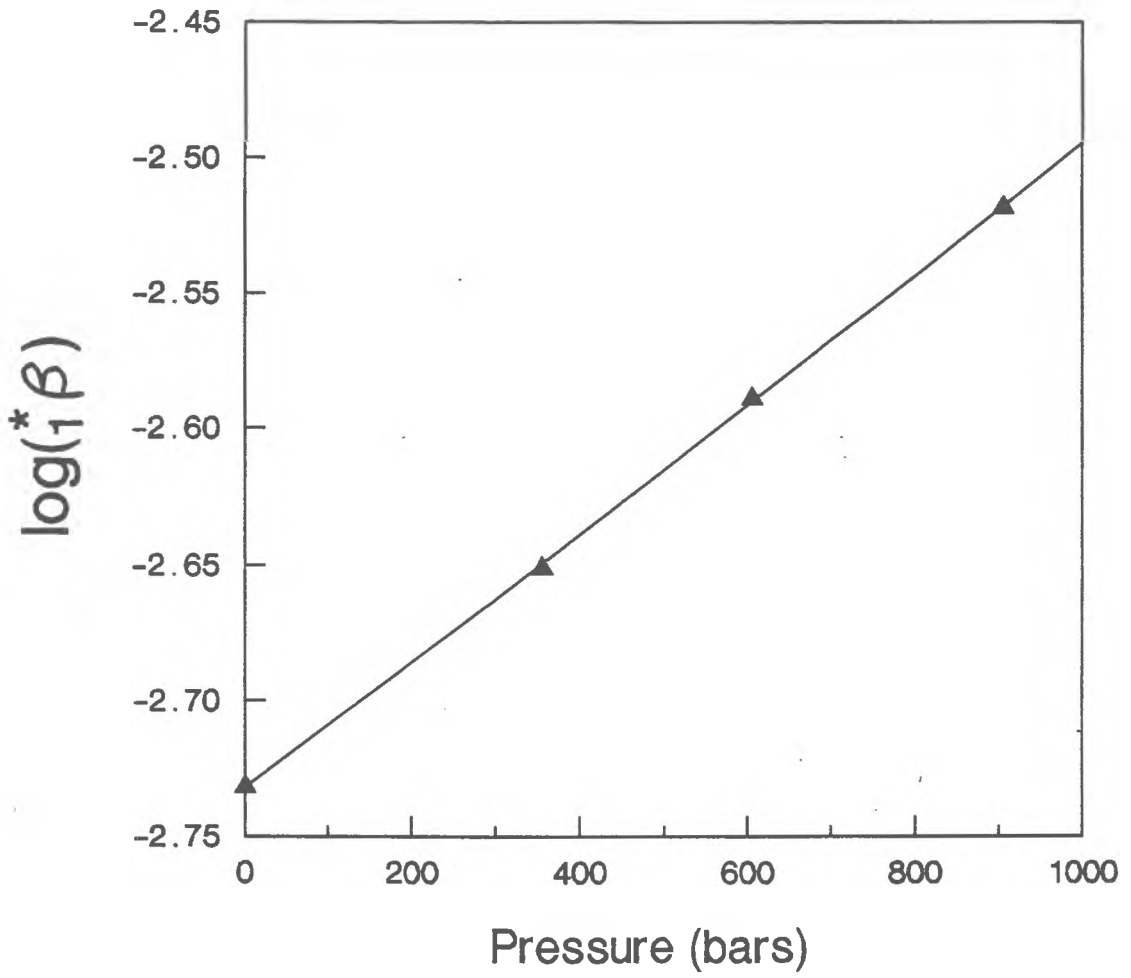
The pressure dependence on ${}^*_1\beta$ was fit to equation 9.

$$\log {}^*_1\beta_P = \log {}^*_1\beta_0 - \frac{\Delta V^*}{2.303RT} P + \frac{0.5\Delta k^*}{2.303RT} P^2 \quad (9)$$

P is the applied pressure beyond one atmosphere. The constants ΔV^* and Δk^* are the stoichiometric partial molal volume change and compressibility change in the 0.68 m NaClO_4 medium respectively. A fit of our ${}^*_1\beta$ data to equation 9 yielded values of $\Delta V^* = -13.1 \text{ cm}^3 \text{ mol}^{-1}$ and $\Delta k^* = 9.3 \times 10^{-4} \text{ cm}^3 \text{ mol}^{-1} \text{ bar}^{-1}$. The calculated Δk^* is quite small and for practical considerations can be ignored at pressures below 500 bars. At pressures above 500 bars compressibility corrections should be included. A plot of ${}^*_1\beta$ as a function of pressure and the best fit line to the data are presented in figure 2.

Our value of 1.85×10^{-3} for ${}^*_1\beta$ determined at atmospheric pressure is in good agreement with the value of $1.90 \pm 0.07 \times 10^{-3}$ determined under similar conditions by Byrne and Kester (1978). It is

Figure 2. Values of $\log({}_1\beta^*)$ in 0.68 m NaClO₄ at 25 °C as a function of pressure. The solid line is the fit to the data using equation 9 with a slight amount of curvature associated with the compressibility term.



also in good agreement with the ${}^*_1\beta$ value of 1.87×10^{-3} of Milburn and Vosburgh (1955) corrected for ionic strength and concentration scale differences.

The ΔV^* value of -13.1 we determined is considerably lower than ΔV values determined by other investigators (3.0: Jost, 1976; 2.2: Martinez et al., 1985; 1.6: Hasinoff, 1979; and 1.1: Swaddle and Merback, 1981) at approximately the same temperature and ionic strength. Previous workers determined the effect of pressure on ${}^*_1\beta$ based on absorbance measurements of a single Fe (III) solution at one wavelength. Under these experimental conditions, independent determination of ${}^*_1\beta$ and molar absorptivities are not possible. Swaddle and Merback (1981) applied corrections for the change in optical density with compression, but in all cases no correction was made for the effect of pressure on the molal absorptivities of Fe^{3+} or FeOH^{2+} . As a result, the ΔV values determined by previous workers are apparent constants which are a function of the effect of pressure on ϵ_{Fe} , ϵ_{FeOH} , and the optical system employed. In contrast, pathlength and optical density variations in this work cancel since all calculations were based on absorbance ratios. By using several Fe(III) solutions at different pH and multiwavelength data, we were able to separate the effects of pressure on ${}^*_1\beta$, E_1 , and E_2 .

Discussion

The effect of pressure on ${}^*_1\beta$ at 25 °C over the pressure range 0 - 1000 bars is given by:

$$\log {}^*_1\beta_P = \log {}^*_1\beta_0 + \frac{13.1}{2.303RT} P + \frac{(0.5)9.3 \times 10^{-4} \Delta k^*}{2.303RT} P^2 \quad (10)$$

The intercept, $\log {}^*_1\beta_0$, is the stoichiometric hydrolysis constant of Fe (III) at atmospheric pressure. Byrne and Kester (1978) have described the temperature and ionic strength dependence on ${}^*_1\beta_0$ using

$$\log {}^*_1\beta_0 = \frac{5.192 + 13.614I^{1/2}}{1 + 3.111I^{1/2}} - 2184.0T^{-1} \quad 0 \leq I \leq 3; 277 \leq T \leq 318. \quad (11)$$

At the present time we do not know how ΔV^* and Δk^* vary with temperature and ionic strength. If we ignore these dependences, as a first approximation, equations 10 and 11 can be combined to yield:

$$\log {}_1^*\beta_P = \frac{5.192 + 13.614I^{1/2}}{1 + 3.111I^{1/2}} - \frac{2184.0}{T} + \frac{0.0684P}{T} + \frac{2.4 \times 10^{-6}P^2}{T} \quad (12)$$

This result provides an estimate of ${}_1^*\beta_P$ for conditions in the marine environment. For example, near the sea surface ($T=298$, $I=0.68$, $P=0$) ${}_1^*\beta = 1.89 \times 10^{-3}$; near hydrothermal vents ($T=279$, $I=0.68$, $P=200$) ${}_1^*\beta = 6.70 \times 10^{-4}$; and at great abyssal depths ($T=274$, $I=0.68$, $P=1000$) ${}_1^*\beta = 7.80 \times 10^{-4}$.

References

- Anderson, M. A.; and Morel, F. M. M. (1982) The influence of aqueous iron chemistry on the uptake of iron by the coastal diatom *Thalassiosira weissflogii*. *Limnology and Oceanography*, 27(5), 789-813.
- Brown, M. F.; and Kester, D. R. (1980) Ultraviolet spectroscopic studies related to iron complexes in marine systems. *Thalassia Jugoslavica*, 16(2-4), 191-201.
- Byrne, R. H., and D. R. Kester (1976) A potentiometric study of ferric ion complexes in synthetic media and seawater. *Marine Chemistry*, 4, 275-278.
- Byrne, R. H., and D. R. Kester (1978) Ultraviolet spectroscopic study of ferric hydroxide complexation. *Journal of Solution Chemistry*, 7(5), 373-83.
- Byrne, R. H., and D. R. Kester (1976) Solubility of hydrous ferric oxide and iron speciation in seawater. *Marine Chemistry*, 4, 255-274.
- Byrne, R. H., and D. R. Kester (1981) Ultraviolet spectroscopic study of ferric equilibria at high chloride concentrations. *Journal of Solution Chemistry*, 10(1), 51-67.

Caceci, M. S.; and Cacheris, W. P. (1984) Fitting curves to data. *Byte*, 9(5), 340-362.

Dickson, A. G. (1984) pH scales and proton-transfer reactions in saline media such as seawater. *Geochimica et Cosmochimica Acta*, 48, 2299-2308.

Elrod, J.; and D. R. Kester (1980) Stability constants of iron(III) borate complexes. *Journal of Solution Chemistry*, 9(11), 885-94.

Hasinoff, B. B. (1979) Fast reaction kinetics of the binding of bromide to iron (III) studied on a high pressure laser temperature jump apparatus. *Canadian Journal of Chemistry*, 57, 77-82.

Jost, A. (1976) Fast reactions in solutions at high pressure. III. The effect of pressure on the reaction of iron (III)-ions with thiocyanate in water up to 2 Kbar @ 25 °C. *Berichte der Bunsen-Gesellschaft für Physikalische Chemie*, 80(4), 316-321.

Kester, D. R. (1986) Equilibrium models in seawater: applications and limitations. In: *The Importance of Chemical Speciation in Environmental Process.*, Bernhard, M.; Brinckman, F. E.; and Sadler, P. J., editors, Dahlem Konferenzen 1986, Springer-Verlag, Berlin, 337-363.

- Kester, D. R., Byrne Jr., R. H.; and Liang, Y.-J. (1975) Redox reactions and solution complexes of iron in marine systems. ACS Symposium Series (18), Marine Chemistry in the Coastal Environment, , 56-79.
- King, D. W.; and Kester, D. R. (1988) The effect of pressure on the dissociation of sulfonephthalein indicators. Journal of Solution Chemistry, submitted.
- le Noble, W. J.; and Schlott, R. (1976) All quartz optical cell of constant diameter for use in high pressure studies. Review of Scientific Instruments, 47, 770.
- Martinez, P., R. van Eldik, and H. Kelm (1985) The effect of ionic strength and pressure on the hydrolysis equilibrium of aquated iron(III) ions. Berichte der Busen-Gesellschaft fur Physikalische Chemie, 89, 81-86.
- Milburn, R. M.; and Vosburgh, W. C. (1955) A spectroscopic study of the hydrolysis of iron (III) ion. Polynuclear species. Journal of the American Chemical Society, 77, 1352-1355.
- Siddall, T. H. and W. C. Vosburgh (1951) A spectrophotometric study of the hydrolysis of iron(III) ion. Journal of the American Chemical Society, 73, 4270-4272.

Swaddle, T. W. and A. E. Merback (1981) High-pressure oxygen-17 fourier transform nuclear magnetic resonance spectroscopy. Mechanism of water exchange on iron(III) in acidic aqueous solution. *Inorganic Chemistry*, 20, 4212-4216.

The Effect of Pressure on the Oxidation Rate of Fe(II) in Seawater.

Abstract

The effect of pressure on the rate of Fe(II) oxidation by O₂ in seawater was determined over the range 0-900 bars and a pH range 7.0-8.2. The pseudo first order oxidation rate constant, k',

$$d\text{Fe(II)}/dt = k'\text{Fe(II)}$$

exhibited a second degree [H⁺] dependence at all pressures. At constant pH, k' increased with increasing pressure. The change in k' was due to the increase in [OH⁻] with pressure from the dissociation of H₂O. The pressure dependence on k' was insignificant when the data were transformed to a constant pOH scale. The overall rate constant, k,

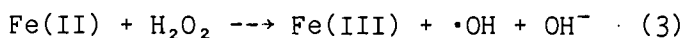
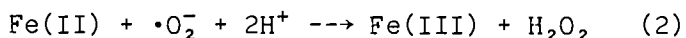
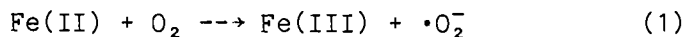
$$d\text{Fe(II)}/dt = k[\text{O}_2][\text{OH}^-]^2\text{Fe(II)}$$

was independent of pressure implying an activation volume of 0 cm³ mol⁻¹ for Fe(II) oxidation by O₂ in natural seawater.

Introduction

In seawater containing dissolved oxygen, Fe(III) is the thermodynamically stable form of iron. Reduced iron, Fe(II), is continuously being input into the oceans from reducing sediments, hydrothermal systems, and possibly through photochemical or biological reduction of Fe(III). Due to the relatively short time scale of Fe(II) oxidation, the concentration and distribution of reduced iron will be controlled by Fe(II) production and oxidation rates rather than large scale mixing and transport processes. It is therefore important to have reliable data for Fe(II) oxidation rates over the full range of oceanic salinities, temperatures and pressures.

The four step Haber-Weiss cycle has been proposed as the mechanism for Fe(II) oxidation (Fallab, 1967).

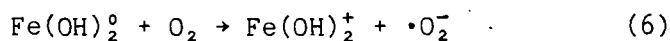


Reaction steps 1 and 3 are considerably slower than steps 2 and 4. In surface waters, the observed rate will be controlled by the rate of Fe(II) oxidation by oxygen and hydrogen peroxide (Moffett and Zika, 1987). In deep sea environments where H_2O_2 is not present, the oxidation rate will be controlled by O_2 alone. In recent years the oxidation rate of Fe(II) by O_2 in seawater has been studied extensively over a range of temperatures and salinities (Kester et al., 1975;

Murray and Gill, 1978; Liang, 1982; Roekens and Grieken, 1983; Waite and Morel, 1984; and Millero et al., 1987). However, no measurements have been made on the effect of pressure on Fe(II) oxidation rates. At constant pH and $[O_2]$, $dFe(II)/dt$ follows pseudo first order kinetics

$$dFe(II)/dt = k' Fe(II) \quad (5)$$

where k' is the pseudo first order rate constant. The effect of pH on k' across a wide pH range (5-9) has been investigated by Roekens and Van Grieken (1983) and Millero et al. (1987). Over the pH range of natural seawater (7.0-8.2) a second degree $[H^+]$ dependence was observed. Similar second degree $[H^+]$ dependence has been established by other investigators (Stumm and Lee, 1961; Liang, 1982; Davison and Seed, 1983). Kester et al. (1975) and Millero (1985) have proposed that the second degree $[H^+]$ dependence could be due to the rate limiting reaction step



with other Fe(II) species such as Fe^{2+} , $FeCl^+$, or $FeOH^+$ having even slower rates of reaction with O_2 . The concentration of $Fe(OH)_2^0$ can be predicted from total Fe(II) concentrations according to equation 7:

$$[Fe(OH)_2^0] = \{Fe(II)\} \alpha \beta_2 / [H^+]^2 \quad (7)$$

where square brackets and curly brackets indicate free and total

concentrations. β_2 is the second hydrolysis constant of Fe(II). α is the free to total ratio of Fe(II). α is a function of Fe(II) complexation in seawater. Over the pH range 6.0 - 8.2, α has an approximate value of 0.7 and is insensitive to pH (Appendix VII) Equations 5, 6, and 7 lead to a rate equation over the pH range 7.0 - 8.2:

$$\begin{aligned} d\text{Fe(II)}/dt &= k_2\{\text{Fe(II)}\}\alpha[\text{O}_2]\beta_2/[\text{H}^+]^2 \\ &= k_2\{\text{Fe(II)}\}\alpha[\text{O}_2][\text{OH}^-]^2\beta_2/(\text{K}_w^*)^2 \quad (8) \end{aligned}$$

where k_2 is the rate constant for Fe(OH)_2^0 oxidation and K_w^* is the molal dissociation constant for seawater. The overall rate constant for Fe(II) oxidation, k , can be written in the simplified form:

$$k = k_2\alpha\beta_2/(\text{K}_w^*)^2 \quad (9)$$

as long as the second degree $[\text{H}^+]$ dependence is obeyed.

We determined Fe(II) oxidation rates as a function of pH over the pressure range 0-1000 bars. Our high pressure data can be combined with published data on the effect of temperature and salinity on Fe(II) oxidation rates at atmospheric pressure to predict Fe(II) oxidation rates over the full range of oceanic environments.

Experimental

Reagents. All reagents were prepared from reagent grade salts and

distilled deionized Milli-Q water. The Fe(II) stock solution, 0.01 M, was prepared from $\text{Fe}(\text{NH}_4)_2(\text{SO}_4)_2$ (J. T. Baker) dissolved in 0.03 M HCl. The Seawater was collected in the Sargasso Sea and diluted by weight with Milli-Q to 35 ‰ salinity. The final concentration of Fe(II) in the seawater samples was 5×10^{-6} M. The addition of the acidic Fe(II) stock to the seawater samples changed the alkalinity by less than 0.6 %.

Determination of k' . Two methods were used to measure the pseudo first order oxidation rate of Fe(II). At atmospheric pressure, a continuous flow analysis system, CFA, was used to measure Fe(II) concentrations continuously with time. Figure 1 is a diagram of the CFA system. The colorimetric reagent Ferrozine was used for the Fe(II) analysis (Stookey, 1970). A tubing pump delivered seawater sample and Ferrozine reagent to a mixing coil at a constant rate. From the mixing coil the solution was passed through a 7 cm flow cell and the solution absorbance measured at 540 nm. The CFA was interfaced to a microcomputer for digital data acquisition. Response of the CFA was linear over the Fe(II) concentration range 0.2 - 5.0 μM . Fe(III) interferences were not detectable. All samples were contained in a stirred vessel thermostated to 25.0 ± 0.1 °C. Figure 2 is a typical plot of Fe(II) concentration as a function of time obtained using the CFA system. The pseudo first order oxidation rate of Fe(II) was determined from the log linearized decrease in Fe(II) with time.

At elevated pressures the CFA system could not be employed. An alternative method was to measure the production of Fe(III) as a function of time. Fe(III) has a strong UV absorbance at 240 nm. The concentration of Fe(III) at any time, t , can be determined using a

Figure 1. Diagram of the continuous flow analysis system used for Fe(II) determinations at atmospheric pressure.

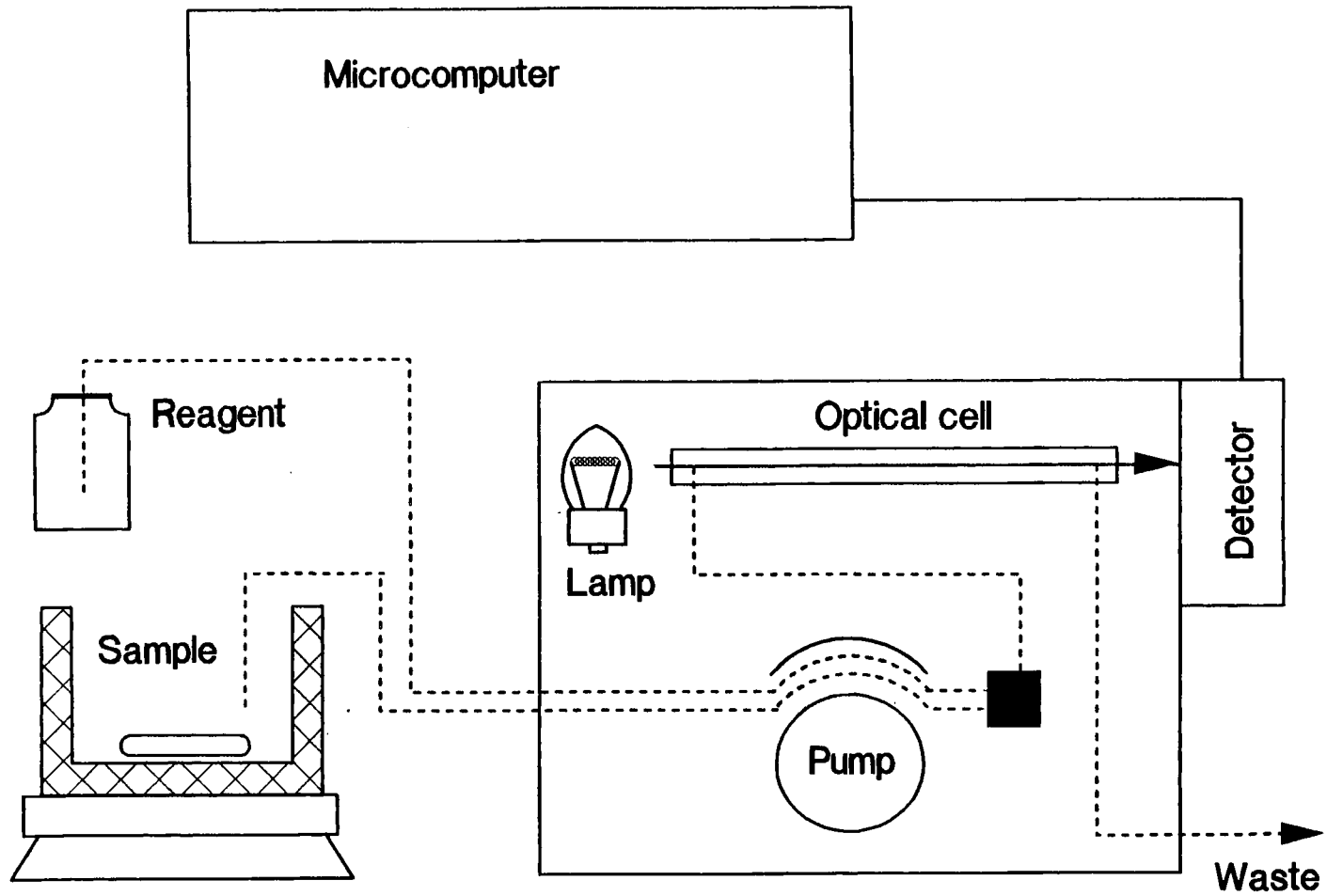
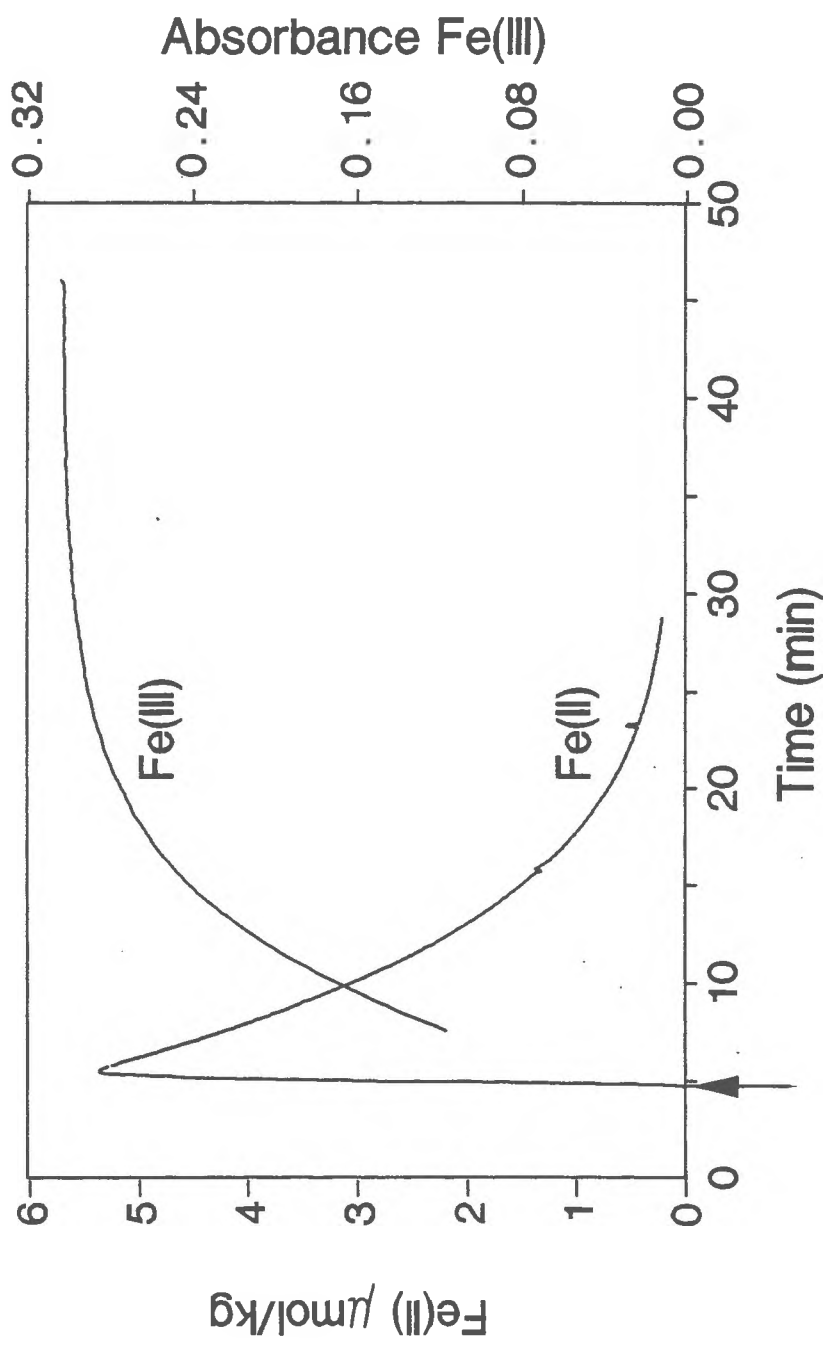




Figure 2. Fe(II) concentrations and Fe(III) absorbances as a function of time. Fe(II) concentrations were determined using the CFA system. Fe(III) absorbances were monitored using the spectrophotometer system. The arrow indicates the addition of $5.4 \mu\text{mol kg}^{-1}$ Fe(II). The seawater pH was 7.749.



simple Beer's law relationship:

$$\{\text{Fe(III)}\}_t = A_t/\ell\epsilon \quad (10)$$

where ϵ is the molar absorptivity of the Fe(III) species and ℓ is the pathlength of the optical cell. The concentration of Fe(II) is determined by mass balance:

$$\{\text{Fe(II)}\}_t = T_{\text{Fe}} - \{\text{Fe(III)}\}_t \quad (11)$$

where T_{Fe} is the total iron concentration. T_{Fe} can be established from the Fe(III) absorbance at t_∞ .

$$T_{\text{Fe}} = A_\infty/\ell\epsilon \quad (12)$$

Since $\{\text{Fe(II)}\}_0 = T_{\text{Fe}}$, equations 10, 11, and 12 can be combined to yield the $\{\text{Fe(II)}\}_t/\{\text{Fe(II)}\}_0$ ratio as a function of time.

$$\frac{\{\text{Fe(II)}\}_t}{\{\text{Fe(II)}\}_0} = \frac{A_\infty - A_t}{A_\infty} \quad (13)$$

The the molar absorptivity and pathlength terms cancel. The Fe(II) pseudo first order oxidation rate was determined by solving equation 14 for k' as a function of Fe(III) absorbance and time.

$$\ln\left(\frac{A_{\infty} - A_t}{A_{\infty}}\right) = -k't \quad (14)$$

For experiments with Fe(II) oxidation half lives less than 5 minutes, A_{∞} could be measured directly and k' determined using a simple linear regression. For experiments with Fe(II) oxidation half lives longer than five minutes, k' and A_{∞} were determined simultaneously using a nonlinear least squares algorithm.

All absorbance measurements were made using a Shimadzu UV 260 scanning spectrophotometer. The spectrophotometer was interfaced to a microcomputer for digital data acquisition and analysis. Over 2000 absorbance measurements were made over the 50 - 80 minute duration of each oxidation experiment. Absorbance measurements at atmospheric pressure were made in thermostated (25.0 ± 0.1 °C) 10 cm quartz cells. Figure 2 shows a typical plot of Fe(III) absorbance as a function of time obtained using the spectrophotometer system at atmospheric pressure. Absorbance measurements at high pressure were made using a custom designed high pressure optical cell described previously (King and Kester, 1988a). The time required for Fe(II) addition and compression of the sample in the high pressure cell was approximately 2 minutes. This set the minimum half life of two minutes for high pressure Fe(II) oxidation experiments. By adjusting the initial pH of the seawater samples to less than 7.9 this requirement was met.

The Fe(III) produced by Fe(II) oxidation will exceed the solubility of Fe(III) by several orders of magnitude (Byrne and Kester, 1976).

The measured absorbance will be the net result of absorbance by dissolved, colloidal, and particulate Fe(III) and scattering by particles. For solutions containing particulate material Beer's law may not be strictly obeyed. In order to confirm the validity of the absorbance method used in these experiments, the pseudo first order Fe(II) oxidation rate at atmospheric pressure were determined using both Fe(III) absorbance and CFA methods.

pH Measurement and Control. The pseudo first order oxidation rate of Fe(II) is strongly pH dependent. Accurate pH measurements are essential for interpretation and intercomparison of Fe(II) oxidation rates. All pH measurements were made on the free hydrogen ion pH scale (Dickson, 1984). The pH of the seawater samples was adjusted by purging the seawater sample with a CO₂/air mixture. All samples were purged for at least one hour to establish a constant pH.

Measurements of pH at atmospheric pressure were made with sulfonephthalein pH indicators (King and Kester, 1988b) and an Orion Ross 8102 combination pH electrode with 4.0 m NaCl filling solution. The pH of seawater solutions without added Fe(II) were determined with the pH indicators. Changes in the pH due to Fe(II) addition were determined using the electrode. The electrode response was within 0.5 % of the theoretical Nernst slope.

Measurements of pH at elevated pressures were made using pH indicators (King and Kester 1988b). The pH at high pressure was determined from the pH change with compression of a sample aliquot without added Fe(II) and the initial pH of the sample at atmospheric pressure. The addition of Fe(II) resulted in a small (0.04) decrease in the pH of the seawater sample. Over the pH range of the high

pressure experiments (7.0-7.8), a 0.04 decrease in initial pH did not affect compressional pH changes by more than 0.004 pH units.

The pOH of the samples were determined from the pH and pK_W^* of the seawater sample ($pOH = pK_W^* - pH$). The effect of temperature and ionic strength on K_W^* at atmospheric pressure was calculated using the equation:

$$\begin{aligned} \ln K_W^* = & 148.9802 - 13847.26/T - 23.6521 \ln T \\ & + 2[I^{1/2}/(1+1.2) + 1.667 \ln(1 + 1.2I^{1/2})] \\ & \times (-5.8901 + 228.2338/T + 0.968144 \ln T) \\ & - I(20.6365 - 945.556/T - 3.00298 \ln T) \\ & - 0.18062[1 - (1 + 2I^{1/2} - 2I)\exp(-2I^{1/2})] \\ & - I^2(-0.05346 + 17.6216/T) \end{aligned} \quad (15)$$

where $T = t + 273.15$ and I is the total ionic strength (Millero et al., 1987). The total ionic strength was calculated from the seawater salinity (Millero, 1982).

$$I = 19.9201 S(10^3 - 1.00488 S) \quad (16)$$

The pressure dependence on K_W^* was calculated from the partial molal volume change, ΔV^* , and partial molal compressibility change, Δk^* , for water dissociation according to equation 17.

$$\log K_{WP}^* = \log K_W^* - \frac{\Delta V^*}{2.303RT} P + \frac{0.5\Delta k^*}{2.303RT} P^2 \quad (17)$$

Values for ΔV^* and Δk^* have not been determined directly in seawater. However, estimates for ΔV^* and Δk^* can be determined from density measurements in simple salt solutions as described by Millero et al. (1972) and Millero (1983). Estimates of ΔV^* and Δk^* in 35 ‰ seawater as a function of temperature were calculated from

$$\Delta V^* = -20.02 + 0.1119t - 1.409 \times 10^{-3}t^2 \quad (18)$$

$$\Delta k^* = -5.13 \times 10^{-3} + 7.94 \times 10^{-5}t. \quad (19)$$

Data for the salinity dependence on ΔV^* and Δk^* are not available. Fortunately, the salinity variations in the deep sea are small so that differences in ΔV^* and Δk^* due to salinity changes should be negligible.

O₂ Solubility. All seawater samples were saturated with air by sparging the solution for more than one hour with the CO₂/air mixture. The partial pressure of CO₂ in the sparging solution was less than 0.005 atm and did not significantly affect O₂ partial pressure. The dissolved oxygen concentrations were calculated from the equilibrium partial pressure of O₂ using the equation of Benson and Krause (1984) converted to the molal concentration scale.

$$\begin{aligned} \ln[O_2] = & -135.29996 + 1.572288 \times 10^5/T \\ & - 6.637149 \times 10^7/T^2 + 1.243678 \times 10^{10}/T^3 \\ & - 8.62106 \times 10^{11}/T^4 - S(0.020573 - 12.142/T + 2362.1/T^2) \\ & + \ln(1 + 10^{-3}S) \quad \mu\text{mol (kg H}_2\text{O)}^{-1} \quad (20) \end{aligned}$$

Seawater samples used in the high pressure experiments were saturated with air at atmospheric pressure. Care was taken to exclude air bubbles from the high pressure samples to prevent changes in O₂ concentration with compression.

Results and Discussion

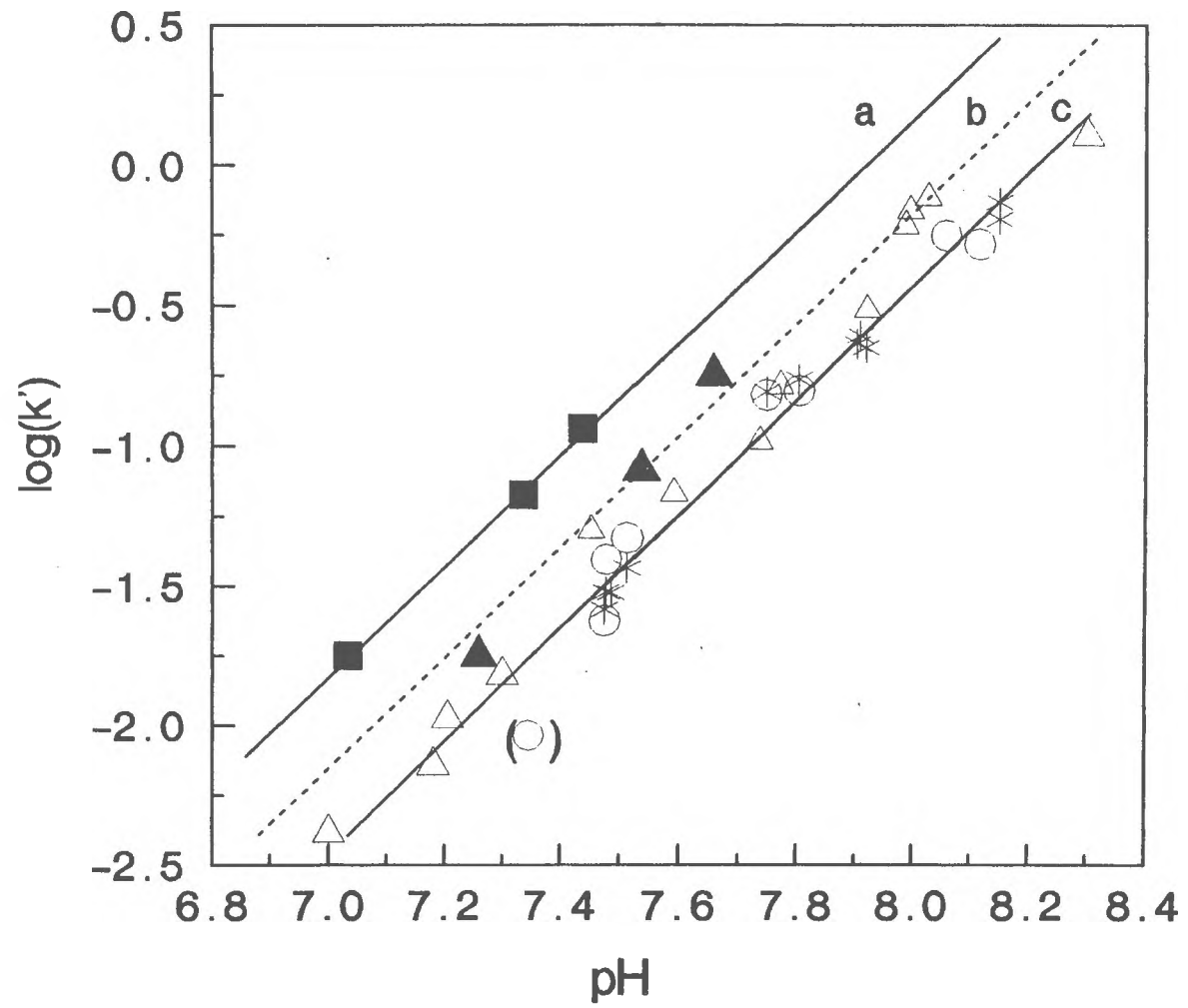
The results of our oxidation experiments are presented in Table I. The pseudo first order rate constant was determined over the pH range 7.0 - 8.2 at three pressures. Figure 3 is a plot of k' as a function of pH. Regression slopes of k' as a function of pH were calculated at each pressure. The slope of 2.01 ± 0.08 obtained at atmospheric pressure is consistent with the second degree [H⁺] dependence observed by other investigators. With the exception of one point at pH 7.35, k' values determined using the absorbance method were in good agreement with k' determined using the CFA method. The agreement between the two methods supports the validity of the absorbance method. The low data point at pH 7.35 was not used in the slope calculation. In this experiment the time for oxidation of 50% of the Fe(II) was 75 minutes. At this and longer times spans the determination of A_{∞} is difficult and other rate processes such as particulate nucleation and gravitational settling may affect the results. Also plotted in Figure 3 are Fe(II) pseudo first order rate constants determined by Millero et al. (1987) under identical conditions. While their data exhibits a bit more scatter, their results are consistent with our k' values.

The regression slope for the pH dependence on k' measured at 901 bars pressure was 1.98 ± 0.08 . This slope is not statistically

Table I. Values of k' determined at 25°C in 35 ‰ salinity seawater using CFA and absorbance methods.

pH	log(k') CFA method	log(k') absorbance method	pOH
<u>0 bars</u>			
7.346		-2.04	6.280
7.476	-1.59	-1.63	6.150
7.479	-1.52	-1.41	6.147
7.487	-1.52		6.139
7.514	-1.44	-1.33	6.112
7.749	-0.81	-0.82	5.877
7.805	-0.77	-0.81	5.821
7.906	-0.64		5.720
7.911	-0.61		5.715
7.921	-0.65		5.705
8.059		-0.25	5.567
8.117		-0.28	5.509
8.151	-0.19		5.475
8.151	-0.13		5.475
<u>441 bars</u>			
7.260		-1.17	6.221
7.538		-1.09	5.943
7.659		-0.75	5.822
<u>901 BARS</u>			
7.034		-1.75	6.284
7.337		-1.17	5.981
7.439		-0.94	5.879

Figure 3. Pseudo first order rate constant for Fe(II) as a function of pH. Open symbols are for k' determined at atmospheric pressure by: * absorbance method, o CFA method, Δ Millero et. al. (1987). The solid symbols are for k' at: \blacktriangle 441, and \blacksquare 901 bars. The solid lines labeled c and a are regression lines through the 0 and 901 bar data. The dashed line, b, is the predicted regression line for the 441 bar data.



different from the slope obtained at atmospheric pressure. The regression slope determined for the 441 bar data was 2.47 ± 0.08 which is not in good agreement with the data obtained at 0 and 901 bars. We think it is unlikely that the pH-dependence mechanism for this reaction is different at 441 bar than at 0 and 901 bars. We would like to have conducted the high pressure experiments over a larger range of pH and time-scales, but the time required to manipulate the loading and pressurization of the pressure cell (2 minutes) sets an upper limit on the pH that can be used. Particulate nucleation and settling set the lower limit on the pH that can be used.

The pH dependence on the pseudo first order rate constant reflects the dependence of the rate on the square of the $[\text{OH}^-]$ concentration. In order to remove the effect of pressure on $[\text{OH}^-]$, the pseudo first order rate has been plotted as a function of pOH in Figure 4. No pressure effect is observed if the pseudo first order rates are compared at constant pOH. The observed pressure dependence on k' at constant pH is due to the effect of pressure on the pK_w^* of water.

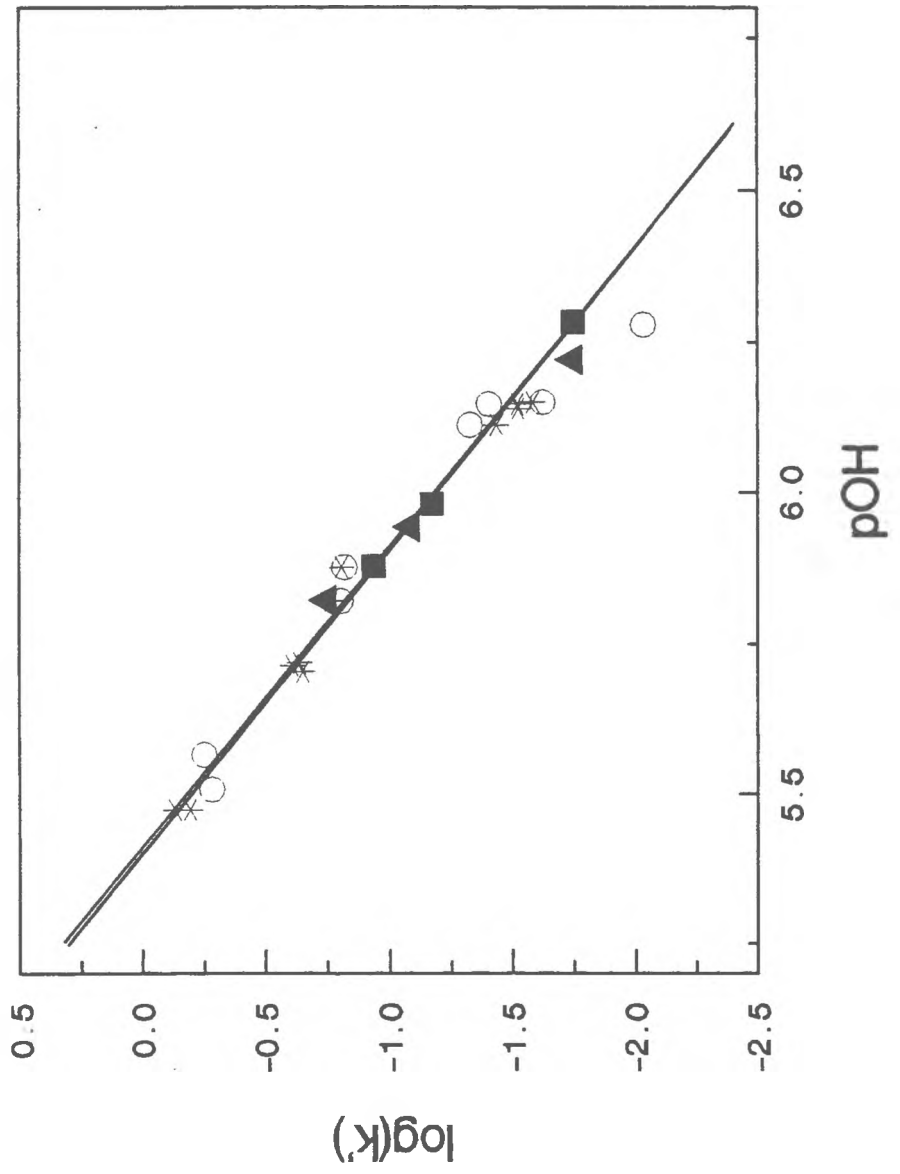
Over the pOH range 5.5 to 6.5 where the second degree $[\text{OH}^-]$ dependence is obeyed, k can be calculated from k' , $[\text{OH}^-]$ and $[\text{O}_2]$.

$$k = k' / [\text{OH}^-]^2 [\text{O}_2] \quad (21)$$

Pooling all our data, we obtain a value for $\log(k)$ of 14.48 ± 0.07 $\text{mol}^{-3} (\text{kg H}_2\text{O})^3 \text{min}^{-1}$ which is in good agreement with values of 14.59 ± 0.06 and 14.50 ± 0.06 obtained by Millero et al. (1987) for Gulf Stream and Biscayne Bay waters respectively.

The effect of pressure on the rate constants can be predicted from

Figure 4. Pseudo first order rate constant for Fe(II) as a function of pOH. Labels are the same as Figure 3.



transition state theory:

$$\partial \ln k / \partial P = -\Delta V^\ddagger / RT \quad (22)$$

where ΔV^\ddagger is the partial molal volume change due to the formation of the activated complex (Stumm and Morgan, 1981). The lack of pressure dependence on k implies a ΔV^\ddagger of 0 for Fe(II) oxidation. The zero ΔV^\ddagger may indicate that the hydration and electrostriction effects are the same for the activated complex and the reacting species. The observed ΔV^\ddagger is actually a hybrid constant reflecting the effect of pressure on Fe(II) speciation and the oxidation rates of the individual Fe(II) species. Data on the effect of pressure on Fe(II) speciation are not available.

Application to Natural Systems. Application of our high pressure data to natural systems requires extrapolation of our results made at 25 °C to lower temperatures and natural Fe(II) concentrations. We do not currently have data on the variation of ΔV^\ddagger with temperature. Assuming ΔV^\ddagger is temperature independent, as a first approximation, k becomes independent of pressure. This implies that k values determined at atmospheric pressure are valid over the full oceanic pressure range. The effect of temperature and salinity on k at atmospheric pressure has been described by Millero et al. (1987).

$$\log k = 21.56 - 1545/T - 3.29\sqrt{I} + 1.52I \quad (23)$$

The pseudo first order rate constant can be determined from $[O_2]$ and pH data. The $[OH^-]$ can be calculated from the observed pH and pK_w^*

calculated using equations 15 and 17.

Our high pressure experiments and the experiments of others (Murray and Gill, 1978; Liang, 1982; Roekens and Grieken, 1983; and Millero et al., 1987) determined the oxidation rate of Fe(II) with initial Fe(II) concentrations greater than $1 \mu\text{mol kg}^{-1}$. Natural Fe(II) concentrations range from 50 nmol kg^{-1} above strongly reducing organic rich sediments to less than 1 nmol kg^{-1} in open ocean waters (Hong and Kester, 1986). At concentrations below 0.5 nmol kg^{-1} , it is possible that other trace species in seawater will compete with Fe(II) for $\cdot\text{O}_2^-$, H_2O_2 , and $\cdot\text{OH}$. If these chain propagating oxide species are scavenged, then the rate of Fe (II) oxidation could be reduced by up to 75% (Moffet and Zika, 1987; King and Kester, 1988c).

Complexation of Fe(II) by dissolved organic material could also reduce Fe(II) oxidation rates by forming stable Fe(II)-organic complexes. Millero et al. (1987) observed a decrease in Fe(II) oxidation rates in organic rich Biscayne Bay water. In a recent study, we observed the same Fe(II) oxidation rates when 28 nmol kg^{-1} Fe(II) was added to Narragansett Bay seawater as in experiments with $> 1 \mu\text{mol kg}^{-1}$. However, the oxidation rate of naturally occurring Fe(II) at $6\text{-}10 \text{ nmol kg}^{-1}$ was 10-15 times less than the rate for added Fe(II). We attribute these differences in the observed oxidation rates to differences in speciation of naturally occurring and added Fe(II) (King and Kester, 1988c).

In environments such a deep sea hydrothermal systems where Fe(II) concentrations are high and Fe(II) speciation is controlled by inorganic complexation, the Fe(II) oxidation rates determined in this study should be applicable. In other environments where Fe(II)

concentrations are below 0.5 nmol kg^{-1} or where Fe(II) forms strong organic or particulate complexes, our high pressure data should be considered an upper limit for Fe(II) oxidation rates.

References

- Benson, B. B.; and Krause Jr., D. (1984) The concentration and isotopic fractionation of oxygen dissolved in freshwater and seawater with the atmosphere. *Limnology and Oceanography*, 29, 620-632.
- Byrne, R. H., and D. R. Kester (1976) Solubility of hydrous ferric oxide and iron speciation in seawater. *Marine Chemistry*, 4, 255-274.
- Davison, W.; and Seed, G. (1983) The kinetics of the oxidation of ferrous iron in synthetic and natural waters. *Geochimica et Cosmochimica Acta*, 47, 67-79.
- Dickson, A. G. (1984) pH scales and proton-transfer reactions in saline media such as seawater. *Geochimica et Cosmochimica Acta*, 48, 2299-2308.
- Fallab, S. (1967) Reactions with molecular oxygen. *Angewandte Chemie International Edition in English*, 6, 496-507.
- Hong, H. and D. R. Kester (1986) Redox state of iron in the offshore waters of Peru. *Limnology and Oceanography*, 31(3), 512-524.

- Kester, D. R., Byrne Jr., R. H.; and Liang, Y.-J. (1975) Redox reactions and solution complexes of iron in marine systems. ACS Symposium Series (18), Marine Chemistry in the Coastal Environment, 56-79.
- King, D. W.; and Kester, D. R. (1988a) Determination of seawater pH from 1.5 to 8.5 using colorimetric indicators. Marine Chemistry, accepted.
- King, D. W.; and Kester, D. R. (1988b) The effect of pressure on the dissociation of sulfonephthalein indicators. Journal of Solution Chemistry, submitted.
- King, D. W.; and Kester, D. R. (1988c) The oxidation rate of naturally occurring Fe(II) in Narragansett Bay. in preparation.
- Liang, Y.-J. (1982) Kinetics of Ferrous Iron Oxygenation and Redox Chemistry of Iron in Natural Waters. Ph.D. Thesis., University of Rhode Island, 237pp.
- Millero, F. J. (1982) Use of models to determine ionic interactions in natural waters. Thallasia Jugoslavica, 18, 253-291.

- Millero, F. J. (1983) Influence of pressure on chemical processes in the sea. *Chemical Oceanography*. vol. 8., Riley, J. P.; and Chester, R. editors, Academic Press, London, 2-88.
- Millero, F. J. (1985) The effect of ionic interactions on the oxidation of metals in natural waters. *Geochimica et Cosmochimica Acta*, 49, 547-553.
- Millero, F. J.; Hoff, E. V.; and Kahn, L. (1972) The effect of pressure on the ionization of water at various temperatures from molal-volume data. *Journal of Solution Chemistry*, 1, 309-327.
- Millero, F. J.; Scotolongo, S.; Izaguirre, M. (1987) The oxidation of Fe (II) in seawater. *Geochimica et Cosmochimica Acta*, 51, 793-801.
- Moffett, J. W.; and Zika, R. G. (1987) Reaction kinetics of hydrogen peroxide with copper and iron in seawater. *Environmental Science and Technology*, 21(8), 804-810.
- Murray, J. W.; and Gill, G. (1978) The geochemistry of iron in Puget Sound. *Geochimica et Cosmochimica Acta*, 42, 9-19.
- Roekens, E. J.; and Van Grieken, R. E. (1983) Kinetics of iron (II) oxidation in seawater of various pH. *Marine Chemistry*, 13, 195-202.

Stookey, L. C. (1970) FerroZine - A new spectrophotometric reagent for iron. *Analytical Chemistry*, 42, 779-81.

Stumm, W.; and Lee, G. F. (1961) Oxygenation of ferrous iron. *Industrial Engineering Chemistry*, 53(2), 143-146.

Stumm, W.; and Morgan, J. J. (1981) *Aquatic Chemistry* 2nd ed., Wiley-Interscience, 780 pp.

Waite, T. D.; and Morel, M. M. (1984) Coulometric study of the redox dynamics of iron in seawater. *Analytical Chemistry*, 56(4), 787-92.

The Oxidation Rate of Fe(II) at Natural Concentrations
in Narragansett Bay Seawater.

Abstract

The oxidation rate of Fe(II) in Narragansett Bay seawater was determined for naturally occurring Fe(II) and Fe(II) added at close to natural concentrations. The oxidation rate of added Fe(II) was in good agreement with predictions based on rate constants for Fe(II) oxidation by O_2 and H_2O_2 . The concentration of Fe(II) in Narragansett Bay was between 6-11 $nmol\ kg^{-1}$. The oxidation of rate naturally occurring Fe(II) was slower than the predicted rate by an order of magnitude. Stabilization of Fe(II) by adsorption onto particles or by organic complexation could explain the reduced Fe(II) oxidation rate. The Fe(II) production rate required to maintain the observed Fe(II) concentrations was $8 \pm 6\ nmol\ kg^{-1},\ hr^{-1}$. This production rate could be sustained by photochemical reduction of particulate Fe(III) to Fe(II).

Introduction

In recent years, the oxidation rate of Fe(II) in seawater has been studied by a number of researchers (Kester et al., 1975; Murray and Gill; Liang, 1982, Roekens and Van Grieken, 1983; Waite and Morel, 1984a and 1984b; Millero et al., 1987; and Moffett and Zika, 1987). With the exception of the low concentration Fe(II) addition work of Waite and Morel (1984b), all oxidation rates were determined by adding more than 100 nmol kg⁻¹ Fe(II) to seawater and monitoring the disappearance of Fe(II) with time. Data are not available for the oxidation rate of naturally occurring Fe(II) in oxic seawater. Moffett and Zika (1987) suggested that Fe(II) oxidation rates determined from experiments with high initial Fe(II) concentrations could overestimate Fe(II) oxidation rates by a factor of four. They proposed that at low Fe(II) concentrations, less than 1 nmol kg⁻¹, the Haber-Weiss oxidation cycle will be terminated after the first reaction step by trace element scavenging of $\cdot\text{O}_2^-$. Millero et al. (1987) observed a decrease in the oxidation rate of Fe(II) in organic rich seawater which they attributed to organic complexation of Fe(II). This observation is consistent with the decrease in the rate of Fe(II) oxidation in coastal Nahant seawater seen by Waite and Morel (1984b). Organic complexation of Fe(II) will be more significant at low Fe(II) concentrations where organic ligand concentrations do not become limiting.

We recently developed a new colorimetric method for Fe(II) analysis which has been used to measure natural Fe(II) concentrations in Narragansett Bay (King et al., 1988). We observed Fe(II)

concentrations of 14.6 and 4.2 nmol kg⁻¹ for unfiltered and filtered samples. Using available data for Fe(II) oxidation rates in air saturated seawater with 100 nmol kg⁻¹ H₂O₂ (Millero et al., 1987; Moffett and Zika, 1987), the pseudo first order rate constant for Fe(II) oxidation is 0.18 min⁻¹. To maintain the Fe(II) concentration in the filtered fraction in steady state, this oxidation rate implies a Fe(II) production rate of over 40 nmol kg⁻¹ hr⁻¹. This production rate is unreasonably large based on rates for photochemical reduction of Fe(II) (Waite and Morel, 1984b) and can be used as indirect evidence that the oxidation rate of naturally occurring Fe(II) is considerably slower than predicted from laboratory experiments.

In order to gain a better understanding of the processes controlling natural Fe(II) oxidation rates and quasi-steady state concentrations, we have determined the oxidation rate of Fe(II) under natural conditions. Experiments were performed to determine the oxidation rate of both naturally occurring Fe(II) and Fe(II) added at natural concentrations.

Method:

Reagents. All solutions were prepared from reagent grade salts and distilled deionized Milli-Q water. Fe(II) stock solution, 0.01 M, was prepared by dissolving Fe(NH₄)₂(SO₄)₂ in 0.03 M HCl. Ferrozine (Hack Chemical Co.) was used without purification. Acetone and methanol were Burdick and Jackson Brand high purity solvents (American Scientific).

Seawater Samples. Narragansett Bay seawater was collected off a stone jetty at the Graduate School of Oceanography, Narragansett, RI. For the Fe(II) addition experiments, the seawater was filtered through

a 0.4 μm filter and placed in the dark for several hours until the natural Fe(II) was completely oxidized. For the oxidation experiments using natural Fe(II), the seawater was collected between 08:00 and 09:00 and returned to the lab for Fe(II) analysis within 15 minutes.

Fe(II) analysis. Fe(II) concentrations were determined colorimetrically using the Ferrozine reagent. The analytical method has been described previously (King et al., 1988); so it will be outlined briefly. Ferrozine forms a strong colored complex with Fe(II) but not Fe(III). The Fe(II) detection limit of the standard wet chemical Ferrozine method is 20 nmol kg^{-1} . The detection limit was improved by immobilizing the Ferrozine on a C-18 Sep-Pak (Waters Associates). The seawater sample was passed through the Sep-Pak with the Fe(II)-Ferozine complex, $\text{Fe}(\text{FZ})_2$, being retained. The $\text{Fe}(\text{FZ})_2$ was eluted off the Sep-Pak in a small volume of acetone and methanol and the absorbance of the combined effluents measured at 562 nm. The detection limit for Fe(II) was 0.5 nmol kg^{-1} .

H_2O_2 and pH determination. H_2O_2 was determined using the fluorometric method of Miller and Kester (1988). The method employs the formation of a fluorescent dimer by the oxidative coupling of H_2O_2 by p-hydroxyphenylacetic acid in the presence of peroxidase. The detection limit was 5 nmol kg^{-1} with a relative precision of 10%. The pH of the seawater samples were determined using an Orion Ross 8102 combination electrode with a filling solution of 4.0 M NaCl. The electrode was calibrated on the free hydrogen ion scale using Tris-seawater buffers.

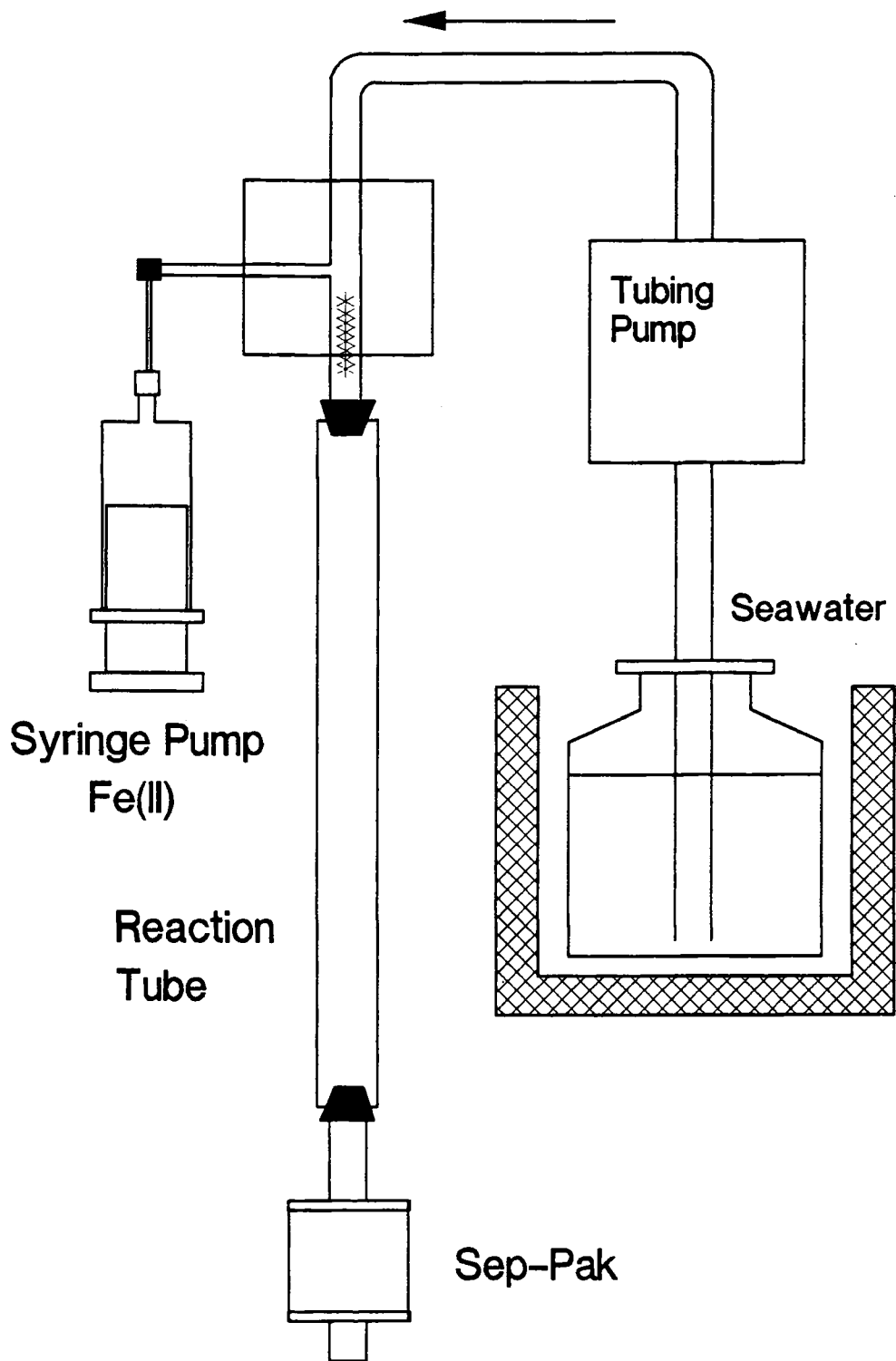
Instrumentation. A Shimadzu UV 260 scanning spectrophotometer was used for all absorbance measurements. A Perkin Elmer model 203

spectrofluorometer was used for H_2O_2 determinations.

Fe(II) oxidation rate. Two experimental techniques were utilized to establish the oxidation rate of Fe(II) in natural systems. In the first set of experiments, Fe(II) was added to seawater samples and the disappearance of Fe(II) monitored with time. The concentration of added Fe(II) was less than 30 nmol kg^{-1} so that experimental conditions would match those observed for natural samples as closely as possible. In the second set of experiments, the oxidation rate of naturally occurring Fe(II) in freshly collected samples was measured directly.

For the low Fe(II) concentrations used in this study, over 150 ml of sample must be processed. The processing time for a sample, approximately 9 minutes, precluded batch experiments since the half life of Fe(II) oxidation was less than 2 minutes. The flow system shown in Figure 1 allowed determination of Fe(II) oxidation rates on the time scale of seconds. Seawater samples were drawn from a thermostated 2 liter sample vessel through a tubing pump (CFA 2000, Scientific Instruments Co.) and into a flow injection chamber. Fe(II) stock solution, $1 \times 10^{-6} \text{ m}$, was injected into the flow stream using a model 341 Sage Instruments Syringe Pump. The Fe(II) concentration in the samples was controlled by adjusting the flow rate of the seawater and Fe(II) stock. Teflon screening just downstream of the Fe(II) injection ensured complete mixing of the Fe(II) with the seawater. The samples then passed through a teflon reaction tube and finally through a Sep-Pak cartridge which had been loaded with Ferrozine. The time span for Fe(II) oxidation was adjusted by changing the length of the reaction tube. The diameter of the reaction tube was 4 mm and ranged

Figure 1. Flow system used to determine the oxidation rate of Fe(II) added to Narragansett Bay seawater.

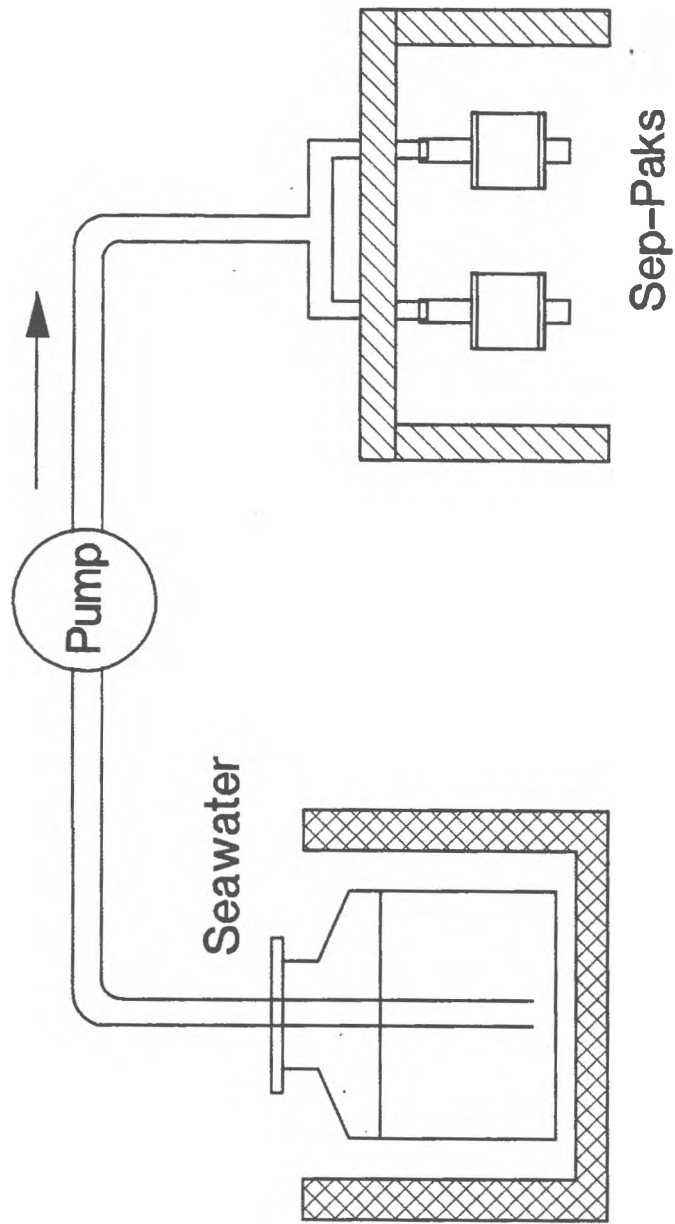


from 3 to 30 cm in length. The seawater flow rate was 2.00 ml min^{-1} . The solution residence time in the reaction tube was between 0.3 and 2.3 minutes. Seawater blanks for the Fe(II) analysis were obtained using the flow system without added Fe(II).

A modification of the flow system was used to determine the oxidation rate of naturally occurring Fe(II). The flow system could be simplified because the oxidation rate of natural Fe(II) was considerably slower than the oxidation rate of added Fe(II). Figure 2 is a diagram of the flow system. Freshly collected Narragansett Bay seawater samples were placed in the 2 l vessel. The vessel was thermostated to within 0.5 °C of the sample temperature at time of collection. The seawater was drawn from the sample vessel through a tubing pump and then passed through two Sep-Paks simultaneously. One Sep-Pak was loaded with Ferrozine and the other Sep-Pak provided a seawater blank. A 150 ml sample volume and 9 minute sampling time span was used for these experiments. The elapsed time from sample collection to the first Fe(II) analysis was less than 15 minutes. The Fe(II) concentration in the sample vessel was determined every 30 minutes for up to two hours.

Over the 9 minute sampling interval used in these experiments the concentration of Fe(II) was decreasing due to oxidation. As a result, the analysis did not provide discrete concentrations, but rather Fe(II) concentrations integrated over the duration of the sampling period. Under conditions where pseudo first order kinetics for Fe(II) oxidation are obeyed, the Fe(II) concentration at the beginning of a sampling

Figure 2. Flow system used to determine the oxidation rate of naturally occurring Fe(II).



period can be estimated using the equation:

$$\{Fe(II)\}_t = \{Fe(II)\}_{int,t} \Delta t k' / (1 - e^{-k' \Delta t}) \quad (1)$$

where $\{Fe(II)\}_t$ is the Fe(II) concentration at the beginning of the sampling interval, $\{Fe(II)\}_{int,t}$ is the integrated Fe(II) concentration measured using the Ferrozine method, Δt is the sampling time interval, and k' is the pseudo first order rate constant. Equation 1 was derived from the mean value theorem. The Fe(II) concentration at time t can be described in terms of the first order decay equation.

$$\{Fe(II)\}_t = \{Fe(II)\}_0 e^{-k't} \quad (2)$$

Substituting equation 1 into equation 2 and reorganizing, a general equation relating measured Fe(II) concentrations in terms of first order decay kinetics was obtained.

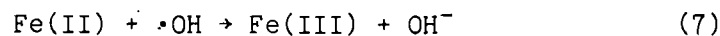
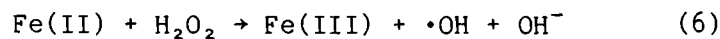
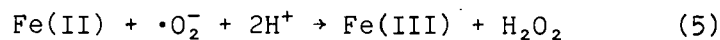
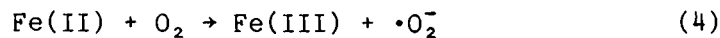
$$\ln \left[\frac{\{Fe(II)\}_{int,t}}{\{Fe(II)\}_{int,0}} \right] = -k't - \ln \left[\frac{\Delta t k'}{1 - e^{-\Delta t k'}} \right] \quad (3)$$

Since the same sampling interval was used for all samples (Δt was constant), equation 3 has a simple linear solution. A plot of left side of equation 3 as a function of time has a slope of $-k'$ and an intercept of $-\ln[\Delta t k' / (1 - e^{-\Delta t k'})]$.

Results and Discussion

Table I lists the results of our Fe(II) oxidation experiments. Included for comparison are the pseudo first order rate constants for Fe(II) oxidation by O_2 and H_2O_2 . Figure 3 is a plot of $\ln[Fe_t/Fe_0]$ as a function of time for each experiment. The oxidation of Fe(II) obeyed first order kinetics in each case. There was a considerable difference between the oxidation rate of Fe(II) added to seawater and the oxidation rate of naturally occurring Fe(II). After correction for pH and temperature differences, the oxidation rate of naturally occurring Fe(II) was 15 times slower.

The oxidation of Fe(II) has been proposed to follow the four step oxidation sequence known as the Haber-Weiss mechanism (Fallab, 1967).



Reaction steps 4 and 6 are slow compared to reactions steps 5 and 7. The extent that Fe(II) oxidation will follow this sequence will be determined by the competing reactions for $\cdot O_2^-$ and $\cdot OH$. Both $\cdot O_2^-$ and $\cdot OH$ will react rapidly with trace components in seawater. Based on the estimated half-life of 20 minutes for $\cdot O_2^-$ in seawater (Petasne and Zika, 1987) and $k_5 = 10^7$ (Rush and Bielski, 1985), reaction 5 will be the primary pathway for $\cdot O_2^-$ reduction when Fe(II) concentrations are greater than 0.5 nmol kg^{-1} . However the

Table I. Oxidation rate of Fe(II) in Narragansett Bay seawater.

Sample	pH	O ₂ μmol/kg	H ₂ O ₂ nmol/kg	t °C	Fe(II) ₀ nmol/kg	k' min ⁻¹	τ min	k _{O₂} ^a min ⁻¹	k _{H₂O₂} ^b min ⁻¹	k _{pred} ^c min ⁻¹	τ _{pred} min
Added Fe(II)											
1A	7.969	228	55	23.0	28.0	0.62	1.1	0.097	0.14	0.50	1.5
Natural Fe(II)											
1B	7.984	246	40	18.7	6.2 ^d	0.021	33	0.047	0.078	0.25	2.8
2B	7.850	242	15	19.6	11.3	0.023	31	0.030	0.023	0.11	6.5
3B	7.852	242	27	19.6	6.0	0.014	50	0.030	0.041	0.14	4.9

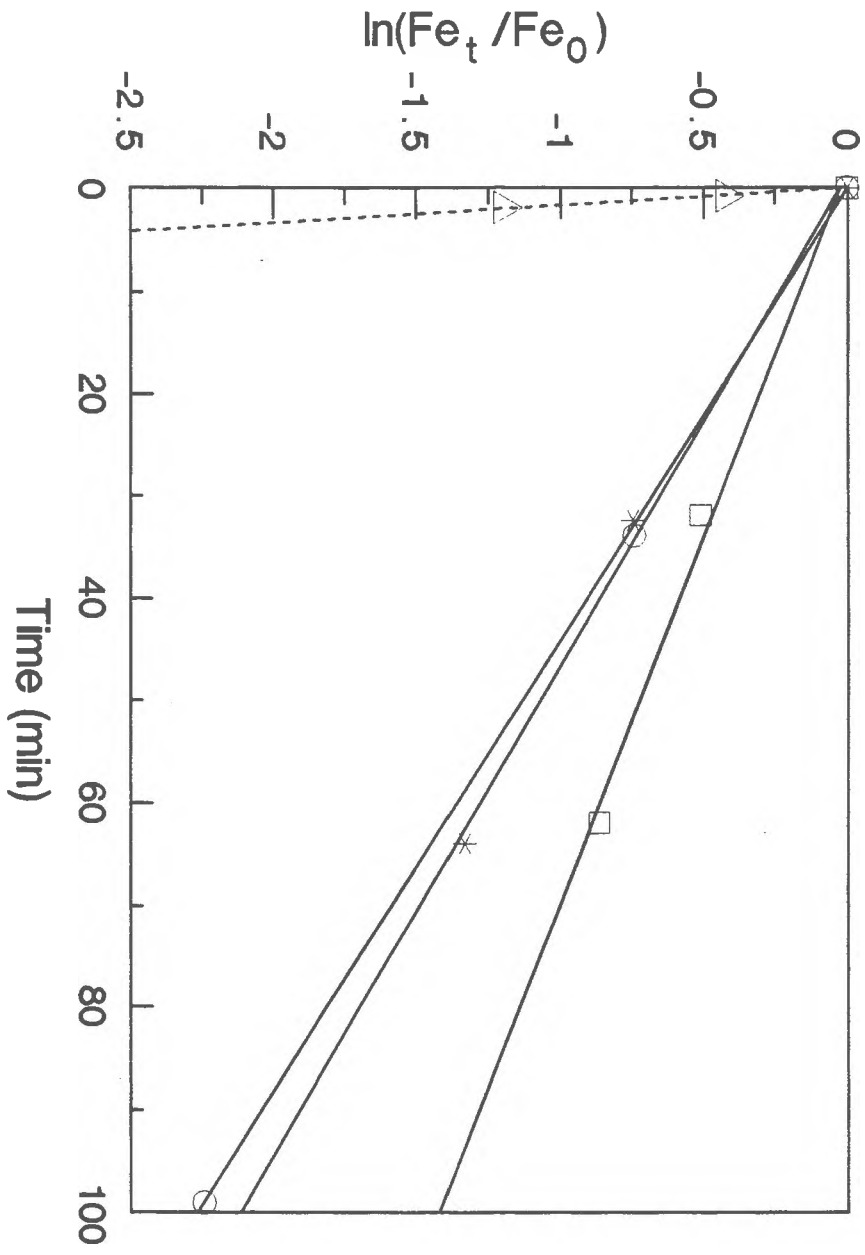
^aFirst order rate calculated from Millero et al. (1987) using $k_{O_2} = k/4$.

^bFirst order rate at t=0 from k₃ data of Moffett and Zika (1987).

^cPredicted overall first order rate determined using equation 9.

^dEstimated Fe(II) concentrations based on extrapolation to time of collection using the observed decay rates.

Figure 3. First order decay plots for Fe(II) oxidation. Samples are labeled: Δ , 1A; *, 1B; o; 2B; \square , 3B. The regression lines for natural Fe(II) and Fe(II) addition experiments are labeled with solid and dashed lines respectively.



same is not true for $\cdot\text{OH}$. Even at $\mu\text{mol kg}^{-1}$ Fe(II) concentrations, the reaction of $\cdot\text{OH}$ with Br^- to form $\cdot\text{Br}$ and OH^- will be the predominant $\cdot\text{OH}$ sink. The $\cdot\text{Br}$ radical is highly reactive and will most likely combine with Br^- to form Br_2^- (Zafiridou, 1974). Based on the observed 2:1 reaction stoichiometry for Fe(II) oxidation by H_2O_2 , Moffett and Zika (1987) have proposed that Br_2^- (or other $\cdot\text{OH}$ reaction products) will react quantitatively with Fe(II). Their experiments were performed using $\mu\text{mol kg}^{-1}$ Fe(II) concentrations. Data are not available to predict whether $\cdot\text{OH}$ reaction products will still react quantitatively with Fe(II) at lower concentrations. Assuming that reaction 7 will still predominate through intermediates at Fe(II) concentrations greater than 1 nmol kg^{-1} , the overall Fe(II) oxidation rate will be determined by reaction steps 4 and 6.

$$d\text{Fe(II)}/dt = 2k_4[\text{Fe(II)}][\text{O}_2] + 2k_6[\text{Fe(II)}][\text{H}_2\text{O}_2] \quad (8)$$

Values for k_4 and k_6 were obtained from Millero et al. (1987) and Moffett and Zika (1987) respectively. From initial Fe(II) and H_2O_2 concentrations, equation 8 was solved numerically as a function of time for each sample. The $[\text{O}_2] \gg [\text{Fe(II)}]$ and $[\text{H}_2\text{O}_2]$ changes slowly in the numerical solution to equation 8. As a very good approximation, $d\text{Fe(II)}/dt$ could be described in terms of pseudo first order kinetics:

$$d\text{Fe(II)}/dt = k'[\text{Fe(II)}] \quad (9)$$

where k' is the pseudo first order rate constant:

$$k' = 2k_4[O_2] + 2k_6[\overline{H_2O_2}] \quad (10)$$

and $[\overline{H_2O_2}]$ is the mean H_2O_2 concentration. Using calculated values for $[Fe(II)]_t$ obtained from the numerical solution of equation 8, k' was calculated from a plot of $\ln(Fe(II)_t/Fe(II)_0)$ versus time. The calculated k' values are listed in table I. The agreement between the predicted and calculated k' was quite good for the Fe(II) addition experiment. The difference in the predicted and observed pseudo first order rate is within the uncertainty of available rate data (King and Kester, 1988). Waite and Morel (1984b) have performed a similar experiment using a coulometric method for Fe(II) determination. They added 6.0 nmol kg^{-1} of Fe(II) to artificial seawater at 20°C with no H_2O_2 . Using our model for Fe(II) oxidation, we obtain an expected Fe(II) half-life of 2.3 min. Their observed half-life was 5 min in reasonable agreement with our results. However, when they repeated the experiment in $0.2 \mu\text{m}$ filtered coastal seawater a significantly longer half-life of 16 min was obtained.

The oxidation rates for naturally occurring Fe(II) were between 5 and 12 times longer than the predicted rates. The observed rates were variable and did not exhibit a trend with temperature, pH, or H_2O_2 . It is evident that some process is stabilizing the Fe(II) in these samples. Three possibilities seem most plausible. The Fe(II) may form stable Fe(II)-organic complex with dissolved organic material. This possibility was suggested by Waite and Morel (1984b) and Millero et al. (1987) to explain observed decreases in Fe(II) oxidation rates in coastal seawater samples. Alternatively, the Fe(II) may be adsorbed onto particles and stabilized as a Fe(II)-particulate complex.

Finally, biologically mediated reduction of Fe(III) could be occurring in natural samples. If biological production of Fe(II) does occur, our oxidation rates will be net rates reflecting contributions of both chemical Fe(II) oxidation and biological Fe(III) reduction. It is difficult to distinguish these three possibilities with our limited data set. If organic complexation were reducing Fe(II) oxidation rates, the effect should be similar in both the Fe(II) addition and natural Fe(II) oxidation experiments unless the kinetics of organic complexation of Fe(II) are slow ($\tau \geq 1$ sec.). Also, the high particulate Fe(II) concentrations observed in Narragansett Bay seawater indicates that up to 60% of the total Fe(II) is particle bound (King et al., 1988). For biological reduction of Fe(III) to be a significant factor in the observed Fe(II) oxidation rates, biological reduction rates would have to be greater than $1-2 \text{ nmol kg}^{-1} \text{ hr}^{-1}$. The rate of biological Fe(III) reduction has not been established in marine waters.

Using the observed decay rates for naturally occurring Fe(II) and the estimated steady state Fe(II) concentrations at time of sample collection, the production rate of Fe(II) in Narragansett Bay was $8 \pm 6 \text{ nmol kg}^{-1} \text{ hr}^{-1}$. We have not established the mechanism for Fe(II) production. However, this production rate is consistent with photochemical reduction of Fe(III) to Fe(II) as observed by Waite and Morel (1984b) in coastal seawater at pH 6.5. They did not see production of Fe(II) seawater at pH 8.2. However, it is unlikely that the mass-transport limited coulometric method they employed will detect Fe(II) bound to particles due to the slow diffusion and dissociation kinetics of particulate Fe(II). The Ferrozine method used in this

study will detect Fe(II) bound to particles due to relatively long contact time of Ferrozine with particulate Fe(II) and the stability of the Fe(FZ)₂ complex. It is possible that considerable concentrations of particulate Fe(II) could be produced photochemically through photoreduction of particulate Fe(III).

Summary:

The oxidation rate of Fe(II) in Narragansett Bay Seawater was determined for naturally occurring Fe(II) and Fe(II) added at close to natural concentrations. The oxidation rate of the added Fe(II) was a factor of 15 faster than the oxidation rate of natural Fe(II). The oxidation rate of the added Fe(II) was in good agreement with the predicted oxidation rate based on literature data for Fe(II) oxidation by O₂ and H₂O₂. The slow oxidation rate and high particulate concentration of natural Fe(II) suggests stabilization of Fe(II) on particles. A Fe(II) production rate of $8 \pm 6 \text{ nmol kg}^{-1} \text{ hr}^{-1}$ is required to maintain the observed steady state Fe(II) concentrations in Narragansett Bay. This production rate is not inconsistent with photochemical reduction of particulate Fe(III) to Fe(II).

References

- Fallab, S. (1967) Reactions with molecular oxygen. *Angewandte Chemie International Edition in English*, 6, 496-507.
- Kester, D. R., Byrne Jr., R. H.; and Liang, Y.-J. (1975) Redox reactions and solution complexes of iron in marine systems. ACS Symposium Series (18), *Marine Chemistry in the Coastal Environment*, 56-79.
- King, D. W.; Lin, J.; and Kester, D. R. (1988) Determination of Fe(II) in seawater at nanomolar concentrations. *Analytical Chemistry*, in preparation.
- Liang, Y.-J. (1982) Kinetics of Ferrous Iron Oxygenation and Redox Chemistry of Iron in Natural Waters. Ph.D. Thesis., University of Rhode Island, 237.
- Miller, W. L.; and Kester, D. R. (1988) Hydrogen peroxide measurement in seawater by P-hydroxyphenylacetic acid dimerization. *Analytical Chemistry*, in press.
- Millero, F. J.; Scotolongo, S.; Izaguirre, M. (1987) The oxidation of Fe(II) in seawater. *Geochimica et Cosmochimica Acta*, 51, 793-801.

- Moffett, J. W.; and Zika, R. G. (1987) Reaction kinetics of hydrogen peroxide with copper and iron in seawater. *Environmental Science and Technology*, 21(8), 804-810.
- Murray, J. W.; and Gill, G. (1978) The geochemistry of iron in Puget Sound. *Geochimica et Cosmochimica Acta*, 42, 9-19.
- Petasne, R. G.; and Zika, R. G. (1987) Fate of superoxide in coastal sea water. *Nature*, 325, 516-518.
- Roekens, E. J.; and Van Grieken, R. E. (1983) Kinetics of iron (II) oxidation in seawater of various pH. *Marine Chemistry*, 13, 195-202.
- Rush, J. D.; and Bielski, B. H. J. (1985) Pulse radiolytic studies of the reaction of perhydroxyl/superoxide O_2^- with iron (II)/iron (III) ions. The reactivity of HO_2/O_2^- with ferric ions and its implication on the occurrence of the Haber-Weiss reaction. *Journal of Physical Chemistry*, 89(23), 5062-6.
- Waite, T. D.; and Morel, F. M. M. (1984a) Coulometric study of the redox dynamics of iron in seawater. *Analytical Chemistry*, 56(4), 787-92.
- Waite, T. D.; and Morel, F. M. M. (1984b) Photoreductive dissolution of colloidal iron oxides in natural waters. *Environmental Science and Technology*, 18, 860-868.

Zafiriu, O. C. (1974) Sources and reactions of OH and daughter radicals in seawater. *Journal of Geophysical Research*, 79, 4491-4497.

Appendix I

Derivation of single indicator equations related to the manuscript entitled "Determination of Seawater pH From 1.5 to 8.5 Using Colorimetric Indicators".

The total concentration of the acidic and basic forms of the indicator as are defined as (HI) and (I) respectively. Charges on the indicator species are not included for brevity. The absorbances A_1 and A_2 of an indicator solution at wavelengths λ_1 and λ_2 are defined by equations 1 and 2 respectively.

$$A_1/\ell = (I)_1\epsilon_I + (HI)_1\epsilon_{HI} \quad (1)$$

$$A_2/\ell = (I)_2\epsilon_I + (HI)_2\epsilon_{HI} \quad (2)$$

The constants ${}_1\epsilon_I$, ${}_1\epsilon_{HI}$, ${}_2\epsilon_I$, and ${}_2\epsilon_{HI}$ are the molar (or molal) absorptivities of (I) and (HI) at wavelengths λ_1 and λ_2 respectively. The pathlength of the optical cell is ℓ . Equations 1 and 2 can be rearranged by dividing by A_1 and A_2 respectively.

$$A_1/\ell A_1 = (I)_1\epsilon_I/A_1 + (HI)_1\epsilon_{HI}/A_1 \quad (3)$$

$$A_2/\ell A_2 = (I)_2\epsilon_I/A_2 + (HI)_2\epsilon_{HI}/A_2 \quad (4)$$

Since the left sides of equations 3 and 4 are equivalent, equations 3 and 4 can be combined into equation 5.

$$(I)_1 \epsilon_I A_2 + (HI)_1 \epsilon_{HI} A_2 = (I)_2 \epsilon_I A_1 + (HI)_2 \epsilon_{HI} A_1 \quad (5)$$

Gathering the concentration terms and rearranging equation 5 yields equations 6 and 7.

$$(I) \{ {}_1 \epsilon_I A_2 - {}_2 \epsilon_I A_1 \} = (HI) \{ {}_2 \epsilon_{HI} A_1 - {}_1 \epsilon_{HI} A_2 \} \quad (6)$$

$$\frac{(I)}{(HI)} = \frac{\{ {}_2 \epsilon_{HI} A_1 - {}_1 \epsilon_{HI} A_2 \}}{\{ {}_1 \epsilon_I A_2 - {}_2 \epsilon_I A_1 \}} \quad (7)$$

Dividing equation 7 by ${}_2 \epsilon_{HI} A_2$ results in equation 8.

$$\frac{(I)}{(HI)} = \frac{\left\{ \frac{A_1}{A_2} - \frac{{}_1 \epsilon_{HI}}{{}_2 \epsilon_{HI}} \right\}}{\left\{ \frac{{}_1 \epsilon_I}{{}_2 \epsilon_{HI}} - \frac{{}_2 \epsilon_I A_1}{{}_2 \epsilon_{HI} A_2} \right\}} \quad (8)$$

The ratios of the molar absorptivities can be described by the constants E_1 , E_2 , and E_3 .

$$E_1 = {}_1 \epsilon_{HI} / {}_2 \epsilon_{HI} \quad (9)$$

$$E_2 = {}_2 \epsilon_I / {}_2 \epsilon_{HI} \quad (10)$$

$$E_3 = {}_1 \epsilon_I / {}_2 \epsilon_{HI} \quad (11)$$

Equation 8 can be rewritten in a more convenient form as equation 14 by defining an additional constant, E_I , and renaming E_1 to E_{HI} .

$$E_I = \frac{1}{2} \epsilon_I / \epsilon_I \quad (12)$$

note:

$$E_3 = E_2 E_I \quad (13)$$

$$\frac{(I)}{(HI)} = \frac{(A_1/A_2 - E_{HI})}{(E_I - A_1/A_2) E_2} \quad (14)$$

Combining equation 14 with the general equation for the dissociation of a weak acid, the pH of a solution with added indicator can be determined as described by equation 15.

$$pH_{ind} = pK'_a + \log \frac{(A_1/A_2 - E_{HI})}{(E_I - A_1/A_2)} - \log(E_2) \quad (15)$$

The pK'_a is the apparent equilibrium constant of the indicator. The pH is the $-\log[H^+]$ where $[H^+]$ is the free proton concentration.

Appendix II

The data listed in this appendix are related to the manuscript entitled "Determination of Seawater pH From 1.5 to 8.5 Using Colorimetric Indicators".

Table 1. Indicator absorbance and pH data used for the determination of indicator apparent dissociation constants.

Sample	A_1	A_2	A_1/A_2	Obs. pH	Pred.pH	Δ pH	σ
Thymol Blue							
N1	1.0097	0.2930	3.4461	1.001	1.000	-0.002	
N22	0.9164	0.2861	3.2031	1.115	1.112	-0.003	
N23	0.8039	0.2802	2.8690	1.256	1.256	-0.000	
N2	0.7111	0.3040	2.3391	1.465	1.475	0.010	
N25	0.5092	0.2835	1.7961	1.682	1.691	0.009	
N3	0.3495	0.3099	1.1278	2.004	1.999	-0.005	
N4	0.1722	0.3158	0.5453	2.478	2.472	-0.006	
N24	0.1132	0.2611	0.4336	2.644	2.642	-0.002	0.006
1CB	0.1956	0.4348	0.4499	2.616			
B10	0.1523	0.4774	0.3190	2.905			
B11	0.1295	0.4605	0.2812	3.037			
Bromophenol Blue							
1CB	0.2173	0.3109	0.6989	2.619	2.616	0.003	
B10	0.4324	0.3495	1.2372	2.901	2.905	-0.004	
B11	0.3606	0.2246	1.6055	3.037	3.036	0.001	0.003
2CB	0.6163	0.1524	4.0440	3.619			
3CB	1.2715	0.1598	7.9568	4.646			
5CB	1.3991	0.1657	8.4436	5.016			

Table 1. continued

Sample	A ₁	A ₂	A ₁ /A ₂	Obs. pH	Pred.pH	ΔpH	σ
Bromocresol Green							
2CB	0.1126	0.1262	0.8922	3.619	3.619	-0.000	
3CB	0.4865	0.1199	4.0575	4.646	4.646	0.000	
5CB	0.7225	0.1406	5.1387	5.016	5.016	-0.000	0.000
5CB	0.7225	0.1406	5.1387	5.016			
4CB	0.8456	0.1429	5.9174	5.486			
6CB	0.7602	0.1400	5.4300	5.152			
Bromocresol Purple							
5CB	0.1305	0.1872	0.6971	5.021	5.016	0.006	
6CB	0.176	0.1921	0.9162	5.155	5.152	0.003	
4CB	0.2369	0.1413	1.6766	5.477	5.486	-0.009	0.007
P1	0.6825	0.1739	3.9247	6.089			
M1	0.706	0.1430	4.9371	6.367			
T4	1.0098	0.1723	5.8607	6.713			
T3	0.9881	0.1577	6.2657	6.949			
Phenol Red							
P1	0.0864	0.3786	0.2282	6.087	6.089	-0.002	
M1	0.196	0.4780	0.4100	6.365	6.367	-0.003	
T4	0.2113	0.2553	0.8277	6.710	6.713	-0.002	
T3	0.4137	0.3156	1.3108	6.957	6.949	0.007	0.004

Appendix III

The data listed in this appendix are related to the manuscript entitled "The Effect of Pressure on the Dissociation of Sulfonephthalein Indicators".

Table 1. Indicator absorbance and pH of buffer solutions as a function of pressure at 25 °C in 35 ‰ salinity seawater.

Indicator Samp. (solution)	P (bars)	pK	A ₁	A ₂	A ₁ /A ₂	pH	ΔpH	
Thymol	1	0	1.438	0.1941	0.3520	0.5514	2.470	0.000
ASW(2):1	2	236	1.429	0.2017	0.3569	0.5651	2.444	-0.026
	3	517	1.418	0.2125	0.3657	0.5811	2.414	-0.056
	4	680	1.411	0.2177	0.3698	0.5887	2.398	-0.071
	5	844	1.405	0.2225	0.3737	0.5954	2.384	-0.086
Bromophenol Blue	1	0	3.695	0.8012	0.1546	5.1824	3.844	0.000
	2	264	3.659	0.7945	0.1554	5.1126	3.794	-0.051
ASW(2):2	3	513	3.624	0.7894	0.1580	4.9962	3.736	-0.108
	4	733	3.594	0.7857	0.1599	4.9137	3.689	-0.155
	5	933	3.566	0.7814	0.1617	4.8324	3.646	-0.199
Bromocresol Green	1	0	4.411	0.7203	0.1246	5.7809	5.371	0.000
	2	203	4.376	0.7153	0.1245	5.7454	5.310	-0.061
ASW(2):3	3	507	4.325	0.7135	0.1253	5.6943	5.222	-0.149
	4	734	4.286	0.7130	0.1262	5.6498	5.154	-0.217
	5	901	4.258	0.7121	0.1270	5.6071	5.099	-0.272
Bromocresol Purple	1	0	5.972	0.8480	0.1580	5.8242	6.695	0.000
	2	440	5.860	0.8360	0.1610	5.6258	6.497	-0.199
ASW(2):4	3	676	5.800	0.8290	0.1630	5.5046	6.388	-0.307
	4	982	5.723	0.8230	0.1650	5.3932	6.269	-0.426

Table 2. Indicator absorbance and pK as a function of pressure at 25 °C in 35 ‰ salinity seawater.

Indicator	Samp.	P (bars)	pH	A ₁	A ₂	A ₁ /A ₂	pK	ΔpK
Thymol Blue 1	1	0	1.582	0.6852	0.3358	2.0405	1.438	0.000
	2	269	1.582	0.6800	0.3380	2.0118	1.427	-0.011
	3	517	1.582	0.6797	0.3415	1.9903	1.418	-0.020
	4	793	1.582	0.6771	0.3446	1.9649	1.408	-0.030
	5	1047	1.582	0.6742	0.3473	1.9413	1.398	-0.040
Thymol Blue 2	1	0	1.863	0.4676	0.3358	1.3925	1.438	0.000
	2	313	1.863	0.4681	0.3430	1.3647	1.424	-0.014
	3	614	1.863	0.4678	0.3496	1.3381	1.411	-0.027
	4	852	1.863	0.4668	0.3542	1.3179	1.401	-0.037
Bromophenol Blue	1	0	2.470	0.1303	0.2517	0.5177	3.689	0.000
	2	295	2.437	0.1356	0.2574	0.5268	3.648	-0.041
	3	531	2.413	0.1416	0.2632	0.5380	3.614	-0.076
	4	751	2.392	0.1472	0.2685	0.5482	3.584	-0.105
	5	899	2.379	0.1526	0.2753	0.5543	3.566	-0.124
	6	314	2.435	0.1353	0.2551	0.5304	3.643	-0.047
Bromocresol Green	1	0	3.847	0.1682	0.1182	1.4230	4.392	0.000
	2	339	3.774	0.1677	0.1213	1.3825	4.335	-0.057
	3	519	3.736	0.1676	0.1230	1.3626	4.305	-0.087
	4	719	3.693	0.1679	0.1250	1.3432	4.270	-0.122
	5	900	3.654	0.1678	0.1268	1.3233	4.239	-0.153
Bromocresol Purple	1	0	5.353	0.3715	0.2996	1.3431	5.972	0.000
	2	263	5.274	0.3728	0.3068	1.3136	5.905	-0.067
	3	509	5.201	0.3741	0.3139	1.2860	5.843	-0.129
	4	737	5.132	0.3751	0.3204	1.2613	5.785	-0.187
	5	906	5.082	0.3761	0.3255	1.2433	5.742	-0.230
Phenol Red	1	0	6.696	0.2270	0.2830	0.8021	7.493	0.000
	2	471	6.480	0.2070	0.2930	0.7065	7.330	-0.163
	3	659	6.399	0.1990	0.2970	0.6700	7.272	-0.222
	4	989	6.265	0.1880	0.3050	0.6164	7.171	-0.322

Appendix IV

Derivation of multiple indicator equations related to the manuscript entitled "Spectral Modeling of Sulfonephthalein Indicators: Application to pH Measurement Using Multiple Indicators".

The general equation for pH determination from absorbance measurements of solutions containing multiple indicators is derived in manner similar to the derivation for single indicator systems. The equation will be derived for two indicators bromocresol green and phenol red. However, the equation is not limited to these indicators and can be generalized for systems with two or more indicators. The acidic and basic forms of bromocresol green and phenol red will be designated as (HG), (G), (HR), and (R) respectively. Bromocresol green will be designated as the master indicator and phenol red as the second indicator. If more indicators were used they would be defined as the third, fourth, fifth indicators etc. The master indicator is used as a reference for normalizing the concentrations of all the indicators in the solution.

The absorbance at wavelengths λ_1 and λ_2 are defined by equations 1 and 2 respectively.

$$A_1/\ell = (G)_1\epsilon_G + (HG)_1\epsilon_{HG} + (R)_1\epsilon_R + (HR)_1\epsilon_{HR} \quad (1)$$

$$A_2/\ell = (G)_2\epsilon_G + (HG)_2\epsilon_{HG} + (R)_2\epsilon_R + (HR)_2\epsilon_{HR} \quad (2)$$

In a manner identical to the single indicator derivation, equations 1

and 2 can be combined and rearranged to yield equation 3.

$$\begin{aligned} & (G)\{ {}_2\varepsilon_{GA_1} - {}_1\varepsilon_{GA_2} \} + (HG)\{ {}_2\varepsilon_{HGA_1} - {}_1\varepsilon_{HGA_2} \} \\ & = -(R)\{ {}_2\varepsilon_{RA_1} - {}_1\varepsilon_{RA_2} \} - (HR)\{ {}_2\varepsilon_{HRA_1} - {}_1\varepsilon_{HRA_2} \} \quad (3) \end{aligned}$$

The total indicator concentration will be defined as TG and TR for bromocresol green and phenol red respectively. The ratio of the base to total indicator will be defined as β_A and the ratio of acid to the total indicator as α_A . These ratios can be calculated for a general indicator according to equations 4 and 5.

$$\beta_A = \frac{(A)}{(A) + (HA)} = \frac{K'_A}{K'_A + [H]} \quad (4)$$

$$\alpha_A = \frac{(HA)}{(A) + (HA)} = \frac{[H]}{K'_A + [H]} \quad (5)$$

Where K'_A is the apparent equilibrium constant for the indicator and $[H]$ is the free proton concentration. Equation 3 can be written in terms of the total concentrations of each indicator by combining equations 3, 4, and 5.

$$\begin{aligned} & (TG)\beta_G\{ {}_2\varepsilon_{GA_1} - {}_1\varepsilon_{GA_2} \} + (TG)\alpha_G\{ {}_2\varepsilon_{HGA_1} - {}_1\varepsilon_{HGA_2} \} \\ & = -(TR)\beta_R\{ {}_2\varepsilon_{RA_1} - {}_1\varepsilon_{RA_2} \} - (TR)\alpha_R\{ {}_2\varepsilon_{HRA_1} - {}_1\varepsilon_{HRA_2} \} \quad (6) \end{aligned}$$

The ratio of the total concentration of the second indicator to the

master indicator, (TR)/(TG), is defined as χ . Dividing equation 6 by (TG) and substituting χ for (TR)/(TG) results in equation 7.

$$\beta_G \{ {}_2\varepsilon_G A_1 - {}_1\varepsilon_G A_2 \} + \alpha_G \{ {}_2\varepsilon_{HG} A_1 - {}_1\varepsilon_{HG} A_2 \} \\ = -\chi \beta_R \{ {}_2\varepsilon_R A_1 - {}_1\varepsilon_R A_2 \} - \chi \alpha_R \{ {}_2\varepsilon_{HR} A_1 - {}_1\varepsilon_{HR} A_2 \} \quad (7)$$

Dividing equation 7 by ${}_2\varepsilon_{HG} A_2$ results in equation 8.

$$\beta_G \left[\frac{{}_2\varepsilon_G A_1}{{}_2\varepsilon_{HG} A_2} - \frac{{}_1\varepsilon_G}{{}_2\varepsilon_{HG}} \right] + \alpha_G \left[\frac{{}_2\varepsilon_{HG} A_1}{{}_2\varepsilon_{HG} A_2} - \frac{{}_1\varepsilon_{HG}}{{}_2\varepsilon_{HG}} \right] \\ = -\chi \beta_R \left[\frac{{}_2\varepsilon_R A_1}{{}_2\varepsilon_{HG} A_2} - \frac{{}_1\varepsilon_R}{{}_2\varepsilon_{HG}} \right] - \chi \alpha_R \left[\frac{{}_2\varepsilon_{HR} A_1}{{}_2\varepsilon_{HG} A_2} - \frac{{}_1\varepsilon_{HR}}{{}_2\varepsilon_{HG}} \right] \quad (8)$$

The ratios of the molar absorptivities are defined by the six constants $E_{1G} - E_{3R}$ in equations 9-14.

$$E_{1G} = {}_1\varepsilon_{HG} / {}_2\varepsilon_{HG} \quad (9)$$

$$E_{2G} = {}_2\varepsilon_G / {}_2\varepsilon_{HG} \quad (10)$$

$$E_{3G} = {}_1\varepsilon_G / {}_2\varepsilon_{HG} \quad (11)$$

$$E_{1R} = {}_1\varepsilon_{HR} / {}_2\varepsilon_{HR} \quad (12)$$

$$E_{2R} = {}_2\varepsilon_R / {}_2\varepsilon_{HR} \quad (13)$$

$$E_{3R} = {}_1\varepsilon_R / {}_2\varepsilon_{HR} \quad (14)$$

A final constant, ψ , is the ratio of the absorbance of (HR) to (HG) at λ_2 when both indicators are completely in the acid form as described by

equation 15.

$$\psi = A_2(\text{red})/A_2(\text{green}) = (\text{TR})_2 \epsilon_{\text{HR}} / (\text{TG})_2 \epsilon_{\text{HG}} \quad (15)$$

Multiplying equations 12 - 14 by ψ and dividing by χ results in a set of mixed optical constant for phenol red which can be substituted into equation 8.

$${}_1 \epsilon_{\text{HR}} / {}_2 \epsilon_{\text{HG}} = E_{1\text{R}} \psi / \chi \quad (16)$$

$${}_2 \epsilon_{\text{R}} / {}_2 \epsilon_{\text{HG}} = E_{2\text{R}} \psi / \chi \quad (17)$$

$${}_1 \epsilon_{\text{R}} / {}_2 \epsilon_{\text{HG}} = E_{3\text{R}} \psi / \chi \quad (18)$$

$${}_2 \epsilon_{\text{HR}} / {}_2 \epsilon_{\text{HG}} = \psi / \chi \quad (19)$$

Substituting equations 9-11 and 16-19 into equation 8 and condensing a few terms results in equation 20.

$$\begin{aligned} & \beta_{\text{G}}(E_{2\text{G}} A_1/A_2 - E_{3\text{G}}) + \alpha_{\text{G}}(A_1/A_2 - E_{1\text{G}}) \\ & = -\psi [\beta_{\text{R}}(E_{2\text{R}} A_1/A_2 - E_{3\text{R}}) + \alpha_{\text{R}}(A_1/A_2 - E_{1\text{R}})] \quad (20) \end{aligned}$$

Equation 20 contains seven optical constants, K'_{G} , K'_{R} , $[\text{H}]$, A_1 , and A_2 . The pH of a solution with added indicator can be determined by solving equation 20 for $[\text{H}]$ (β and α are a function of $[\text{H}]$) as a function of A_1/A_2 . The equation can be solved iteratively or using the quadratic equation. Equation 20 can be reduced to a simple quadratic solution using the following steps:

$$C_1 = E_{2G} A_1/A_2 - E_{3G} \quad (21)$$

$$C_2 = A_1/A_2 - E_{1G} \quad (22)$$

$$C_3 = E_{2R} A_1/A_2 - E_{3R} \quad (23)$$

$$C_4 = A_1/A_2 - E_{1R} \quad (24)$$

$$[H]^2(C_1 + C_4\psi) + [H](K_G C_1 + K_R C_2 + K_G C_4\psi + K_R C_3\psi) + K_G K_R (C_1 + \psi C_3) = 0 \quad (25)$$

Equation 20 can be expanded to include more than two indicators. The general form of equation 20 is defined by equation 26. The master indicator is labeled as M. The second through n indicators will be labeled A, B, C,n etc.

$$\begin{aligned} & \beta_M(E_{2M} A_1/A_2 - E_{3M}) + \alpha_M(A_1/A_2 - E_{1M}) \\ & = -\psi_A[\beta_A(E_{2A}A_1/A_2 - E_{3A}) + \alpha_A(A_1/A_2 - E_{1A})] \\ & \quad -\psi_B[\beta_B(E_{2B}A_1/A_2 - E_{3B}) + \alpha_B(A_1/A_2 - E_{1B})] \\ & \quad , \dots -\psi_n[\beta_n(E_{2n}A_1/A_2 - E_{3n}) + \alpha_n(A_1/A_2 - E_{1n})] \quad (26) \end{aligned}$$

If more than two indicators are used the pH is most conveniently determined by solving equation 26 for [H] using a numerical iteration scheme.

This derivation used the optical constants E_1 , E_2 , and E_3 . These constants can be related to the constants E_A , E_{HA} and E_2 through the following equalities:

$$E_{HA} = E_1 \quad (27)$$

$$E_A = E_3/E_2 \quad (28)$$

$$E_2 = E_2 \quad (29)$$

Making the appropriate substitutions, equation 26 can be written in terms of the optical constants E_{HA} , E_A , and E_2 .

$$\begin{aligned} & \beta_M(E_2 M A_1/A_2 - E_M E_{2M}) + \alpha_M(A_1/A_2 - E_{HM}) \\ = & -\psi_A[\beta_A(E_2 A A_1/A_2 - E_A E_{2A}) + \alpha_A(A_1/A_2 - E_{HA})] \\ & -\psi_B[\beta_B(E_2 B A_1/A_2 - E_B E_{2B}) + \alpha_B(A_1/A_2 - E_{HB})] \\ & \dots -\psi_n[\beta_n(E_2 n A_1/A_2 - E_n E_{2n}) + \alpha_n(A_1/A_2 - E_{Hn})] \quad (30) \end{aligned}$$

Appendix V

Figures of the observed and predicted spectra of sulfonephthalein indicators in seawater related to the manuscript entitled "Spectral Modeling of Sulfonephthalein Indicators: Application to pH Measurement Using Multiple Indicators".

The curve fitting of sulfonephthalein indicators can be evaluated by comparing the observed and predicted spectra of the indicators (thymol blue, bromophenol blue, bromocresol green, bromocresol purple, and phenol red) in seawater media. The predicted spectra were calculated from values of ν^{ϵ_A} , $\nu^{\epsilon_{HA}}$, pK'_A , pH, and indicator concentration. Figures 1 - 5 are examples of the curve fits for each indicator in seawater media.

Figure 1. Observed and predicted spectra of thymol blue in seawater at pH 1.684. The solid line is the observed spectrum. The dashed lines labeled A1, A2, B1 denote the first and second acidic and basic Gaussian peaks. The x symbol is the predicted spectrum.

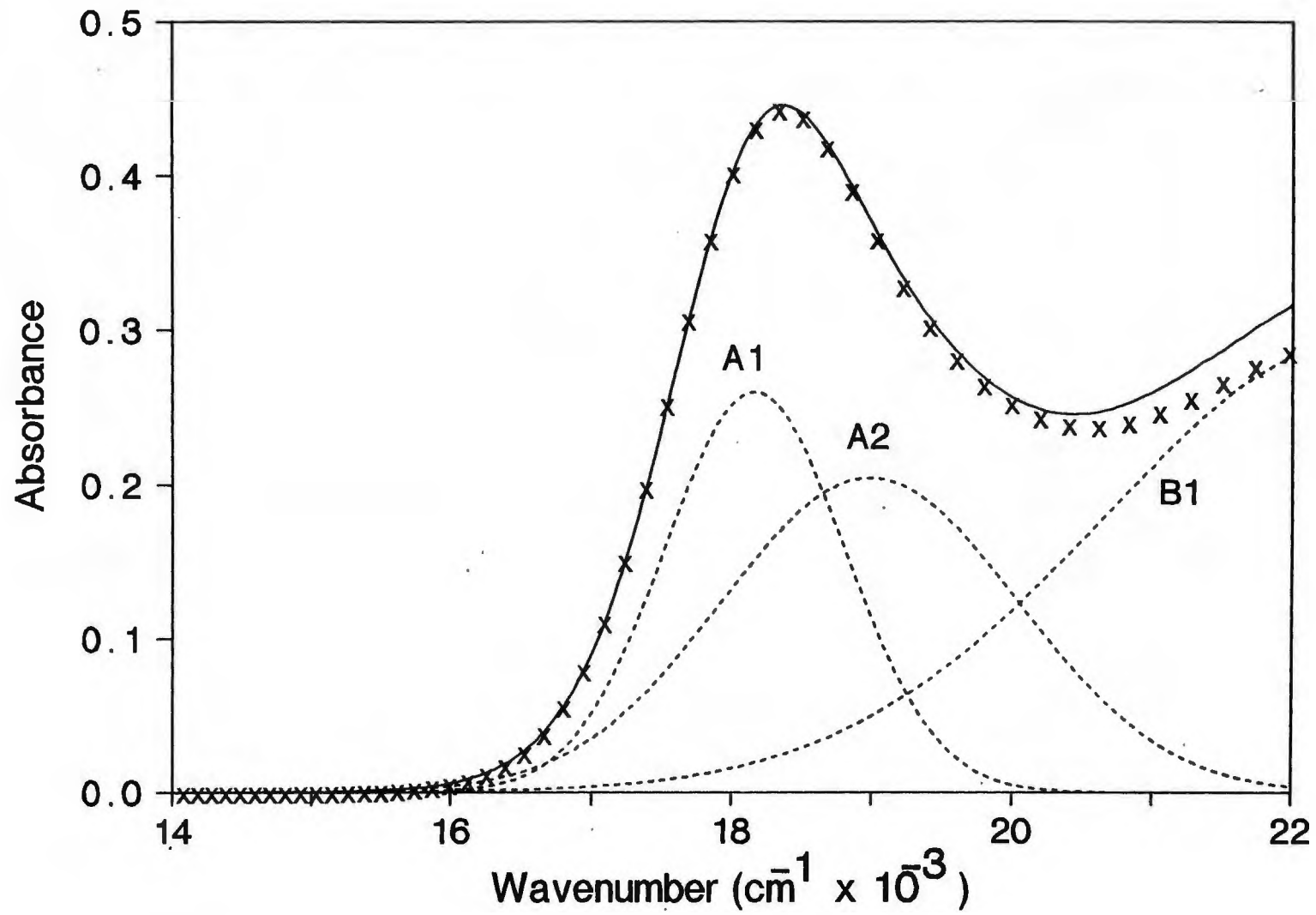


Figure 2. Observed and predicted spectra of bromophenol blue in seawater at pH 3.751. The solid line is the observed spectrum. The dashed lines labeled A1, B1, B2, and B3 denote the acidic and first, second, and third basic Gaussian peaks. The x symbol is the predicted spectrum.

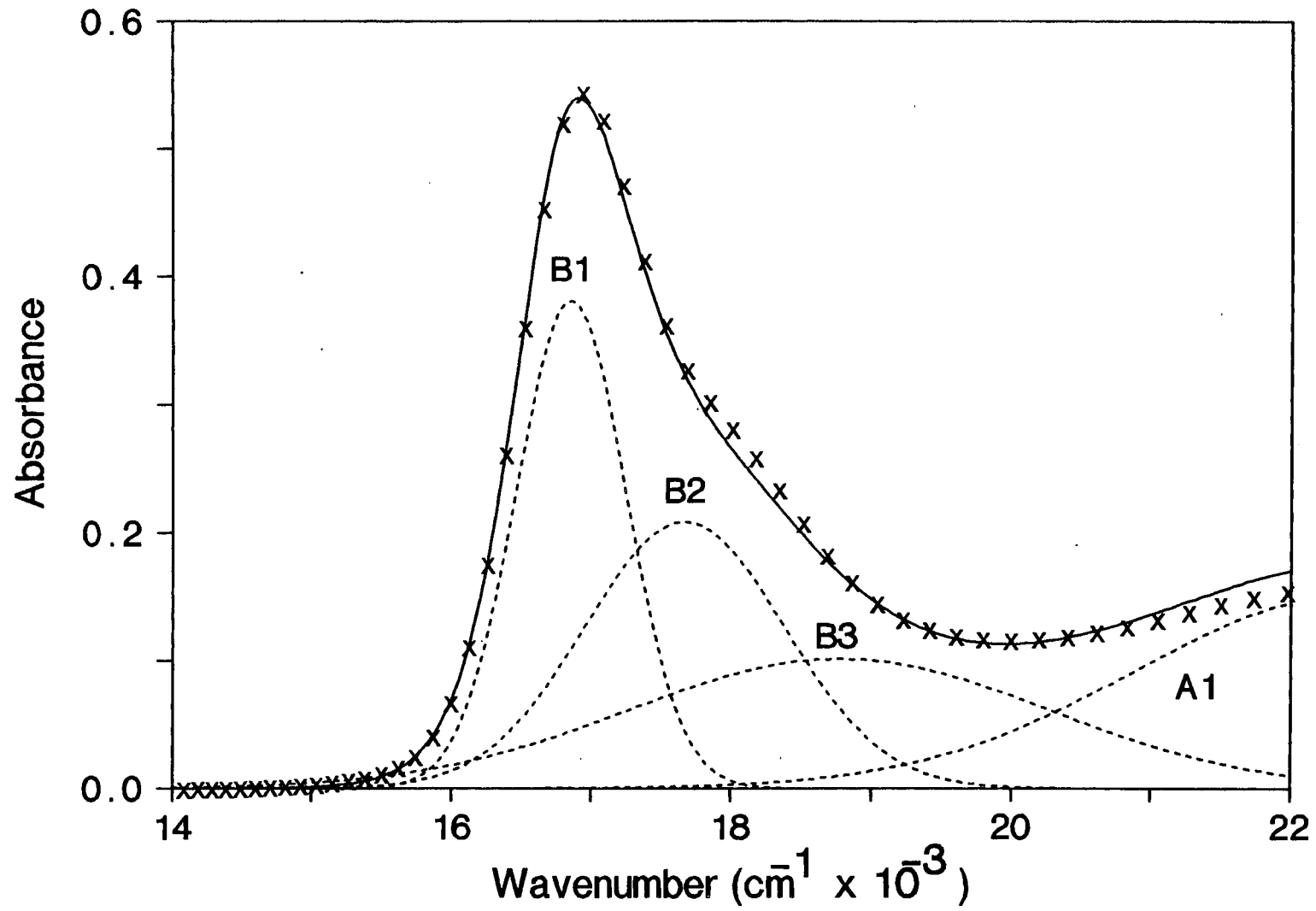


Figure 3. Observed and predicted spectra of bromocresol green in seawater at pH 4.625. The solid line is the observed spectrum. The dashed lines labeled A1, B1, B2, and B3 denote the acidic and first, second, and third basic Gaussian peaks. The x symbol is the predicted spectrum.

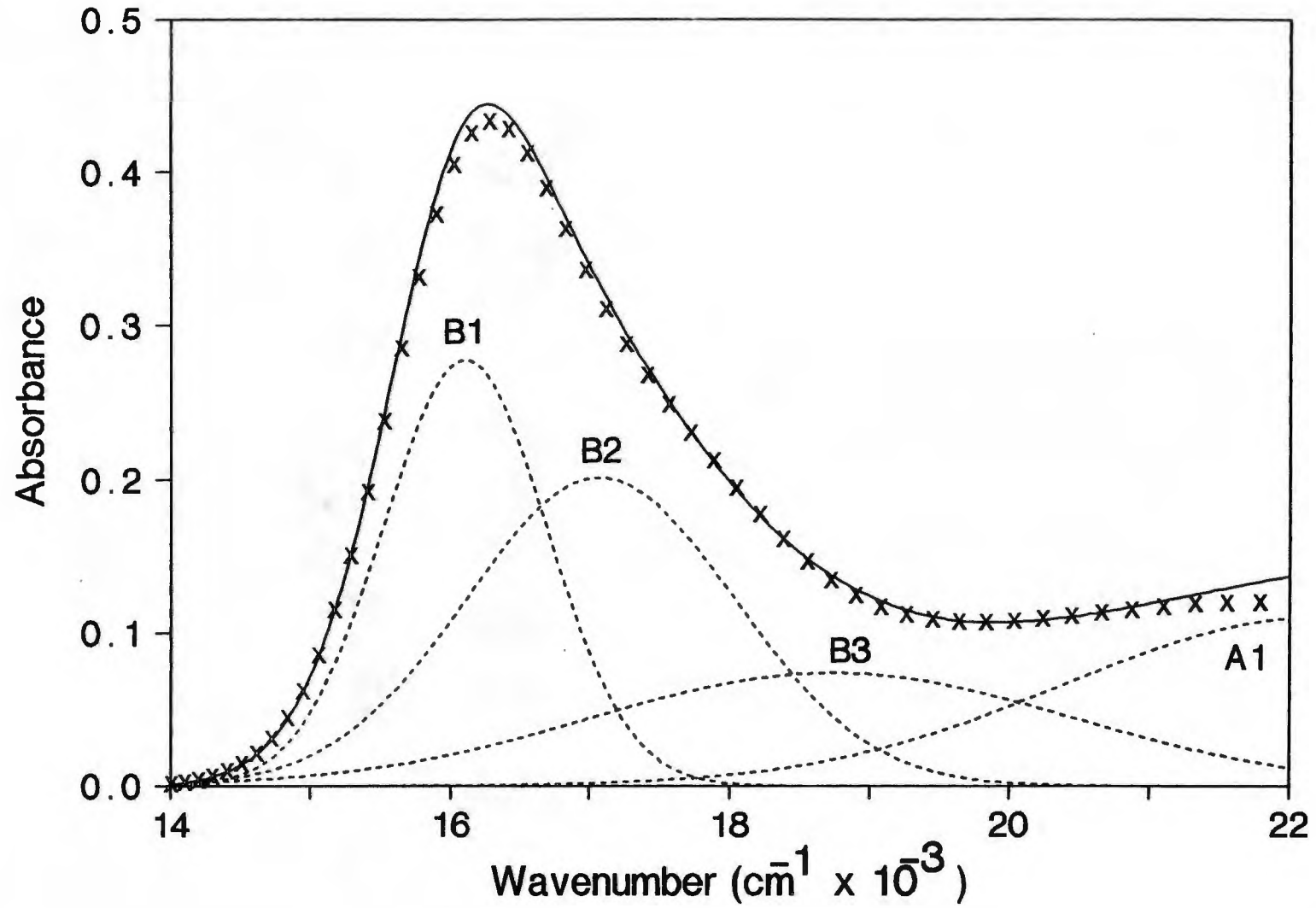


Figure 4. Observed and predicted spectra of bromocresol purple in seawater at pH 5.654. The solid line is the observed spectrum. The dashed lines labeled A1, B1, B2, and B3 denote the acidic and first, second, and third basic Gaussian peaks. The x symbol is the predicted spectrum.

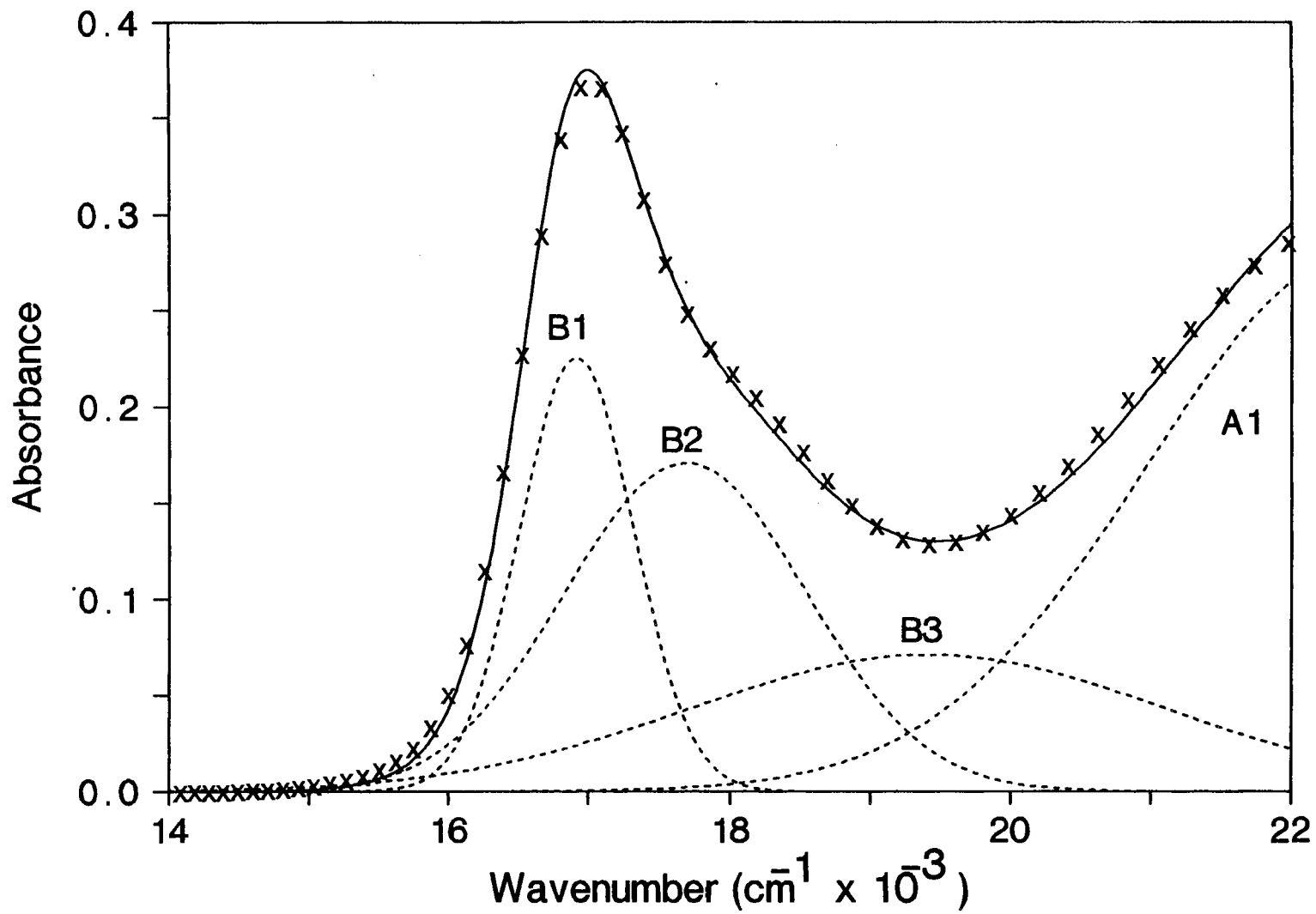
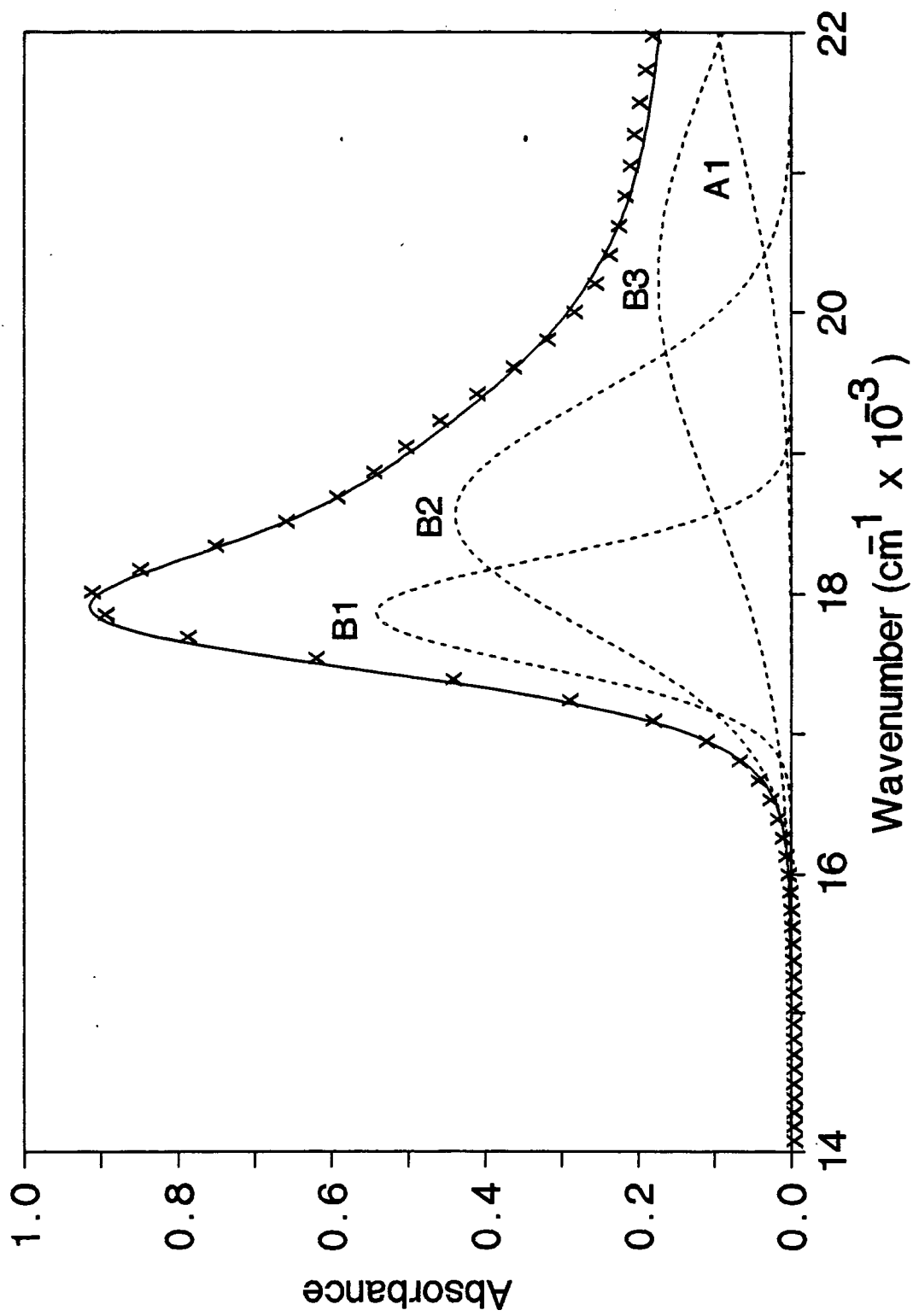


Figure 5. Observed and predicted spectra of phenol red in seawater at pH 7.986. The solid line is the observed spectrum. The dashed lines labeled A1, B1, B2, and B3 denote the acidic and first, second, and third basic Gaussian peaks. The x symbol is the predicted spectrum.



Appendix VI

The data listed in this appendix are related to the manuscript entitled "The Effect of Pressure on the Hydrolysis of Fe(III)".

Table 1. Absorbance of Fe(III) solutions as a function of pH, wavelength, and pressure.

[H ⁺]	λ	A _λ /A _{iso}
Pressure = 0 bars		
2.438E-02	290	0.3488
5.200E-03	290	0.5464
8.954E-04	290	0.9981
2.438E-02	295	0.2882
5.200E-03	295	0.5080
8.954E-04	295	0.9944
2.438E-02	300	0.2333
5.200E-03	300	0.4867
8.954E-04	300	0.9758
2.438E-02	310	0.1822
5.200E-03	310	0.4080
8.954E-04	310	0.9108
2.438E-02	330	0.1254
5.200E-03	330	0.2972
8.954E-04	330	0.6582
Pressure = 355 bars		
2.438E-02	290	0.3613
5.200E-03	290	0.5573
8.954E-04	290	0.9355
2.438E-02	295	0.3000
5.200E-03	295	0.5079
8.954E-04	295	0.9239
2.438E-02	300	0.2440
5.200E-03	300	0.4783
8.954E-04	300	0.9040
2.438E-02	310	0.1863
5.200E-03	310	0.4012
8.954E-04	310	0.8478
2.438E-02	330	0.1286
5.200E-03	330	0.2787
8.954E-04	330	0.6130

Table 1. continued

[H ⁺]	λ	A_λ/A_{iso}
Pressure = 605 bars		
2.438E-02	290	0.3731
5.200E-03	290	0.5732
8.954E-04	290	0.9028
2.438E-02	295	0.3035
5.200E-03	295	0.5209
8.954E-04	295	0.8748
2.438E-02	300	0.2477
5.200E-03	300	0.4831
8.954E-04	300	0.8424
2.438E-02	310	0.1955
5.200E-03	310	0.3895
8.954E-04	310	0.7703
2.438E-02	330	0.1328
5.200E-03	330	0.2652
8.954E-04	330	0.5495
Pressure = 905 bars		
2.438E-02	290	0.3831
5.200E-03	290	0.5918
8.954E-04	290	0.8842
2.438E-02	295	0.3106
5.200E-03	295	0.5303
8.954E-04	295	0.8447
2.438E-02	300	0.2550
5.200E-03	300	0.4842
8.954E-04	300	0.8079
2.438E-02	310	0.2010
5.200E-03	310	0.3902
8.954E-04	310	0.7356
2.438E-02	330	0.1420
5.200E-03	330	0.2621
8.954E-04	330	0.5199

Appendix VII

A model for the inorganic speciation of Fe(II) related to the manuscript entitled "The Effect of Pressure on the Oxidation Rate of Fe(II) in Seawater".

Available data on Fe (II) equilibria indicate that Fe (II) speciation in seawater is controlled predominantly by the Cl^- , SO_4^{2-} and free Fe (II) species (Kester, 1986). I have used an equilibrium model similar to the one used by Kester (1986) to look at the effect of pH on the higher order Fe (II) hydrolysis species. The equilibrium model of Kester (1986) was used to determine the free concentrations of the major ions in seawater. Equilibrium constants for Fe (II) species were obtained from the compilation of Turner et al. (1981). Turner et al. fit the available equilibrium data for a wide number of metals to the function:

$$\log K_i^* = \log K_i^0 - 0.511\Delta Z\sqrt{I}/(1 + B\sqrt{I}) + CI + DI^2 \quad (1)$$

where I is the effective ionic strength, K_i^* and K_i^0 are the stoichiometric and thermodynamic equilibrium constants respectively, and $\Delta Z = \sum Z^2$ (products) - $\sum Z^2$ (reactants). B , C , and D are empirical constants used to describe the ionic strength dependence on K_i^0 . Table I. lists these constants for the major Fe (II) species. My calculated values of K_i^* at 25 °C in 35 ‰ salinity seawater are also listed in Table I.

Table I. Values of $\log K_i^0$, B, C, D, and ΔZ for equation 2 and $\log K_i^*$ determined at 25 °C in 35 ‰ salinity seawater.^a

Fe (II) species	$\log K_i^0$	B	C	D	ΔZ	$\log K_i^*$
FeCl ⁺	0.32	1.57	0.17	0	-4	-0.30
FeSO ₄ ⁰	2.20	1.63	0.05	0	-8	0.80
FeF ⁺	1.42	1.57	0.17	0	-4	0.80
FeCO ₃ ⁰	4.73	1.63	0.05	0	-8	3.32
FeOH ⁺	-9.50	2.10	0.01	0	-2	-9.80
FE(OH) ₂ ⁰	-20.60	2.01	-0.12	0	-2	-21.00
Fe(OH) ₃ ⁻	-31.00	0	-0.09	-0.07	0	-31.09
Fe(OH) ₄ ²⁻	-46.00	1.0	-0.34	0	4	-45.31

^a K_i values for Fe (II) hydrolysis species are hydrolysis constants usually written as β_i .

The total concentration of Fe (II) in solution, TFe, will equal the sum of the Fe (II) species:

$$\begin{aligned} \text{TFe} = & [\text{Fe}^{2+}] + [\text{FeOH}^+] + [\text{Fe}(\text{OH})_2^0] + [\text{Fe}(\text{OH})_3^-] \\ & + [\text{Fe}(\text{OH})_4^{2-}] + [\text{FeF}^+] + [\text{FeCl}^+] + [\text{FeSO}_4^0] + [\text{FeCO}_3^0] \quad (2) \end{aligned}$$

where brackets denote the species concentrations. Equation 2 can be written in terms of the free Fe (II), anion, and hydrogen ion concentrations:

$$\begin{aligned} \text{TFe}/[\text{Fe}^{2+}] = 1/\alpha = & \{1 + \beta_1/[\text{H}^+] + \beta_2/[\text{H}^+]^2 + \beta_3/[\text{H}^+]^3 + \beta_4/[\text{H}^+]^4 \\ & + K_F[\text{F}^-] + K_{\text{Cl}}[\text{Cl}^-] + K_{\text{SO}_4}[\text{SO}_4^{2-}] + K_{\text{CO}_3}[\text{CO}_3^{2-}]\} \quad (3) \end{aligned}$$

where α is the free to total ratio of Fe (II). The concentration of each Fe (II) species can be calculated from:

$$[\text{Fe}^{2+}] = \text{TFe } \alpha \quad (4)$$

$$[\text{FeOH}^+] = \text{TFe } \alpha \beta_1/[\text{H}^+] \quad (5)$$

$$[\text{Fe}(\text{OH})_2^0] = \text{TFe } \alpha \beta_2/[\text{H}^+]^2 \quad (6)$$

$$[\text{Fe}(\text{OH})_3^-] = \text{TFe } \alpha \beta_3/[\text{H}^+]^3 \quad (7)$$

$$[\text{Fe}(\text{OH})_4^{2-}] = \text{TFe } \alpha \beta_4/[\text{H}^+]^4 \quad (8)$$

$$[\text{FeF}^+] = \text{TFe } \alpha K_F[\text{F}^-] \quad (9)$$

$$[\text{FeCl}^+] = \text{TFe } \alpha K_{\text{Cl}}[\text{Cl}^-] \quad (10)$$

$$[\text{FeSO}_4^0] = \text{TFe } \alpha K_{\text{SO}_4}[\text{SO}_4^{2-}] \quad (11)$$

$$[\text{FeCO}_3^0] = \text{TFe } \alpha K_{\text{CO}_3}[\text{CO}_3^{2-}]. \quad (12)$$

The speciation of Fe (II) was calculated over the pH range 5 - 9 for

35 ‰ salinity seawater at 25 °C. The results of the speciation calculations are presented in Figures 1 and 2. As can be seen from Figure 1, the predominant Fe (II) species are Fe^{2+} , FeCl^+ , and FeSO_4^0 . Over the pH range 5.0 to 8.2 the concentration of these major Fe (II) species are insensitive to pH. Above pH 8.2, the increasing carbonate concentration causes a slight decrease in $[\text{Fe}^{2+}]$.

Figure 2 shows the speciation of the Fe (II) hydrolysis products on a considerably expanded scale. With the exception of FeOH^+ above pH 8.2, the contribution of the hydrolysis products to the total Fe (II) concentration is negligible. Due to the pH dependence on the hydrolysis reaction, the relative concentration of each hydrolysis species increases with increasing pH. The slope of $\log(\% \text{ total iron})$ versus pH for each hydrolysis species is in agreement with the predicted slope based on the hydrolysis order (FeOH^+ $m = 1$, Fe(OH)_2^0 $m = 2$, Fe(OH)_2^- $m = 3$, Fe(OH)_4^{2+} $m = 4$).

Literature Cited

- Kester, D. R. (1986) Equilibrium models in seawater: applications and limitations. In: The Importance of Chemical Speciation in Environmental Process., Bernhard, M.; Brinckman, F. E.; and Sadler, P. J., editors, Dahlem Konferenzen 1986, Springer-Verlag, Berlin,, 337-363.
- Turner, D. R., M. Whitfield, and A. G. Dickson (1981) The equilibrium speciation of dissolved components in freshwater and seawater at 25°C and 1 atm pressure. *Geochimica et Cosmochimica Acta*, 45, 844-881.

Figure 1. Variation of Fe (II) species in 35 ‰ salinity seawater at 25 °C as a function of pH.

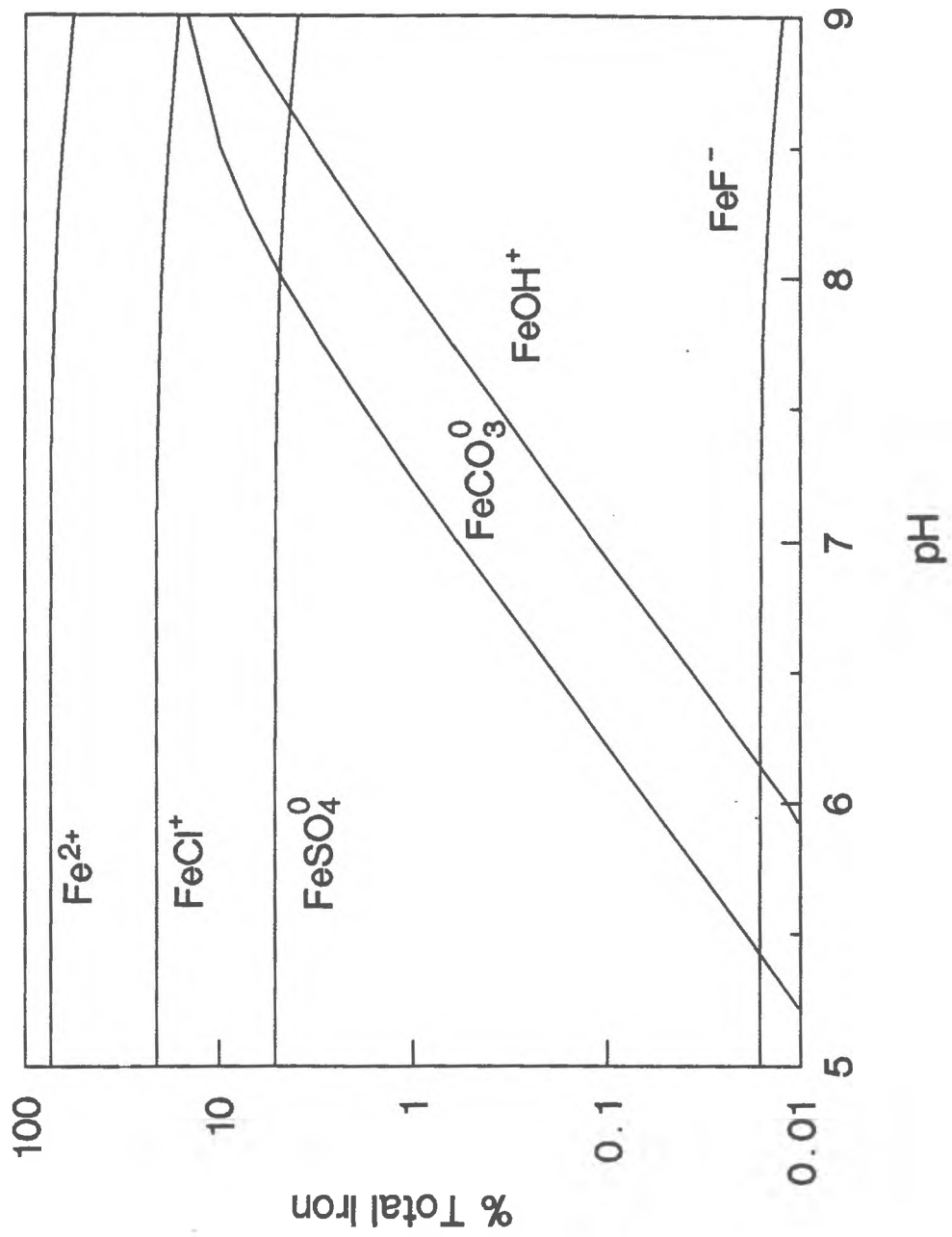
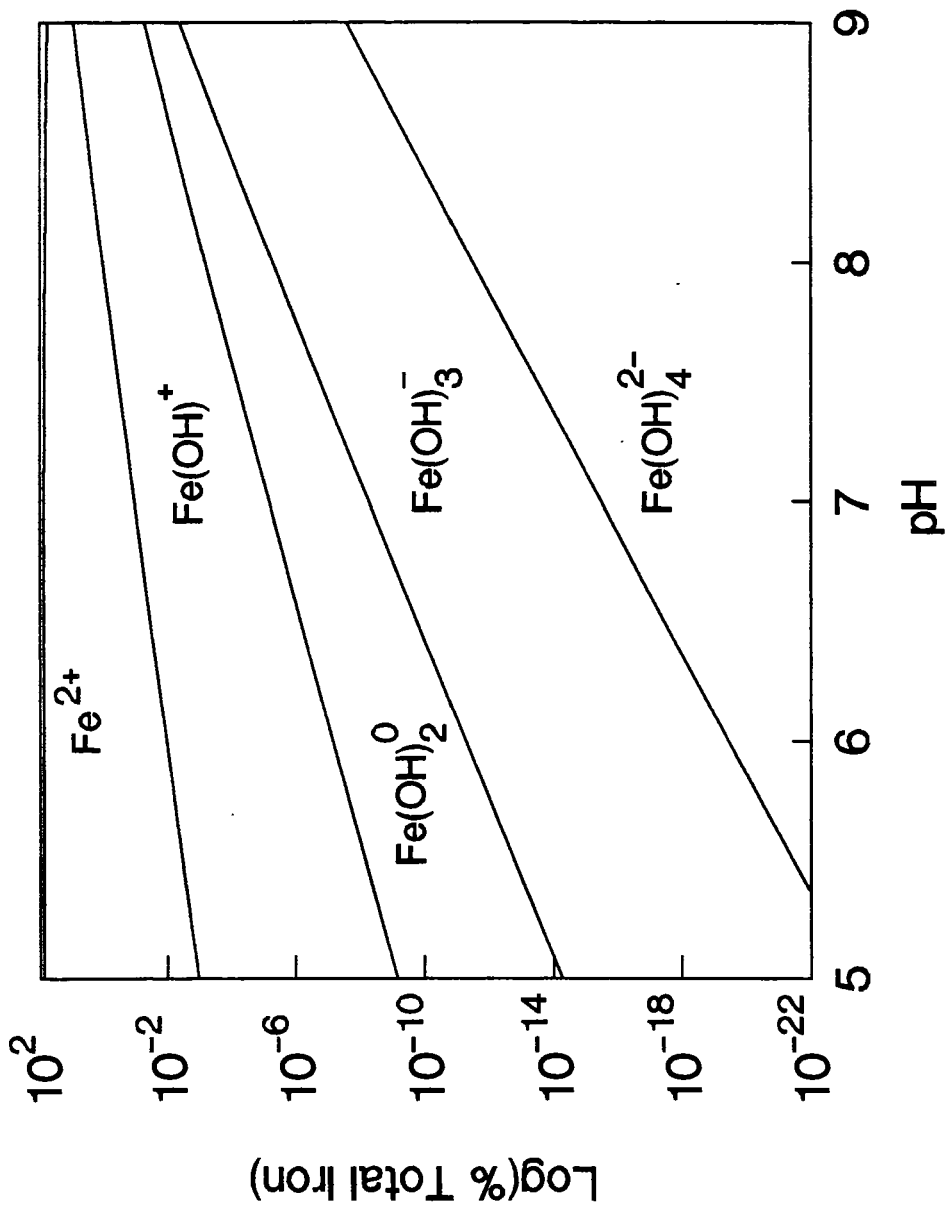


Figure 2. Variation of Fe (II) hydrolysis species in 35 ‰ salinity seawater at 25 °C as a function of pH.



Thesis Bibliography

- Anderson, M. A.; and Morel, F. M. M. (1982) The influence of aqueous iron chemistry on the uptake of iron by the coastal diatom *Thalassiosira weissflogii*. *Limnology and Oceanography*, 27(5), 789-813.
- Baker, F. W.; Parish, R. C.; and Stock, L. M. (1967) Dissociation constants of bicyclo[2.2.2]oct-2-ene-1-carboxylic acids, dibenzobicyclo[2.2.2]octa-2,5-diene-1-carboxylic acids, and cubanecarboxylic acids. *Journal of the American Chemical Society*, 89, 5677-5685.
- Barlin, G. B.; and Perrin, D. D. (1972) Dissociation constants in the elucidation of structure. In: *Elucidation of Organic Structures by Physical and Chemical Methods Part I, 2nd Edition.*, Bentley, K. W.; and Kirby, G. W., editors, Wiley-Interscience, New York, 611-676.
- Bates, R. G. (1965) *Determination of pH: Theory and Practice*, Wiley and Sons, New York, 435.
- Bates, R. G.; and Calais, J. G. (1981) Thermodynamics of the dissociation of BisH^+ in seawater from 5 to 40 °C. *Journal of Solution Chemistry*, 10, 269-279.
- Bates, R. G.; and Macaskill, J. B. (1975) Acid-base measurements in seawater In: *Analytical Methods in Seawater. Advances in Chemistry Series, No. 147*, Gibbs Jr., R. P., editors, American Chemical Society, Washington, D.C., 110-123.

- Benson, B. B.; and Krause Jr., D. (1984) The concentration and isotopic fractionation of oxygen dissolved in freshwater and seawater with the atmosphere. *Limnology and Oceanography*, 29, 620-632.
- Betteridge, D.; Dagless, E. L.; Fields, B.; and Graves, N. F. (1978) A highly sensitive flow-through phototransducer for unsegmented continuous-flow analysis demonstrating high-speed spectroscopy at parts per 10^9 level and a new method of refractometric determinations. *The Analyst*, 103(1230), 897-908.
- Biggs, A. I.; and Robinson, R. A. (1961) The ionization constants of some substituted anilines and phenols: a test of the Hammett relation. *Journal of the Chemical Society*, , 388-393.
- Brown, M. F.; and Kester, D. R. (1980) Ultraviolet spectroscopic studies related to iron complexes in marine systems. *Thalassia Jugoslavica*, 16(2-4), 191-201.
- Byrne, R. H. (1984) Absorbance corrections in self-adjusting, variable path-length-diameter, high-pressure cells. *Review of Scientific Instruments*, 55(1), 131-32.
- Byrne, R. H. (1987) Standardization of standard buffers by visible spectrometry. *Analytical Chemistry*, 59(10), 1479-1481.
- Byrne, R. H., and D. R. Kester (1976) A potentiometric study of ferric ion complexes in synthetic media and seawater. *Marine Chemistry*, 4, 275-278.
- Byrne, R. H., and D. R. Kester (1978) Ultraviolet spectroscopic study of ferric hydroxide complexation. *Journal of Solution Chemistry*, 7(5), 373-83.

- Byrne, R. H., and D. R. Kester (1976) Solubility of hydrous ferric oxide and iron speciation in seawater. *Marine Chemistry*, 4, 255-274.
- Byrne, R. H., and D. R. Kester (1981) Ultraviolet spectroscopic study of ferric equilibria at high chloride concentrations. *Journal of Solution Chemistry*, 10(1), 51-67.
- Caceci, M. S.; and Cacheris, W. P. (1984) Fitting curves to data. *Byte*, 9(5), 340-362.
- Culberson, C. H. (1981) Direct potentiometry In: *Marine Electrochemistry.*, Whitfield, M.; and Jagner, D., editors, Wiley and Son, New York, 188-261.
- Culberson, C. H.; Pytkowicz, R. M.; and Hawley, J. E. (1970) Seawater alkalinity determination by the pH method. *Journal of Marine Research*, 28, 15-21.
- Davison, W.; and Seed, G. (1983) The kinetics of the oxidation of ferrous iron in synthetic and natural waters. *Geochimica et Cosmochimica Acta*, 47, 67-79.
- Dickson, A. G. (1984) pH scales and proton-transfer reactions in saline media such as seawater. *Geochimica et Cosmochimica Acta*, 48, 2299-2308.
- Disteche, A. and S. Disteche (1967) The effect of pressure on the dissociation of carbonic acid from measurements with buffered glass electrode cells. *Journal Electrochemical society*, 114(4), 330-340.
- Dunn, L. A.; and Stokes, R. H. (1969) Pressure and temperature dependence of the electrical permittivities of formamide and water. *Transactions of the Faraday Society*, 65, 2906-2912.

- Dyrssen, D.; and Hansson, I. (1973) Ionic medium effects in seawater - a comparison of acidity constants of carbonic acid and boric acid in sodium chloride and synthetic seawater. *Marine Chemistry*, 1, 137-149.
- Dyrssen, D.; and Sillen, L. G. (1967) Alkalinity and total carbonate in sea water. A plea for p-T-independent data. *Tellus*, 19b, 113-121.
- Elrod, J.; and D. R. Kester (1980) Stability constants of iron(III) borate complexes. *Journal of Solution Chemistry*, 9(11), 885-94.
- Fallab, S. (1967) Reactions with molecular oxygen. *Angewandte Chemie International Edition in English*, 6, 496-507.
- Grant, M. W. (1973) Kinetics and thermodynamics of the formation of the monoglycinate complexes of cobalt(II), nickel(II), copper(II), and zinc(II) in water, at pressures from 1 bar to 3 kbar. *Journal of the Chemical Society, Faraday Transactions 1.*, 69, 560-569.
- Hamann, S. D.; and Linton, M. (1974) Influence of pressure on the ionization of substituted phenols. *Journal of the Chemical Society Faraday Transactions 1.*, 70, 2239-2249.
- Hansson, I. (1973) A new set of pH-scales and standard buffers for sea water. *Deep-Sea Research*, 20, 479-491.
- Harvie, C. E.; Moller, N.; and Weare, J. H. (1984) The prediction of mineral solubilities in natural waters: The Na-K-Mg-Ca-H-Cl-SO₄-OH-HCO₃-CO₃-CO₂-H₂O system to high ionic strengths at 25 °C. *Geochimica et Cosmochimica Acta*, 48, 723-751.
- Hasinoff, B. B. (1979) Fast reaction kinetics of the binding of bromide to iron (III) studied on a high pressure laser temperature jump apparatus. *Canadian Journal of Chemistry*, 57, 77-82.

- Hasinoff, B. B. (1976) The kinetic activation volumes for the binding of chloride to iron(III), studied by means of a high pressure laser temperature jump apparatus. *Canadian Journal of chemistry*, 54, 1820-1826.
- Hong, H. and D. R. Kester (1986) Redox state of iron in the offshore waters of Peru. *Limnology and Oceanography*, 31(3), 512-524.
- Johnson, K. S.; Beehler, C. L.; and Sakamoto-Arnold, C. M. (1986) A submersible flow analysis system. *Analytica Chimica Acta*, 179, 245-257.
- Jost, A. (1976) Fast reactions in solutions at high pressure. III. The effect of pressure on the reaction of iron (III)-ions with thiocyanate in water up to 2 Kbar @ 25 °C. *Berichte der Bunsen-Gesellschaft für Physikalische Chemie*, 80(4), 316-321.
- Kendrick, K. L.; and Gilkerson, W. R. (1987) The state of aggregation of methyl orange in water. *Journal of Solution Chemistry*, 16(4), 257-267.
- Kester, D. R. (1986) Equilibrium models in seawater: applications and limitations. In: *The Importance of Chemical Speciation in Environmental Process.*, Bernhard, M.; Brinckman, F. E.; and Sadler, P. J., editors, Dahlem Konferenzen 1986, Springer-Verlag, Berlin,, 337-363.
- Kester, D. R., Byrne Jr., R. H.; and Liang, Y.-J. (1975) Redox reactions and solution complexes of iron in marine systems. *ACS Symposium Series (18), Marine Chemistry in the Coastal Environment*, 56-79.

- Kester, D. R.; Duedall, I. W.; Connors, D. N.; and Pytkowicz, R. M. (1967) Preparation of artificial seawater. *Limnology and Oceanography*, 12(1), 176-179.
- Khoo, K. H.; Ramette, R. N.; Culberson, C. H.; and Bates, R. G. (1977) Determination of hydrogen ion concentration in seawater from 5 to 40 °C: Standard potentials at salinities from 20 to 45 ‰. *Analytical Chemistry*, 49, 29-34.
- King, D. W.; Lin, J.; and Kester, D. R. (1988) Determination of Fe(II) in seawater at nanomolar concentrations. *Analytical Chemistry*, in preparation.
- King, D. W.; and D. R. Kester (1988) Spectral modeling of sulfonephthalein indicators: Application to pH measurements using multiple indicators. In preparation.
- King, D. W.; and Kester, D. R. (1988) Determination of seawater pH from 1.5 to 8.5 using colorimetric indicators. *Marine Chemistry*, accepted.
- King, D. W.; and Kester, D. R. (1988) The effect of pressure on the dissociation of sulfonephthalein indicators. In preparation.
- Kirkwood, J. G.; and Westheimer, F. H. (1938) Electrostatic influence of substituents on the dissociation constants of organic acids. *Journal of Chemical Physics*, 6, 506.
- Kitamura, Y.; and Itoh, T. (1987) Reaction volume of protonic ionization for buffering agents. Prediction of pressure dependence of pH and pOH. *Journal of Solution Chemistry*, 16(9), 715-725.
- Kolthoff, I. M.; and Rosenblum, C. (1937) *Acid-Base Indicators*, MacMillan Co., New York, 413.

- le Noble, W. J.; and Schlott, R. (1976) All quartz optical cell of constant diameter for use in high pressure studies. Review of Scientific Instruments, 47, 770.
- Liang, Y.-J. (1982) Kinetics of Ferrous Iron Oxygenation and Redox Chemistry of Iron in Natural Waters. Ph.D. Thesis., University of Rhode Island, 237 pp.
- Martinez, P., R. van Eldik, and H. Kelm (1985) The effect of ionic strength and pressure on the hydrolysis equilibrium of aquated iron(III) ions. Berichte der Busen-Gesellschaft fur Physikalische Chemie, 89, 81-86.
- Milburn, R. M.; and Vosburgh, W. C. (1955) A spectroscopic study of the hydrolysis of iron (III) ion. Polynuclear species. Journal of the American Chemical Society, 77, 1352-1355.
- Miller, W. L.; and Kester, D. R. (1988) Hydrogen peroxide measurement in seawater by P-hydroxyphenylacetic acid dimerization. Analytical Chemistry, , submitted.
- Millero, F. J. (1983) The estimation of the pK_{HA}^* of acids in seawater using the Pitzer equation. Geochimica et Cosmochimica Acta, 47(12), 2121-2129.
- Millero, F. J. (1983) Influence of pressure on chemical processes in the sea. Chemical Oceanography. vol. 8., Riley, J. P.; and Chester editors, Academic Press, London, 2-88.
- Millero, F. J. (1985) The effect of ionic interactions on the oxidation of metals in natural waters. Geochimica et Cosmochimica Acta, 49, 547-553.
- Millero, F. J. (1986) The pH of estuarine waters. Limnology and Oceanography, 31(4), 839-837.

- Millero, F. J. (1982) Use of models to determine ionic interactions in natural waters. *Thalassia Jugoslavica*, 18, 253-291.
- Millero, F. J.; Hoff, E. V.; and Kahn, L. (1972) The effect of pressure on the ionization of water at various temperatures from molal-volume data. *Journal of Solution Chemistry*, 1, 309-327.
- Millero, F. J.; Scotolongo, S.; Izaguirre, M. (1987) The oxidation of Fe (II) in seawater. *Geochimica et Cosmochimica Acta*, 51, 793-801.
- Moffett, J. W.; and Zika, R. G. (1987) Reaction kinetics of hydrogen peroxide with copper and iron in seawater. *Environmental Science and Technology*, 21(8), 804-810.
- Murray, J. W.; and Gill, G. (1978) The geochemistry of iron in Puget Sound. *Geochimica et Cosmochimica Acta*, 42, 9-19.
- Owen, B. B.; Miller, R. C.; Milner, C. E.; and Cogan, H. L. (1961) Dielectric constant of water as a function of temperature and pressure. *Journal of Physical Chemistry*, 65, 2065.
- Perez, F. F.; and Fraga, F. (1987) The pH measurements in seawater on the NBS scale *Marine Chemistry*, 21, 315-327.
- Perrin, D. D.; Dempsey, B.; and Serjeant, E. P. (1981) *pKa Prediction for Organic Acids and Bases*, Chaptman and Hall, London, 146 pp.
- Petasne, R. G.; and Zika, R. G. (1987) Fate of superoxide in coastal sea water. *Nature*, 325, 516-518.
- Pytkowicz, R. M. (1969) Use of apparent equilibrium constants in chemical oceanography, geochemistry, and biochemistry. *Geochemical Journal*, 3, 181-184.
- Pytkowicz, R. M.; Kester, D. R.; and Burgener, B. C. (1966) Reproducibility of pH measurements in seawater *Limnology and Oceanography*, 11(3), 417-419.

- Ramette, R. W., C. H. Culberson, and R. G. Bates (1977) Acid-base properties of tris(hydroxymethyl)aminomethane (Tris) buffers in seawater from 5 to 40 °C. *Analytical Chemistry*, 49(6), 867-670.
- Robert-Baldo, G. L.; Morris, M. J.; and Byrne, R. H. (1985) Spectroscopic determination of seawater pH using phenol red. *Analytical Chemistry*, 57, 2564-67.
- Roekens, E. J.; and Van Grieken, R. E. (1983) Kinetics of iron (II) oxidation in seawater of various pH. *Marine Chemistry*, 13, 195-202.
- Rush, J. D.; and Bielski, B. H. J. (1985) Pulse radiolytic studies of the reaction of perhydroxyl/superoxide O_2^- with iron (II)/iron (III) ions. The reactivity of HO_2/O_2^- with ferric ions and its implication on the occurrence of the Haber-Weiss reaction. *Journal of Physical Chemistry*, 89(23), 5062-5066.
- Siddall, T. H. and W. C. Vosburgh (1951) A spectrophotometric study of the hydrolysis of iron(III) ion. *Journal of the American Chemical Society*, 73, 4270-4272.
- Stookey, L. C. (1970) FerroZine - A new spectrophotometric reagent for iron. *Analytical Chemistry*, 42, 779-781.
- Stumm, W.; and Lee, G. F. (1961) Oxygenation of ferrous iron. *Industrial Engineering Chemistry*, 53(2), 143-146.
- Stumm, W.; and Morgan, J. J. (1981) *Aquatic Chemistry* 2nd ed., Wiley-Interscience, 780 pp.
- Swaddle, T. W. and A. E. Merback (1981) High-pressure oxygen-17 fourier transform nuclear magnetic resonance spectroscopy. Mechanism of water exchange on iron(III) in acidic aqueous solution. *Inorganic Chemistry*, 20, 4212-4216.

- Turner, D. R., M. Whitfield, and A. G. Dickson (1981) The equilibrium speciation of dissolved components in freshwater and seawater at 25°C and 1 atm pressure. *Geochimica et Cosmochimica Acta*, 45, 844-881.
- Waite, T. D.; and Morel, F. M. M. (1984) Coulometric study of the redox dynamics of iron in seawater. *Analytical Chemistry*, 56(4), 787-92.
- Waite, T. D.; and Morel, F. M. M. (1984) Photoreductive dissolution of colloidal iron oxides in natural waters. *Environmental Science and Technology*, 18, 860-868.
- Whitfield, M.; Butler, R. A.; and Covington, A. K. (1985) The determination of pH in estuarine waters. I. Definition of pH scales and the selection of buffers. *Oceanologica Acta*, 8(4), 423-432.
- Wilcox, C. F.; and Leung, C. (1968) Transmission of substituent effects. Dominance of field effects. *Journal of the American Chemical Society*, 90, 336-341.
- Zafirioiu, O. C. (1974) Sources and reactions of OH and daughter radicals in seawater. *Journal of Geophysical Research*, 79, 4491-4497.